

Sulfur cycling in oceanic oxygen minimum zones

Cameron M. Callbeck ^{1,2*} Donald E. Canfield ³ Marcel M. M. Kuypers,² Pelin Yilmaz,² Gaute Lavik,²
Bo Thamdrup ³ Carsten J. Schubert ^{1,4} Laura A. Bristow ³

¹Swiss Federal Institute of Aquatic Science and Technology (Eawag), Kastanienbaum, Switzerland

²Max Planck Institute for Marine Microbiology, Bremen, Germany

³Department of Biology, Nordcee, University of Southern Denmark, Odense M, Denmark

⁴Institute of Biogeochemistry and Pollutant Dynamics, ETH, Zurich, Switzerland

Abstract

The sulfur cycle is an important, although understudied facet of today's modern oxygen minimum zones (OMZs). Sulfur cycling is most active in highly productive coastal OMZs where sulfide-rich sediments interact with the overlying water column, forming a tightly coupled benthic-pelagic sulfur cycle. In such productive coastal systems, highly eutrophic and anoxic conditions can result in the benthic release of sulfide leading to an intensification of OMZ-shelf biogeochemistry. Active blooms involving a succession of sulfide-oxidizing bacteria detoxify sulfide and reduce nitrate to N₂, while generating nitrite and ammonium that augment anammox and nitrification. Furthermore, the abiotic interactions of sulfide with trace metals may have the potential to moderate nitrous oxide emissions. While sulfide/sulfur accumulation events were previously considered to be rare, new evidence indicates that events can develop in OMZ shelf waters over prolonged periods of anoxia. The prevalence of these events has ramifications for nitrogen loss and greenhouse gas emissions, including other linked cycles involving carbon and phosphorus. Sulfur-based metabolisms and activity also extend into the offshore OMZ as a result of particle micro-niches and lateral transport processes. Moreover, OMZ waters ubiquitously host a community of organosulfur-based heterotrophs that ostensibly moderate the turnover of organic sulfur, offering an exciting avenue for future research. Our synthesis highlights the widespread distribution and multifaceted nature of the sulfur cycle in oceanic OMZs.

Large-scale thermohaline circulation maintains a well-oxygenated ocean, with the exception of certain regions called oxygen minimum zones (OMZs). OMZs are situated along continental margins where coastal upwelling of nutrient rich waters causes intensified primary productivity in surface waters (Carr 2001). As a result, the downward flux of organic matter stimulates microbial respiration that lowers dissolved oxygen concentrations in the water column. Most marine waters typically have lower oxygen concentrations below the euphotic zone; however, in OMZs, this deficit is exacerbated by poor regional ventilation. Traditionally, the low-oxygen water mass is demarcated at a cutoff of < 20 μM of O₂. At this cutoff, OMZs comprise approximately 1% of the global ocean volume (Lam and Kuypers 2011). The major OMZs are located in the eastern

tropical South Pacific (ETSP), the eastern tropical North Pacific (ETNP), the eastern tropical South Atlantic (ETSA), the Arabian Sea (AS), and the Bay of Bengal. However, in some of these regions, dissolved oxygen concentrations can fall far below the 20 μM definitional threshold, to levels even below the detection limit (a few nanomoles per liter) of the most sensitive oxygen sensors, (Karstensen et al. 2008; Revsbech et al. 2009; Tiano et al. 2014), which we refer to hereafter as anoxic.

OMZ waters, especially those with low nanomolar to undetectable oxygen, host a diverse assemblage of anaerobic microorganisms that transform nitrate, nitrite and ammonium through the processes of anammox (anaerobic ammonium oxidation using nitrite) and denitrification, to produce N₂ gas. The production of N₂ effectively removes fixed nitrogen from the biosphere, which is referred to as nitrogen loss. Consequently, these low-oxygen waters promote substantial fixed nitrogen loss that strongly impact the marine nitrogen budget (Dalsgaard et al. 2003; Kuypers et al. 2003, 2005; Ward et al. 2009). Estimates indicate that OMZs are responsible for 60–90 Tg N yr⁻¹ (DeVries et al. 2012), or roughly 20–40% of marine nitrogen loss (Codispoti et al. 2001), and are major emitters of the climate-active gas, N₂O (Naqvi et al. 2000; Arevalo-Martinez et al. 2015; Arévalo-Martínez et al. 2019).

*Correspondence: cameron.callbeck@eawag.ch, cameron.callbeck@uni-bas.ch

This is an open access article under the terms of the Creative Commons Attribution License, which permits use, distribution and reproduction in any medium, provided the original work is properly cited.

This work was conducted by C. M. Callbeck in partial fulfillment of the requirements for a Ph.D. from the University of Bremen, 2017 (Callbeck 2017). Associate editor: Florence Schubotz

A growing body of work indicates the presence of a widespread and persistent sulfur cycle in OMZs. Indeed, the potential for sulfur cycling is large. Even though sulfate reduction has a low free energy yield, holding one of the lowest positions on the redox tower (after nitrate, manganese oxides, and iron oxyhydroxides), marine sulfate concentrations (28 mM) are much higher than concentrations of other more favorable electron acceptors, which are found in nanomolar to micromolar levels. The large sulfate pool, in combination with the high organic matter load of OMZs, provides a large supply of substrate for heterotrophic sulfate-reducing bacteria (Jørgensen 1982). This is hypothesized to be the basis of the sulfur cycle and generates inorganic sulfide, in turn, fueling sulfide-oxidizing bacteria and the production of reduced sulfur intermediates, such as elemental sulfur, sulfite, and thiosulfate (Canfield et al. 2005).

Moreover, the large sulfate pool supports assimilatory sulfate reduction that generates organic sulfur. The inventory of organic sulfur further drives organosulfur-based heterotrophs that thrive from the breakdown of organic sulfur-containing compounds to reduced inorganic sulfur species. Together, the sulfur cycle encompasses the transformation of both inorganic and organic sulfur (Fig. 1). The various sulfur transformation processes also have the potential to span a wide range of redox conditions. The sulfur cycle is well known to be active in sulfide-rich anoxic sediments (Wasmund et al. 2017; Jørgensen et al. 2019), with recent discoveries of microniches inside particles and sulfur storage in some sulfur-based microbes further expanding the niche for sulfur cycling to the sulfide-poor OMZ (Canfield et al. 2010; Bianchi et al. 2018; Callbeck et al. 2018). In addition, many organosulfur-based heterotrophs can use oxygen as the electron acceptor for growth, which broadens the extent of the sulfur cycle to include the oxycline overlying the OMZ where dissolved organic sulfur (DOS) concentrations are large.

The organisms that mediate the transformation of inorganic and organic sulfur in OMZs are phylogenetically diverse. The diversity of sulfur-based microbes was recently examined in the permanently stratified and sulfide-rich waters of the Black Sea—an important model environment for oceanic OMZs (van Vliet et al. 2020). The survey by van Vliet et al. (2020) find that sulfur-based microbes span 11 phyla, and that many of these taxonomic assemblages occur in both oceanic OMZs and stratified basins, demonstrating broad community similarities between these two environments. Understanding sulfur-based microbes in oceanic OMZs may therefore provide important insight into factors driving diversification in sulfur-utilizing groups in analogously stratified basins and vice versa. On the other hand, some sulfur-based microbes appear to be more prevalent in oceanic OMZs. Moreover, sulfur-related microbes in oceanic OMZs can have different metabolic capabilities compared to their sister lineages in stratified basins. Thus, by understanding sulfur-based taxa in the context of oceanic OMZs we may also reveal adaptations unique to these environments.

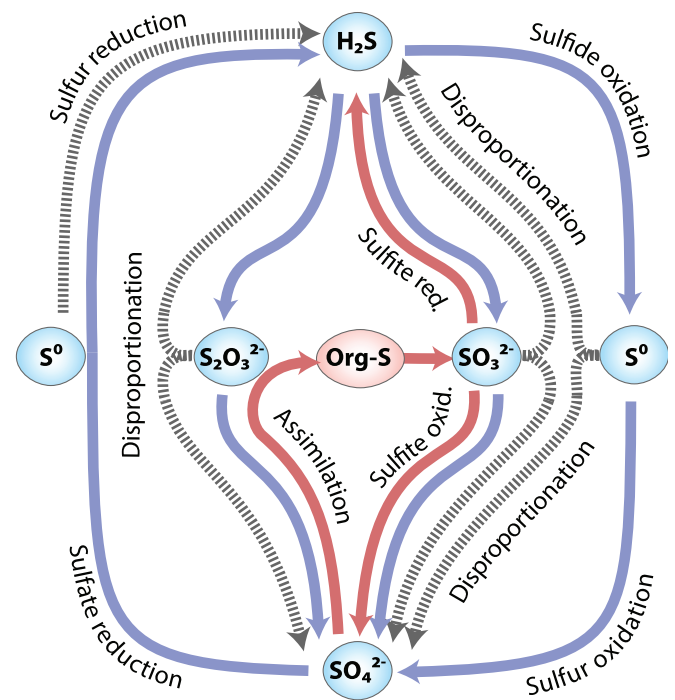


Fig. 1. The microbial sulfur cycle in oxygen minimum zones. The sulfur cycle is comprised of both inorganic and organic sulfur species. The blue and red lines indicate inorganic and organic sulfur transformation pathways, respectively. Pathways shown by dotted lines are expected to occur in OMZ waters, but have limited evidence for to date. Complementary pathways of microbial sulfate reduction and sulfide oxidation produce/consume sulfide (H_2S), respectively. These pathways also generate intermediate sulfur species that include elemental sulfur (S^0), thiosulfate ($\text{S}_2\text{O}_3^{2-}$) and sulfite (SO_3^{2-}), which can be released into the environment. Produced intermediates, can be further reduced/oxidized to yield sulfate or sulfide, respectively. Produced sulfur intermediates can also be disproportionated to yield sulfide and sulfate. Sulfur-containing organic matter is produced from the assimilation of sulfate into biomass. Reduced sulfur intermediates, thiosulfate, sulfite and sulfide can be generated from the degradation of organic sulfur-containing metabolites (Org-S). For instance, produced sulfite from organic sulfur degradation can be oxidized or reduced to sulfate or sulfide, respectively. In this reaction, the organic matter sulfur moiety ultimately serves as the source of sulfur.

A deep examination of sulfur-related microbes will further provide insight into other linked biogeochemical cycles involving nitrogen, carbon and phosphorous. Functional gene surveys have uncovered potential for sulfur-based microbes to influence regional greenhouse gas emissions and nitrogen loss, as well as provide key substrates driving anammox—one of the most important nitrogen removal pathways in OMZs. In addition, some sulfur-related microbes have a capacity for nitrogen and carbon fixation, contributing to the generation of organic matter; while others may facilitate the release of dissolved phosphate with possible feedback effects on primary productivity in waters overlying the OMZ. Thus, investigating these sulfur-based microbes including their distribution and activity in OMZs will help to predict/quantify chemical fluxes of other linked cycles. Such findings will not only have

implications for oceanic OMZs, but will help to constrain processes in analogously stratified basins.

Here, we provide a synoptic view of oceanic OMZ sulfur cycling spanning from eutrophic upper shelf waters (< 200 m water depth) where highly active sulfur cycling prevails, to the offshore OMZ detached from the benthic fluxes of reduced sulfur (> 200 m water depth). For detailed insight into key functional genes and metabolic pathways associated to sulfur-based microbes in OMZs and shelf sediments we recommend the reviews by van Vliet et al. 2020 and Wasmund et al. 2017. Our synthesis here highlights the ecophysiology of key sulfur-based microbes, their affinities for sulfur, their niche partitioning between various habitats, and their impact on the tightly coupled nitrogen, carbon, and phosphorous cycles in oceanic OMZs. We also partly draw on research from stratified basins that are either seasonally or permanently sulfidic including the Cariaco Basin, Black Sea, Saanich Inlet, and Mariager Fjord. Finally, we discuss the hydrodynamic processes that shape the distribution and activity of sulfur-based microbes—and explore the potential for widespread organic sulfur degradation in oceanic OMZs.

Sulfidic events and sulfur cycling associated with the upper shelf

The benthic-pelagic coupled sulfur cycle

The first indications of an active sulfur cycle operating in OMZs dates as far back as the 19th century. In 1852, off the coast of Peru, Dr. J. L. Burttt depicted the release of sulfide, which can be characteristically detected by its odor:

The first premonition of what was to produce a remarkable destruction among fish, was the discoloration of the water of the bay, from a marine green to a dirty milk-white hue, followed by a decided odor of the gas; so much of it being present on many occasions as directly to blacken a clean piece of silver, and to blacken paint work in a few hours. (Burttt 1852)

These phenomena, otherwise known as “sulfidic events” can result in sudden fish death, which were shrouded in mystery for over a century since Dr. Burttt’s first account. In the past decades, scientific advances in biogeochemistry and microbial ecology, coupled with large research expeditions and remote sensing technologies have provided a holistic understanding of sulfidic events and the active sulfur cycle that prevails over the OMZ shelf.

The intensified input of organic matter along the coastal upwelling region fuels enhanced activity of heterotrophic sulfate-reducing bacteria in the shelf OMZ sediments (Fossing 1990; Ferdelman et al. 1997, 1999; Brüchert et al. 2003). In dissimilatory sulfate reduction, sulfate is transported into the cell, where it is activated with ATP sulfurylase (Sat) generating adenosine-5'-phosphosulfate (APS). APS is reduced by the soluble APS reductase to sulfite with two electrons (Ramos et al. 2012) and then further to sulfide with six electrons

Table 1. Gibbs free energy of key sulfur-based reactions under both standard and nonstandard conditions representing the OMZ. Nonstandard state conditions were calculated according to the following concentrations: 41 μM O_2 , 28 mM sulfate, 1 nM sulfide, 1 μM sulfite, 1 μM thiosulfate, 10 μM nitrate, 5 μM nitrite, 3 μM ammonium, 10 nM N_2O , 10 μM acetate ($\text{C}_2\text{H}_3\text{O}_2^-$), 10 μM acetaldehyde (CH_3CHO), 1 nM taurine ($\text{C}_2\text{H}_7\text{NSO}_3$), 2.2 mM bicarbonate (HCO_3^-). Other conditions were as follows: temperature 14°C and pH 7.5. The abbreviation DNRA stands for dissimilatory nitrate reduction to ammonium.

Reaction stoichiometry	ΔG°	$\Delta G'$		
	(kJ mol ⁻¹)			
Oxygen/nitrate reduction coupled to sulfide oxidation				
$\text{HS}^- + 2 \text{O}_2 \rightarrow \text{SO}_4^{2-} + \text{H}^+$	-763	-756	Inorganic sulfur transformation	
$\text{HS}^- + \frac{5}{8} \text{NO}_3^- + \frac{3}{8} \text{H}^+ \rightarrow \text{SO}_4^{2-} + \frac{1}{8} \text{N}_2 + \frac{1}{8} \text{H}_2\text{O}$	-769	-661		
$\text{HS}^- + 2 \text{NO}_3^- + \text{H}^+ \rightarrow \text{SO}_4^{2-} + \text{N}_2\text{O} + \text{H}_2\text{O}$	-668	-567		
$\text{HS}^- + 4 \text{NO}_3^- \rightarrow \text{SO}_4^{2-} + 4 \text{NO}_2^- + \text{H}^+$	-461	-468		
$\text{HS}^- + \frac{3}{5} \text{NO}_3^- + \frac{7}{5} \text{H}^+ \rightarrow \text{S}^0 + \frac{1}{5} \text{N}_2 + \frac{6}{5} \text{H}_2\text{O}$	-252	-135		
Elemental sulfur oxidation				
$\text{S}^0 + \frac{5}{8} \text{NO}_3^- + \frac{3}{8} \text{H}_2\text{O} \rightarrow \text{SO}_4^{2-} + \frac{1}{8} \text{N}_2 + \frac{1}{8} \text{H}^+$	-517	-526		
Sulfite and thiosulfate oxidation				
$\text{S}_2\text{O}_3^{2-} + \frac{5}{8} \text{NO}_3^- + \frac{1}{8} \text{H}_2\text{O} \rightarrow 2 \text{SO}_4^{2-} + \frac{1}{8} \text{N}_2 + \frac{3}{8} \text{H}^+$	-743	-701		
$\text{SO}_3^{2-} + \frac{3}{5} \text{NO}_3^- + \frac{7}{5} \text{H}^+ \rightarrow \text{SO}_4^{2-} + \frac{1}{5} \text{N}_2 + \frac{1}{5} \text{H}_2\text{O}$	-260	-209		
DNRA coupled to sulfide oxidation				
$\text{HS}^- + \text{NO}_3^- + \text{H}^+ + \text{H}_2\text{O} \rightarrow \text{SO}_4^{2-} + \text{NH}_4^+$	-489	-411		
Sulfate reduction				
$\text{SO}_4^{2-} + \text{C}_2\text{H}_3\text{O}_2^- \rightarrow \text{HS}^- + 2 \text{HCO}_3^-$	-46	-88		
Sulfite reduction				
$\text{SO}_3^{2-} + \frac{3}{4} \text{C}_2\text{H}_3\text{O}_2^- + \frac{1}{4} \text{H}^+ \rightarrow \text{HS}^- + \frac{3}{2} \text{HCO}_3^-$	-108	-103		
Disproportionation – inorganic sulfur ‘fermentation’				
$\text{SO}_3^{2-} + \frac{1}{4} \text{H}^+ \rightarrow \frac{1}{4} \text{HS}^- + \frac{3}{4} \text{SO}_4^{2-}$	-68	-44		
$\text{S}_2\text{O}_3^{2-} + \text{H}_2\text{O} \rightarrow \text{HS}^- + \text{SO}_4^{2-} + \text{H}^+$	+26	-39		
$\text{S}^0 + \text{H}_2\text{O} \rightarrow \frac{3}{4} \text{H}_2\text{S} + \frac{1}{4} \text{SO}_4^{2-} + \frac{1}{2} \text{H}^+$	+59	-30		
Taurine^a - oxidative processes				
$\text{C}_2\text{H}_7\text{NSO}_3 + 3 \text{O}_2 + \text{H}_2\text{O} \rightarrow \text{SO}_4^{2-} + \text{NH}_4^+ + 3 \text{H}^+ + 2 \text{HCO}_3^-$	-1251	-1365	Organic sulfur transformation	
$\text{C}_2\text{H}_7\text{NSO}_3 + \frac{1}{2} \text{NO}_3^- \rightarrow \text{SO}_4^{2-} + \frac{5}{8} \text{N}_2 + \text{NH}_4^+ + 2 \text{HCO}_3^- + \frac{3}{8} \text{H}^+ + \frac{1}{8} \text{H}_2\text{O}$	-1269	-1239		
Taurine^a - fermentative processes^b				
$\text{C}_2\text{H}_7\text{NSO}_3 + \text{H}_2\text{O} \rightarrow \text{HS}^- + \frac{1}{2} \text{C}_2\text{H}_3\text{O}_2^- + \text{HCO}_3^- + \text{NH}_4^+ + 2 \text{H}^+$	-92	-225		
$\text{C}_2\text{H}_7\text{NSO}_3 + \frac{1}{2} \text{H}_2\text{O} \rightarrow \frac{1}{2} \text{S}_2\text{O}_3^{2-} + \text{C}_2\text{H}_3\text{O}_2^- + \text{NH}_4^+ + \text{H}^+$	-82	-140		
Taurine^a “degradation”				
$\text{C}_2\text{H}_7\text{NSO}_3 + \text{H}_2\text{O} \rightarrow \text{SO}_3^{2-} + \text{CH}_3\text{CHO}^c + \text{NH}_4^+ + 2 \text{H}^+$	-47	-12		
$\text{C}_2\text{H}_7\text{NSO}_3 + \frac{1}{2} \text{O}_2 + \text{H}_2\text{O} \rightarrow \text{SO}_3^{2-} + \text{C}_2\text{H}_3\text{O}_2^- + \text{NH}_4^+ + 2 \text{H}^+$	-189	-302		

^a G_f° for taurine: -509.4 kJ mol⁻¹

^b Stoichiometry according to Denger et al. 1997 and Lie et al. 1999

^c Acetaldehyde was used as the product of taurine degradation to balance sulfite formation (at 25°C).

catalyzed by dissimilatory sulfite reductase (Dsr) (Santos et al. 2015). The soluble reductase enzymes are coupled to membrane-bound complexes for energy conservation: AprAB-QmoABC and DsrABC-MKJOP complexes. The Dsr pathway is highly conserved among sulfate-reducing prokaryotes and is currently found in five bacterial and two archaeal lineages (Muyzer and Stams 2008), although the majority of sulfate- and sulfur-reducing microbes in OMZ sediments are affiliated with the class *Deltaproteobacteria* and the family *Desulfobacteraceae* (Wasmund et al. 2017).

The activity levels of heterotrophic sulfate-reducing bacteria in sediments depends on the quantity and quality of available organic matter. Preferred organic matter substrates include volatile fatty acids, as well as more complex carbon sources such as hydrocarbons, monocarboxylic acids, alcohols, amino acids, sugars, and aromatic compounds (Canfield et al. 2005; Muyzer and Stams 2008). The oxidation of these organic substrates via substrate-level phosphorylation can be subdivided into two distinct metabolisms: the incomplete oxidation of organics producing acetate, or the complete oxidation to CO₂ (Widdel 1988). While sulfate-reducing bacteria can oxidize a variety of organic matter substrates, they generally thrive from the by-products of fermentation, such as acetate, which is a key compound fueling sulfate reduction in sediments (Beulig et al. 2018; Jørgensen et al. 2019). Using acetate as the electron donor, sulfate-reducing bacteria gain moderate amounts of energy ($\Delta G' = -88 \text{ kJ mol}^{-1}$) from the reduction of sulfate to sulfide when calculated under OMZ conditions (Table 1).

In OMZs, high organic matter concentrations, along with the general absence of pore-water oxygen and nitrate, promote enhanced rates of sulfate reduction particularly in the upper most sediment layer, where rates can reach hundreds of $\text{nmol cm}^{-3} \text{ d}^{-1}$ (Brüchert et al. 2003; Maltby et al. 2016; Jørgensen et al. 2019). Rates of sulfate reduction decrease with depth and also decrease when moving away from the eutrophic upper shelf (Fossing 1990; Ferdelman et al. 1997, 1999; Schubert et al. 2000, 2005; Brüchert et al. 2003; Maltby et al. 2016). The sulfide generated by sulfate-reducing bacteria in the upper sediment layer is recycled back to sulfate by co-occurring filamentous sulfide-oxidizing bacteria (e.g., *Thioploca*), and to a small extent removed by pyrite formation (Fossing et al. 1995; Schulz et al. 1999; Böning et al. 2004; Dale et al. 2009; Maltby et al. 2016). This tightly coupled production/consumption of sulfide contributes to the presence of a pore-water “sulfide deficit” in the uppermost sediment layer (Schulz et al. 1999; Schmaljohann et al. 2001; Gutiérrez et al. 2008; Prokopenko et al. 2013; Dale et al. 2016).

However, if stagnant and highly eutrophic conditions arise over the upper OMZ shelf, the increased organic matter input enhances rates of sulfate reduction at the water-sediment interface. Increased sulfide production can eventually overrun the capacity of sulfide-oxidizing bacteria to remove sulfide in the upper sediment layer resulting in the

accumulation of sulfide. The release of sulfide into the water column, otherwise known as a “sulfidic event”, is exacerbated during the formation of stagnant and stratified bottom waters, which promotes the consumption of water-column oxygen and nitrate (Dale et al. 2016; Sommer et al. 2016). The release of sediment-generated sulfide into the overlying water column can occur via passive molecular diffusion, but can also be facilitated by ebullition with methane bubbles (Martens and Val Klump 1980; Martens et al. 1998). Indeed, the sulfide-rich muds of OMZs are generally accompanied by active methanogenesis, with rates reaching up to $1.1 \text{ nmol cm}^{-3} \text{ d}^{-1}$ that can contribute to gas charging in sediments (Maltby et al. 2016).

The benthic sulfide flux to overlying waters can be substantial in OMZs, particularly when anoxic and stratified conditions prevail (Pratihary et al. 2014; Sommer et al. 2016). On the ETSP upper shelf, the sulfide flux has been measured at up to $14 \text{ mmol m}^{-2} \text{ d}^{-1}$ (Sommer et al. 2016), and could possibly reach up to $20 \text{ mmol m}^{-2} \text{ d}^{-1}$ at its peak (Dale et al. 2016). This sulfide flux is similar in magnitude to the benthic ammonium flux of $18\text{--}21 \text{ mmol m}^{-2} \text{ d}^{-1}$ (Sommer et al. 2016), and greatly exceeds the release of phosphate and iron from OMZ sediments of $0.2\text{--}1 \text{ mmol m}^{-2} \text{ d}^{-1}$ (Noffke et al. 2012; Lomnitz et al. 2016; Schlosser et al. 2018). Additional sulfide is supplied by moderate rates of sulfate reduction in shelf bottom waters of $0.2\text{--}6.8 \text{ nmol L}^{-1} \text{ d}^{-1}$, or up to $0.02 \text{ mmol m}^{-2} \text{ d}^{-1}$ (measured 3 m above the sediment), albeit, this is considered a minor contribution compared to the benthic sulfide flux (Brüchert et al. 2006; Lavik et al. 2009). In most eutrophic OMZ shelf regions, sulfide accumulates to low micromolar concentrations in bottom waters over the course of days (Kasten and Jørgensen 2000), with the larger events reaching up to $15\text{--}33 \mu\text{M}$ of sulfide (Naqvi et al. 2000; Lavik et al. 2009; Shenoy et al. 2012; Schunck et al. 2013; Galán et al. 2014; Lomnitz et al. 2016; Callbeck et al. 2018; Shirodkar et al. 2018).

The benthic-generated sulfide flux is eventually opposed by an overlying nitrate flux. At the overlap of nitrate and sulfide, a diverse consortium of sulfide/sulfur-oxidizing nitrate-reducing bacteria catalyzes the detoxification of the sulfidic event producing nontoxic sulfate with nitrate as the electron acceptor (Lavik et al. 2009). Many OMZ sulfide-oxidizing bacteria employ the periplasmic sulfur-oxidizing multienzyme SOX system (*soxABCDXYZ*) and/or the “reverse” siroheme-containing sulfite reductase (*rdsr*) pathways (in conjunction with other enzymes: the sulfide-quinone oxidoreductase (*sqr*) or flavocytochrome C (*fcc*) oxidoreductase) to oxidize a range of reduced sulfur species (see also Wasmund et al. 2017; van Vliet et al. 2020).

The oxidation of sulfide is coupled to denitrification, which is the stepwise reduction of nitrate to N₂ via four consecutive enzymatic steps involving nitrate reductase (*nar/nap*: $\text{NO}_3^- \rightarrow \text{NO}_2^-$), nitrite reductase (*nirS/nirK*: $\text{NO}_2^- \rightarrow \text{NO}$), nitric oxide reductase (*nor*: $\text{NO} \rightarrow \text{N}_2\text{O}$), and finally, nitrous oxide reductase (*nosZ*: $\text{N}_2\text{O} \rightarrow \text{N}_2$). Nitrate can also be reduced to form

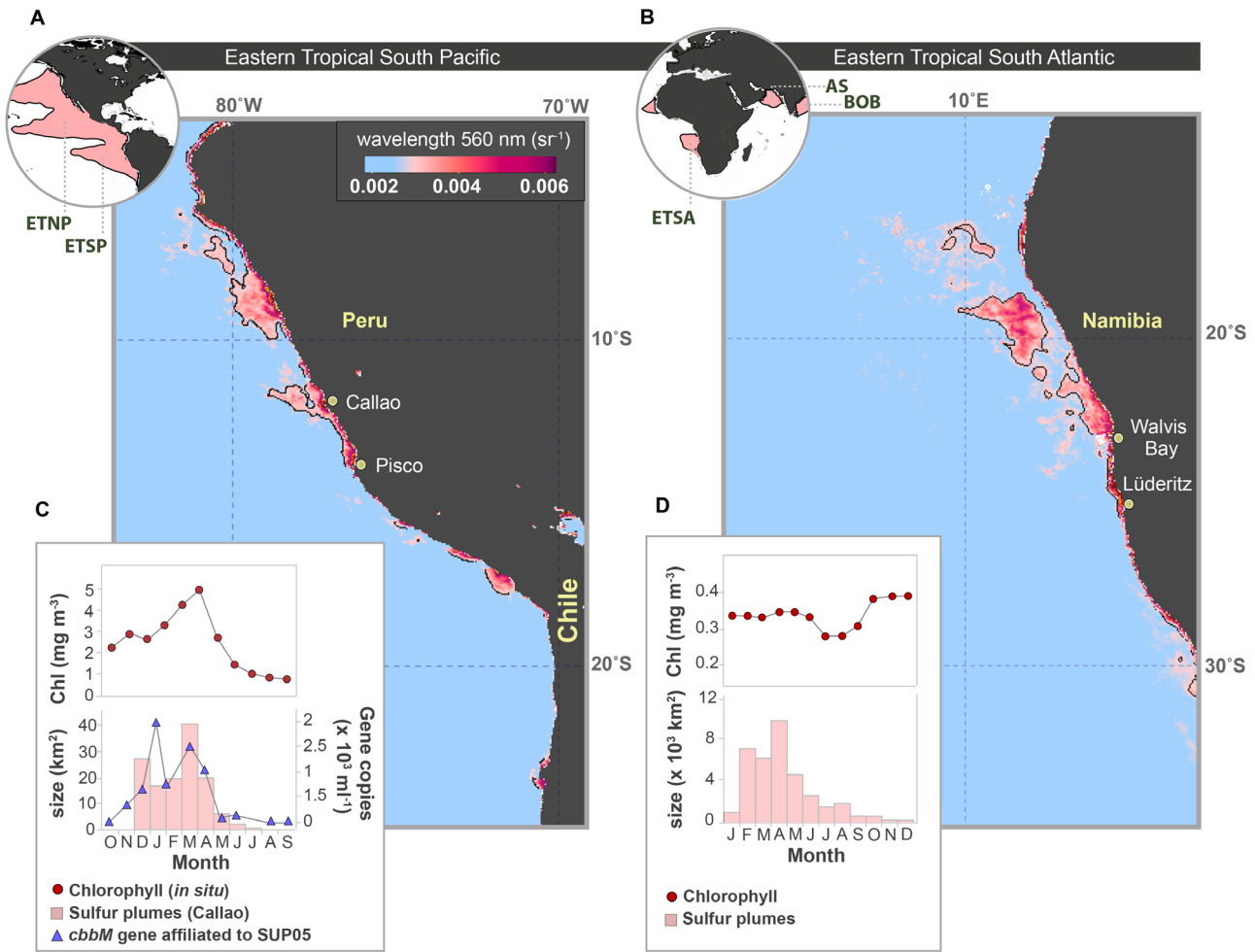


Fig. 2. Distribution and prevalence of sulfur plume activity in oxygen minimum zones. Sulfur plumes develop in eutrophic upper shelf waters (< 200 m water depth). Sulfur plumes can also be transported into the offshore OMZ (> 200 m water depth) due to lateral transport processes (e.g., mesoscale eddies). **(A,B)** Remote sensing images of sulfur plumes using the water-leaving reflectance wavelength of 560 nm (optimal waveband for sulfur plume detection; Ohde et al. 2007; Ohde and Dadou 2018). The images shown are seasonal composites from 21 December to 20 March 2004–2005. The images were acquired by moderate resolution imaging spectroradiometer (MODIS) downloaded from the NASA Ocean Color Database and processed using SeaDas software (www.seadas.gsfc.nasa.gov/). In the world atlas globes, the contour line indicates 20 μM of O_2 , which represents the traditional upper boundary of the OMZ water mass. The total area of the OMZ (at a 20 μM O_2 cutoff) is indicated by the red shading. The oxygen data is based on world atlas data from 2013. Abbreviations indicated stand for: eastern tropical South Pacific (ETSP), eastern tropical North Pacific (ETNP), eastern tropical South Atlantic (ETSA), Arabian Sea (AS), and the Bay of Bengal (BOB). **(C,D)** Seasonality of chlorophyll and sulfur plume development in the ETSP and ETSA regions reproduced from Ohde 2018 and Echevin et al. 2008, and from Ohde and Dadou 2018 and Lamont et al. 2018, respectively. Panel c also includes a marker gene associated to the SUP05 clade; the *ccbM* gene is involved in carbon fixation via the Calvin–Benson–Bassham cycle, data is reproduced from Léniz et al. 2017. Shown are the maximum *ccbM* copy numbers of the three sampled depths by Léniz et al. 2017. Note that panel **C** is representing local remote sensing data off the coast of Callao from 11.8°S to 12.4°S; while panel **D** presents regional remote sensing covering the Namibian shelf from 22°S to 26°S, hence the differences in sulfur plume size between the two studies.

ammonium, otherwise known as dissimilatory nitrate reduction to ammonium (DNRA; involving *nrfA*). As a carbon source, sulfide-oxidizing bacteria either fix CO_2 into biomass or assimilate organic carbon for growth (e.g., acetate), designated as chemolithoautotrophy and chemolithoheterotrophy, respectively. The former was generally believed to dominate sulfide oxidation in shelf waters, with recent evidence now suggesting that the latter also contributes to sulfide oxidation during a sulfidic event (Callbeck et al. 2019).

At the pelagic nitrate-sulfide chemocline, with nitrate in excess, sulfide-oxidizing bacteria gain a moderate to high amount of energy ($\Delta G' = -661 \text{ kJ mol}^{-1}$; Table 1) from the oxidation of sulfide to sulfate. If sulfide is in excess over nitrate, then elemental sulfur is a more common by-product of sulfide oxidation ($\Delta G' = -135 \text{ kJ mol}^{-1}$). Since elemental sulfur oxidation to sulfate is the rate-limiting step (Cervantes et al. 2009), elemental sulfur tends to accumulate at the nitrate-sulfide chemocline reaching up to 20 μM (Lavik et al.

2009; Callbeck et al. 2018, 2019), similar to stratified basins (Zopfi et al. 2001a; Hayes et al. 2006; Li et al. 2008). The presence of elemental sulfur gives the water a milky-turquoise discoloration (Weeks et al. 2002, 2004), which is very likely what Dr. Burt had observed off the coast of Peru. These sulfur-rich water masses can also be detected by satellite remote sensing as elemental sulfur plumes exhibit a maximum reflectance at a wavelength of 560 nm (Ohde et al. 2007). This wavelength is distinct from the spectral profile of other features, such as algal blooms and sediment resuspension. At their apex, sulfur plumes can reach over 10,000 km² in size and envelope large swaths of the upper shelf off the coast of Namibia and Peru (Ohde et al. 2007) (e.g., Fig. 2). Apart from elemental sulfur, sulfide oxidation at the nitrate-sulfide chemocline generates other reduced sulfur species such as thiosulfate and sulfite, reaching concentrations of up to 400 nM at the chemocline (Callbeck et al. 2018). Eventually microbial activity oxidizes the elemental sulfur, along with other reduced sulfur species to sulfate ($\Delta G' = -209$ to -701 kJ mol⁻¹; Table 1).

Sulfide, thus, is generally detoxified in shelf bottom waters with little to no impact on higher life in the oxygenated surface waters. In some cases, however, the giant toxic sulfide plume can enter the oxic layer, as happened in January 2009 off the coast of Callao, Peru (Schunck et al. 2013). In severe cases where sulfide permeates the oxygenated surface waters, it can result in mass migrations and die-offs of fish and invertebrates (Copenhagen 1954; Levin et al. 2009), akin to the scene illustrated by Dr. Burt in 1852. Understanding the conditions that promote moderate and severe sulfidic events will help enable their forecasting in the future, and this will be important for managing critically important food stocks. Indeed, the highly productive marine upwelling regions support some 17% of global fish catches (Carr 2001).

Seasonal patterns and controls of upper shelf sulfur cycling

Using a benthic-pelagic model, Dale et al. 2017 estimated that the release of benthic sulfide is triggered when organic matter rain rates generally exceed 20 mmol m⁻² d⁻¹. In addition, the formation of stratified, stagnant bottom waters that aid in drawing down water-column oxygen and nitrate concentrations is another important prerequisite to the release of benthic sulfide (Sommer et al. 2016). A myriad of factors governs water-column anoxia and primary production in upwelling regions, and these factors can vary on local, seasonal and interannual time scales. We briefly explore these factors as well as the frequency of sulfide/sulfur accumulation in upper shelf waters in the AS, ETSP and ETSA regions.

Arabian Sea (West Indian shelf)

The monsoon-driven upwelling AS region, located in the North Indian Ocean, maintains high chlorophyll *a* concentrations in surface waters and a perennial offshore OMZ (Naqvi

et al. 2000, 2006; Jensen et al. 2011). However, the AS shelf off Western India is ventilated by a deep upwelling water mass that maintains low, but persistent O₂ concentrations of ~ 20 μM. Oxygen and nitrate in these nearshore waters become depleted following the heavy rainfall of the summer monsoon. This heavy rainfall induces a fresh/warm water lens overtop of saline/cold upwelled waters, isolating the bottom waters from the coastal upwelling and prompting water-column stratification (Naqvi et al. 2006; Levin et al. 2009). In addition, the monsoon period renews nutrients to the surface waters by vertical mixing, which stimulates a strong increase in surface primary productivity from August to September in the postmonsoon period (Naqvi et al. 2006). The combination of water-column stratification causing the drawdown of oxygen and nitrate, along with enhanced organic matter export, promotes sediment sulfate reduction and the release of benthic sulfide. The accumulation of sulfide in bottom waters has been well documented from ship-based measurements to arise in September–October and dissipates in November (Naqvi et al. 2006; Shenoy et al. 2012). The sulfide plume, at its peak, can span a large section of the West Indian upper shelf (~ 19,000 km²) based on transects made off the coast of Goa to Kochi (Naqvi et al. 2000; Shirodkar et al. 2018). Unfortunately, sulfur plume detection by remote sensing is difficult as a result of the intensive cloud coverage off the West Indian shelf.

The West Indian shelf, in contrast with other marine upwelling regions off the coast of Peru/Chile and Namibia, is arguably one of the most anthropogenically influenced OMZs. This region receives significant monsoonal river runoff from the surrounding agricultural-dominated landscape and major urban environments (Naqvi et al. 2006). The added fertilizer input intensifies coastal eutrophication and contributes to expanding low-oxygen regions (Diaz and Rosenberg 2008). Given the densely populated surroundings, the AS shelf is expected to host larger and more intense sulfidic events in the future as a result of increasing agricultural demands and growing coastal eutrophication.

Eastern tropical South Pacific (Peruvian and Chilean shelf)

In contrast to the AS region, the eastern boundary upwelling in the ETSP and ETSA (Fig. 2A,B) promotes upper shelf anoxia over much broader periods of time. In the ETSP region, the perennial coastal upwelling of nutrient-rich waters sustains some of the highest rates of primary production in the ocean (Carr 2001). The high rates of organic matter export combined with the long water residence time maintain a permanent OMZ (Fuenzalida et al. 2009). Over the upper shelf, the general absence of oxygen (with the exception of El Niño events; Stramma et al. 2016) means that nitrate is the last possible oxidant for microbial sulfide oxidation, and hence, the last barrier to the release of benthic sulfide to the water column.

Nitrate-rich conditions prevail over the ETSP shelf in autumn and winter as a consequence of strong vertical mixing induced by upwelling (Echevin et al. 2008; Dale et al. 2017). In contrast, lower vertical mixing rates and a shift toward nitrate-depleted bottom waters coincides with the spring–summer phytoplankton bloom (Fig. 2C). This same period corresponds with a fivefold increase in the organic matter rain rates to the sediment, from 37 ± 22 to 206 ± 116 mg C m⁻² d⁻¹ from the winter to the summer (Echevin et al. 2008; Dale et al. 2015, 2017). As a result, the eutrophic and anoxic spring–summer period produces an increase in the number of remotely detected sulfur plumes from December to May (Ohde 2018), which is in line with benthic-pelagic models of the ETSP region (Dale et al. 2017). The increase in sulfur plume development in spring–summer is also demarcated by a rise in the number of genes associated with key sulfide-oxidizing bacteria within the SUP05 clade (Fig. 2C) (Léniz et al. 2017). The presence of SUP05 bacteria has served as a marker of sulfidic/anoxic conditions in previous studies (Forth et al. 2015).

Across the ETSP upper shelf, hotspots of sulfide/sulfur accumulation develop off the coast of Peru, from Callao to Pisco, and consistently off the coast of Chile in Concepción Bay (Fig. 2A) (Schunck et al. 2013; Sommer et al. 2016; Callbeck et al. 2018; Ohde 2018). The area from Callao to Pisco (12–15°S) is characterized by diatomaceous, rapidly accumulating muds. These muds are subject to high particulate organic carbon rain rates (over 20 mmol m⁻² d⁻¹) in the austral summer (Dale et al. 2015), and therefore exhibit a high organic carbon content and high rates of sulfate reduction in surface sediments (Böning et al. 2004). Moreover, this area is frequented by wind-driven mesoscale eddies (Chaigneau et al. 2008, 2009, 2013), which enhance anoxia over the upper shelf, resulting in a drawdown of nitrate and the release of benthic sulfide (Sommer et al. 2016; Thomsen et al. 2016b; Callbeck et al. 2018).

In contrast, the upper shelf sediments north of 11°S have lower particulate organic matter rain rates (Dale et al. 2015), and hence, the calcareous mud accumulating here has lower organic carbon concentrations (Suess et al. 1987) and lower rates of sulfate reduction in surface sediments compared to the southern shelf (Böning et al. 2004). While remotely detected sulfur plumes are apparent in the northern ETSP region (Fig. 2A), there are currently no reports of sulfide accumulation verified by ship-based measurements.

Apart from seasonal and local patterns, sulfidic events also exhibit strong intraseasonal and interannual variability driven by remote wind-forcing (Ohde 2018). Wind-driven equatorial Kelvin waves produce nearshore coastal-trapped waves that propagate along the length of the ETSP coastline (Belmadani et al. 2012). Coastal-trapped waves, identified by their distinct anomalies in sea-surface height, have an important influence over the Peru-Chile undercurrent (PCUC). The PCUC is a strong (10–15 cm s⁻¹) subsurface poleward flow that ventilates

the ETSP shelf (Chaigneau et al. 2013). Downwelling coastal trapped waves tend to intensify the nearshore PCUC causing it to broaden in size and increase in velocity up to 30 cm s⁻¹ over a period of 20–80 d (Chaigneau et al. 2013; Pietri et al. 2013). The intensification of the PCUC promotes a deepening of the oxycline enabling greater ventilation and enhanced nitrate concentrations in upper shelf bottom waters (Graco et al. 2017; Espinoza-Morriberón et al. 2019; Lüdke et al. 2019). Oxygenation events, induced by coastal trapped waves, exhibit intraseasonal variability and are often associated with strong El Niño phases (Chaigneau et al. 2013; Pietri et al. 2013; Lüdke et al. 2019). Consequently, the El Niño phase is associated with a complete lack of sulfur plumes, with sulfur plumes then confined to the neutral or La Niña phases (Ohde 2018).

Eastern tropical South Atlantic (Namibian shelf)

Similar to the ETSP region, the ETSA Namibian shelf is characterized by perennial upwelling (Hutchings et al. 2009), which supports high primary productivity in surface waters nearly year-round. The austral summer, however, is associated with especially high surface primary productivity and organic matter export rates to sediments compared to the austral winter (Fig. 2D), which promote active sulfate reduction in upper sediments (Schulz et al. 1999; Brüchert et al. 2003, 2006; Neumann et al. 2016). Over this same period, a more oxygen-poor water mass prevails over the shelf (Monteiro and van der Plas 2006; Monteiro et al. 2008; Ohde and Dadou 2018; Lamont et al. 2019). The combination of high organic matter export from the photic zone during the summer bloom, and the persistence of a more stratified and oxygen depleted water mass over the shelf, contribute to the observed spike in medium to large scale (1500–10,000 km²) sulfur plumes in February–August, spanning from 18°S to 25.5°S (Ohde and Dadou 2018) (Fig. 2B,D). This strong seasonal pattern is also consistent with shipboard and remote sensing-based studies (Weeks et al. 2004; Ohde et al. 2007; Lavik et al. 2009). Furthermore, during the peak sulfur plume season there are reports of mass die-offs of fish and invertebrates related to sulfide toxicity and anoxia (Hamukuaya et al. 1998; Cockcroft 2002; Monteiro et al. 2008).

In contrast, from September to January, only small sulfur plumes are observed of less than 1500 km² (Fig. 2D). This same time period is associated with strong vertical mixing and the presence of distinctly more oxygenated waters over the upper shelf (Monteiro and van der Plas 2006; Ohde et al. 2007; Lavik et al. 2009; Ohde and Dadou 2018). Apart from these seasonal patterns, ETSA coastal-trapped waves further play a role in regulating the intraseasonal activity of sulfur-plume development (Ohde and Dadou 2018). Overall, the spring–summer period of the ETSP and ETSA sustains a broad anoxic window, lasting 180–200 d of the year (with the exception of the El Niño phase), which enables the release of benthic sulfide and the detection of sulfur plumes.

Termination of sulfidic events by a succession of sulfide-oxidizing bacteria

Even though anoxic periods can prevail in spring–summer across large sections of the ETSP/ETSA upper shelf (< 200 m water depth), individual sulfur plumes fluctuate in intensity over a time span of days as a consequence of small-scale hydrodynamic features such as internal waves and mesoscale eddies (Ohde et al. 2007; Lavik et al. 2009; Callbeck et al. 2018, 2019). From our own observations, sulfide-containing bottom waters can rapidly change within a few hours at the same sampling station. Some sulfide-oxidizing nitrate-reducing bacteria employ strategies (e.g., intracellular sulfur storage) to cope with the variable fluxes of reduced sulfur and nitrate, enabling survival over a long period (e.g., *Thioploca* and SUP05 bacteria). Other sulfide-oxidizing bacteria appear to bloom opportunistically on shorter time scales when induced by exceptionally high sulfide (> 10 μM) and organic matter concentrations (e.g., *Arcobacter*). Overall, a diverse microbial community of sulfide/sulfur-oxidizing bacteria is responsible for detoxifying sulfide/sulfur-containing upper shelf OMZ waters.

Benthic sulfide oxidation

The oxidation of benthic sulfide proceeds first near the water–sediment interface where dense mats of giant sulfur bacteria such as *Thioploca* thrive. *Thioploca* bacteria are recognized by their long filamentous sheaths that organize into a trichome bundle (Maier and Gallardo 1984). These sheaths are anchored up to 20 cm deep in the sediment with the top extending a couple of centimeters into the overlying water column (Huettel et al. 1996). Densely packed mats of *Thioploca* have been reported to cover vast sections of the upper shelf across all major OMZs (Fossing et al. 1995; Schulz et al. 1999; Schmaljohann et al. 2001; Gutiérrez et al. 2008; Prokopenko et al. 2013). As a result of the large benthic sulfide flux, upper Peruvian shelf sediments are densely populated by *Thioploca* sp. (Dale et al. 2016; Sommer et al. 2016). Inside their long filamentous sheaths, *Thioploca* filaments migrate between the nitrate-rich overlying waters and the sulfide-rich underlying sediments (Zopfi et al. 2001b). In the presence of high concentrations of sulfide of over 200 μM , *Thioploca* oxidizes sulfide at enhanced rates (6220 $\mu\text{mol S per dm}^3$ cell biovolume per h) and produces elemental sulfur that is then stored in intracellular vacuoles (Huettel et al. 1996; Hogslund et al. 2009) (Fig. 3E). When sulfide concentrations are low, *Thioploca* oxidizes stored intracellular sulfur to sulfate.

The ability of *Thioploca* to balance sulfur oxidation under varying sulfide fluxes is complemented with a capacity to store nitrate, providing added flexibility under nitrate-depleted conditions (Fossing et al. 1995). Another closely related giant sulfur bacterium, *Thiomargarita namibiensis*, is found at the ETSA water–sediment interface. *T. namibiensis*, which is comprised of chains of coccoid cells that are separated by a sheath

(Schulz et al. 1999), exhibits a similar capacity to store intracellular sulfur and nitrate like its sister group *Thioploca* (Schulz et al. 1999; Winkel et al. 2016). Both ETSA-*Thiomargarita* and ETSP-*Thioploca* are, thus, well adapted to the dynamic sulfide and nitrate fluxes in OMZ shelf regions (Thamdrup and Canfield 1996; Ferdelman et al. 1997).

In the sulfide-rich sediments off the coast of Chile, microscopy and metagenomic sequencing has recently identified a novel nonvacuolated filamentous sulfur bacterium, “*Candidatus Venteria ishoeyi*” within the family Thiotrichaceae, a distant relative to *Thioploca* (Fonseca et al. 2017). The draft genome indicates that it contains an abundance of sulfide/sulfur oxidation pathways (Fonseca et al. 2017). However, the prevalence of “*Ca. Venteria ishoeyi*” in the Chilean upper shelf and how it responds to changing sulfide fluxes differently than *Thioploca/Thiomargarita* is not yet clear. Apart from large sulfur bacteria, sulfide-oxidizing microbes within the epsilonproteobacteria and gammaproteobacteria are also likely to contribute to benthic sulfide oxidation (Wasmund et al. 2017). Overall, however, the abundance of giant sulfur bacteria in many of the major OMZs suggests that they play an important role in buffering the release of benthic sulfide, as evidenced by the sulfide deficit in upper sediment pore-water profiles (Schulz et al. 1999; Schmaljohann et al. 2001; Gutiérrez et al. 2008; Prokopenko et al. 2013; Dale et al. 2016).

Sulfide oxidation by blooms of epsilonproteobacteria and gammaproteobacteria

When the benthic sulfide flux exceeds the buffering capacity of giant sulfur bacteria, the release of sulfide into the overlying water column stimulates pelagic blooms of sulfide/sulfur-oxidizing bacteria, that reach up to 10^6 cells mL^{-1} at the nitrate-sulfide chemocline (Lavik et al. 2009; Callbeck et al. 2018, 2019). Under high sulfide concentrations (> 10 μM), the community of pelagic sulfide-oxidizing bacteria is dominated by epsilonproteobacteria within the genera *Arcobacter* and *Sulfurovum* spp. (Grote et al. 2008, 2012; Lavik et al. 2009; Wright et al. 2012; Rodriguez-Mora et al. 2013; Schunck et al. 2013; Forth et al. 2015; Callbeck et al. 2019; Michiels et al. 2019) (Fig. 3F,G).

The genus *Arcobacter*, for example, was shown to dominate the microbial community reaching > 10^6 cells mL^{-1} (or 25% of the total microbial community) when bottom-water sulfide concentrations exceeded 10 μM H_2S (Callbeck et al. 2019). At stations containing lower bottom-water sulfide concentrations (< 10 μM H_2S), *Arcobacter* abundances decreased to < 10^5 cells mL^{-1} , or below 3% of the microbial community. Other studied *Arcobacter* members, have also been shown to tolerate high sulfide concentrations (Sievert et al. 2007). *Arcobacter peruensis*, cultivated from ETSP upper shelf waters, showed a capacity to metabolize sulfide and nitrate while using organic matter (e.g., acetate) for growth (Fig. 3G). The assimilation of acetate into biomass is energetically more favorable than the assimilation of CO_2 via a chemolithoautotrophic metabolism

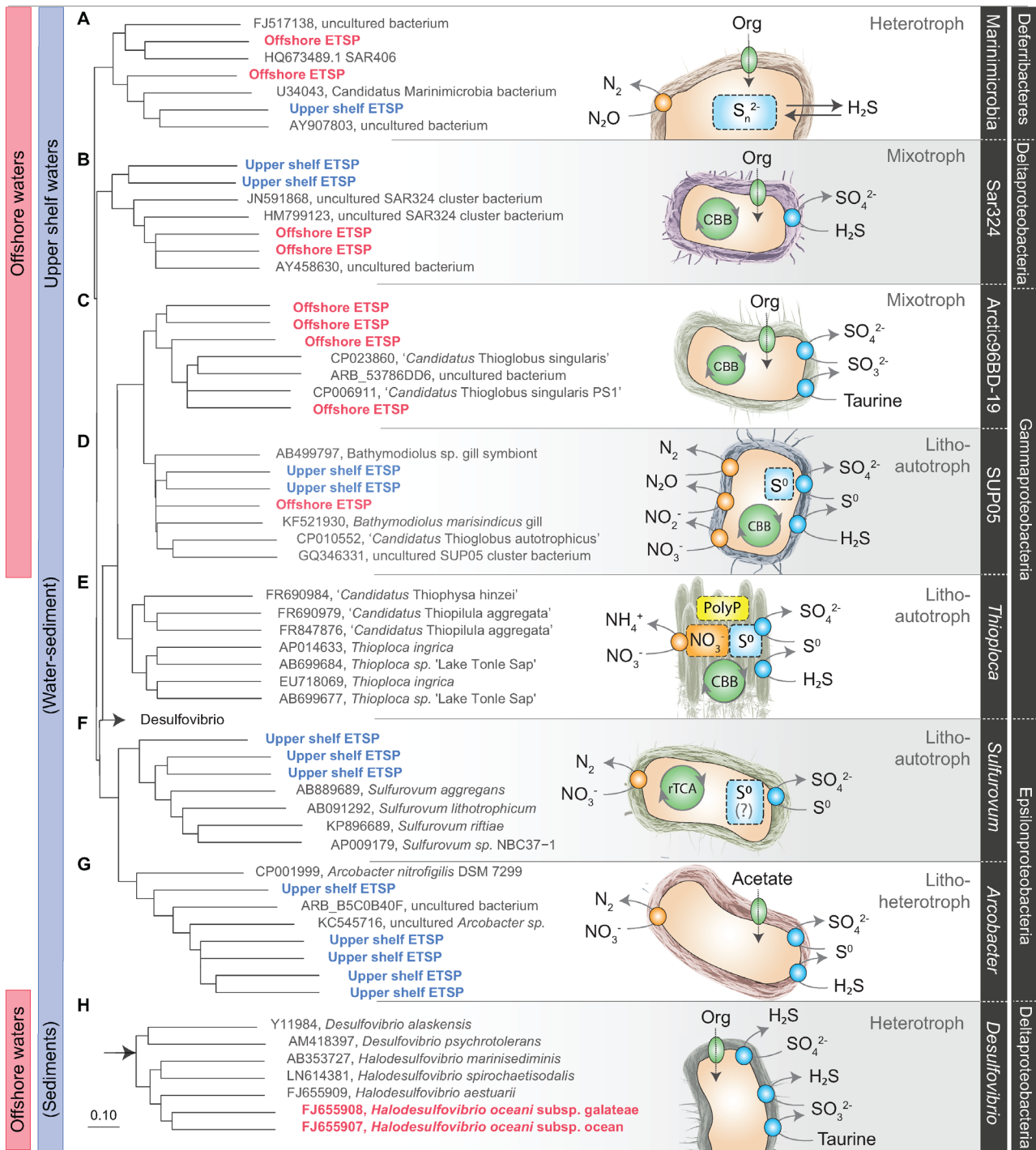


Fig. 3. Ecophysiology and niche partitioning of sulfur-based microbes in OMZs. Phylogenetic diversity of near-full length 16S rRNA genes recovered from waters of the ETSP upper shelf (blue; < 200 m water depth), and the offshore OMZ (red; > 200 m water depth). The ETSP 16S rRNA gene sequences recovered from the upper shelf and offshore region (RV *Meteor* M93 expedition) were previously deposited under the accession numbers MG518493-MG518517 and MH916845-MH916849, see also Callbeck et al. 2018, 2019. The unrooted consensus tree was calculated using the neighbor joining, parsimony, and maximum likelihood methods. The metabolic model of key sulfur-based metabolisms identified are based on ETSP recovered metagenomes, and when available, empirically tested by physiology experiments from ETSP or Saanich Inlet cultivated isolates, described in-text. Shown are pathways related to dissimilatory sulfur and nitrogen transformation processes identified in key sulfur-based microbes in OMZs (oxygen respiration not shown). The microbes with a capacity to store intracellular metabolites such as elemental sulfur/polysulfide (blue), nitrate (orange), and polyphosphate (PolyP; yellow) are shown. Also indicated is the central carbon metabolism (green): Heterotrophy is represented by an abundance of organic matter transport systems and relies on organic matter for assimilable carbon, while a strict autotroph relies on carbon fixation for growth (e.g., by the Calvin-Benson-Bassham (CBB) or reductive tricarboxylic acid (rTCA) cycles) and a mixotroph employs a mixture of both metabolisms.

(Callbeck et al. 2019). The favorable energetics of a chemolithoheterotrophic metabolism explain how *Arcobacter* are able to rapidly bloom in the sulfide- and organic-rich upper shelf waters off the coast of Peru and Namibia (Lavik et al. 2009; Callbeck et al. 2019). Off the coast of Peru, for instance, surface and benthic-influenced bottom waters contain up to 80 to 100 μM of dissolved organic matter (Loginova et al. 2016), which is possibly utilized by *Arcobacter* during a sulfidic event.

Arcobacter also co-occurs with specialist sulfur-oxidizing bacteria that are believed to be supported by the large inventory of elemental sulfur reported in ETSP/ETSA upper shelf waters (Lavik et al. 2009; Callbeck et al. 2018), which can reach up to 7.0×10^8 mol of S^0 (Callbeck et al. 2018). For instance, in the sulfide/sulfur-rich bottom waters off the coast of Peru blooms of epsilonproteobacteria comprised mainly of *Arcobacter* and *Sulfurovum/Sulfurimonas* (Fig. 3F) (Schunck et al. 2013; Callbeck et al. 2019). Other chemocline studies have shown that the latter members are chemolithoautotrophs with a known role in sulfur oxidation. *Sulfurimonas*, for instance, has a capacity to activate cyclooctasulfur (S_8), which could provide an advantage at utilizing elemental sulfur (Pjevac et al. 2014). Some members have a truncated Sox pathway that produces thiosulfate from elemental sulfur oxidation (Lahme et al. 2020). Meier et al. 2017 have additionally shown that *Sulfurovum/Sulfurimonas* have a variable sulfur binding site in the SoxY gene, possibly providing an advantage at responding to changing reduced sulfur fluxes. Single-cell analysis (by nanoSIMS) of ETSP *Arcobacter-Sulfurovum* aggregates found that *Sulfurovum* spp. were highly active with respect to carbon fixation (0.72 fmol C cell⁻¹ d⁻¹), and the cells appeared to be enriched in sulfur, particularly in comparison to *Arcobacter* and SUP05 (Callbeck et al. 2019). Indeed, some members of *Sulfurovum* have been reported to accumulate intracellular sulfur globules (Smith et al. 2017). We therefore suspect that *Sulfurovum/Sulfurimonas*, which compete for produced sulfur, act in consortium with *Arcobacter* to oxidize sulfide/sulfur accumulation in the upper shelf OMZ waters.

When sulfide concentrations fall to < 10 μM in upper shelf waters, the microbial community shifts from epsilonproteobacteria-dominated to a dominance by gammaproteobacteria, mostly within the SUP05 clade (Grote et al. 2008, 2012; Lavik et al. 2009; Wright et al. 2012; Schunck et al. 2013; Hawley et al. 2014; Forth et al. 2015; Callbeck et al. 2018). Key members of the SUP05 clade include “*Candidatus Thioglobus perditus*” (Callbeck et al. 2018), and “*Candidatus Thioglobus autotrophicus*” (Shah and Morris 2015), which have been identified in the ETSP and the seasonally stratified Saanich Inlet, respectively. SUP05 members are predominantly chemolithoautotrophic with a capacity to fix CO_2 via the Calvin–Benson–Bassham pathway, while using either oxidized nitrogen species (e.g., nitrate) or oxygen for respiration (Walsh et al. 2009; Schunck et al. 2013; Hawley et al. 2014; Shah et al. 2016, 2019) (Fig. 3D).

Physiological experiments demonstrate that SUP05 grows best at low sulfide concentrations (< 10 μM), reaching 10^6 cells mL⁻¹, whereas concentrations exceeding this threshold hinder growth (Shah et al. 2019). SUP05 bacteria in the ETSP region have been found to reach 10^6 cells mL⁻¹ at stations with less than 10 μM sulfide (Callbeck et al. 2018, 2019), while in the stratified Black Sea, SUP05 cell abundances show a negative correlation with increasing sulfide concentrations (Glaubitz et al. 2013). Similarly, SUP05 bacteria at hydrothermal vent sites tend to occupy the sulfide-diffuse outer edge where sulfide concentrations are more uniform, while epsilonproteobacteria *Sulfurovum* and *Sulfurimonas* dominate at the sulfide-rich vent inlet (Meier et al. 2017). These studies therefore indicate that SUP05 has an affinity for low sulfide concentrations, especially relative to epsilonproteobacteria.

Furthermore, single-cell analysis indicates that ETSP-SUP05 bacteria, identified off the coast of Peru, have a capacity to store intracellular elemental sulfur (Callbeck et al. 2018; Shah et al. 2019). This conclusion was also supported by the presence of sulfur-storage globule proteins (Sgp) as well as a truncated Sox pathway in recovered SUP05 metagenomes (Walsh et al. 2009; Callbeck et al. 2018; Shah et al. 2019). The truncated Sox pathway, missing the *soxCD* genes, is especially common in microbes that have the capacity to store intracellular sulfur (Dahl et al. 2005; Ghosh and Dam 2009; Walsh et al. 2009). The ability of SUP05 to store intracellular sulfur (Callbeck et al. 2018; Shah et al. 2019), combined with its affinity for low-sulfide concentrations, could explain how they are able to persist throughout the spring–summer anoxic period in the ETSP region (Léniz et al. 2017) (Fig. 2C), and even when dissolved sulfide is absent (Crowe et al. 2018).

Sulfide/sulfur metabolizing microbes of growing interest

Another microbe group that may contribute to the transformation of sulfur in OMZ settings is Marinimicrobia, previously known as SAR406, or Marine Group A. While various Marinimicrobia clades exist, spanning different redox conditions (Hawley et al. 2017), some members thrive in the sulfide/sulfur-rich bottom waters of OMZs (Schunck et al. 2013; Bertagnolli et al. 2017; Hawley et al. 2017; Plominsky et al. 2018; Callbeck et al. 2019). Recovered genomes of Marinimicrobia encode a polysulfide reductase that may be involved in either sulfur oxidation or polysulfide/sulfur reduction to sulfide (Wright et al. 2014; Bertagnolli et al. 2017; Hawley et al. 2017; Thrash et al. 2017) (Fig. 3A). In this regard, Hawley et al. 2017 found that polysulfide reductase (*psrABC*) was up-regulated in waters containing low nitrate and sulfide (Hawley et al. 2017). Whether the polysulfide reductase recovered in Marinimicrobia serves an oxidative or reductive role in the transformation of sulfur is still ambiguous. Nevertheless, Marinimicrobia has a putative role in the transformation of sulfur and sulfur-polysulfides in upper shelf OMZ waters and in stratified basins.

Some unexpected sulfide-oxidizing candidates have also been identified in recent years in OMZs. *Nitrococcus*, is an abundant nitrite-oxidizing bacteria in some OMZs (Füssel et al. 2012, 2017). A study of ETSA *Nitrococcus* found genes encoding for the sulfide/quinone oxidoreductase *sqr* (Füssel et al. 2017), which is responsible for oxidizing sulfide to elemental sulfur or polysulfide (Frigaard and Dahl 2008; Ghosh and Dam 2009). In line with its genomic capacity for sulfide oxidation, the ETSA *Nitrococcus* cell abundances peaked in the anoxic bottom waters near the sulfide-rich sediments. These cells were also shown to be enriched in sulfur (Füssel et al. 2017). Füssel (2017) further demonstrated that *N. mobilis*, a closely related type-strain to the ETSA *Nitrococcus*, was able to oxidize sulfide in laboratory experiments, raising the possibility that *Nitrococcus* has an alternative mode of growth involving the sulfur cycle. Another study of sulfide-rich Peruvian shelf waters recovered a novel heterotrophic N₂-fixing diazotroph within the *Roseobacter* group that has a genomic capacity to oxidize sulfide (Martínez-Pérez et al. 2018). Together, these studies highlight that sulfide oxidation possibly extends to phyla other than epsilon- and gammaproteobacteria, widening the diversity of sulfide-oxidizing bacteria in OMZ shelf waters.

Anoxygenic photosynthesis

The nitrate-sulfide chemocline could additionally support anoxygenic photosynthesis by anaerobic green- and purple-sulfur bacteria. For instance, in permanently stratified basins and freshwater lakes, with sufficient light penetration, anoxygenic photosynthesis contributes substantially to the oxidation of sulfide in the chemoclines (Overmann and Manske 2006). In the chemocline of the Black Sea, the anoxic chlorophyll maximum is dominated by the green sulfur bacteria, *Chlorobium*. *Chlorobium* has a special capacity to grow under extremely low-light conditions ($0.001 \mu\text{mol photons m}^{-2} \text{s}^{-1}$) oxidizing sulfide while generating elemental sulfur, otherwise known as anoxygenic photosynthesis (Overmann and Manske 2006; Marschall et al. 2010).

In the ETSP region, a functional and phylogenetic gene survey have identified green sulfur bacteria closely affiliated to *Chlorobium limicola* and *Chlorobium tepidum* (Stewart 2011). In the sulfide-rich upper shelf waters off the coast of Peru, recent work has also identified sequences belonging to *Chlorobium* (Christiansen and Löscher 2019; Preprint), and the presence of a small anoxic chlorophyll maximum (Schunck et al. 2013). To the best of our knowledge, these studies are the first to identify green sulfur bacteria in the modern OMZ, albeit, in situ evidence of active anoxygenic photosynthesis by green sulfur bacteria is still needed. In the Proterozoic ocean (ca. 2400 million years ago), the once sulfide-rich bottom waters were hypothesized to have supported widespread anoxygenic photosynthesis (Johnston et al. 2009). If anoxygenic photosynthesis is active in today's modern OMZ, then these sulfide-rich upper shelf waters could serve as an important model ecosystem for the past ancient ocean.

Sulfur disproportionation

Organisms disproportionating sulfur compounds might also occupy the OMZ chemocline. Sulfur compound disproportionation catalyzes the inorganic “fermentation” of intermediate sulfur compounds to produce sulfide and sulfate (Finster 2011). Specifically, inorganic sulfur compounds such as elemental sulfur, thiosulfate and sulfite act as both the electron acceptor and electron donor, with concentrations of these intermediates peaking in the ETSP OMZ chemocline (Callbeck et al. 2018). Known thiosulfate disproportionating bacteria of the genus *Desulfocapsa* have been identified in the chemocline of some stratified basins (Finster 2011; Forth et al. 2015). Moreover, natural abundance sulfur isotope signatures indicate that disproportionation is active in the chemoclines of some permanent and seasonally stratified basins (Neretin et al. 2003; Sørensen and Canfield 2004). In OMZs, it remains unknown whether sulfur-compound disproportionation is a significant process contributing to the turnover of elemental sulfur, thiosulfate, and sulfide. One difficulty in identifying this sulfur compound disproportionation is that the genes involved are largely indistinguishable from those required for sulfate reduction (Finster 2011). We hypothesize that because the thermodynamics of disproportionation are near the energetic limit ($\Delta G' = -30$ to -44 kJ mol^{-1} ; Table 1), this mode of growth is difficult to sustain due to the episodic nature of the reduced sulfur fluxes in OMZ upper shelf waters.

Virus–microbe interactions influence sulfidic event termination

Once the flux of benthic sulfide subsides, the blooms of sulfide-oxidizing bacteria in upper shelf waters are likely to decline in size. In addition to sulfide availability, virus–microbe interactions might also moderate bloom termination. A record of microbe–virus interactions can be assessed from metagenomic surveys and from single-cell genomic sequencing (Cassman et al. 2012; Roux et al. 2014). In Saanich Inlet, which experiences seasonal anoxic/sulfidic conditions, nearly one-third of SUP05 cells identified were infected by the viruses: *Caudovirales* (common to marine environments), and *Microviridae* (exclusive to a SUP05 subclade) (Roux et al. 2014). The clonality of recovered *Microviridae* sequences, and the augmented infection rate, suggested that the virus–host interaction is an important mechanism regulating the SUP05 bloom (Roux et al. 2014). In addition, the acquisition of *Dsr* genes by the virus, and its hijacking of the host's metabolic system, could potentially trigger the host to accelerate sulfur oxidation. A broader analysis of OMZ viral populations, indeed, finds a number of viromes with *sox* and *dsr* genes, as well as genes involved in assimilatory sulfate reduction, inorganic sulfur metabolism and dimethylsulfoniopropionate degradation (Cassman et al. 2012; Roux et al. 2014, 2016). This growing body of work indicates that viruses shape the flow of sulfur-based genes in the OMZ possibly contributing to the metabolic flexibility of some sulfur-based microbes.

Offshore OMZ sulfur cycle

Aside from active sulfur cycling in benthic influenced coastal OMZ waters, biogeochemical and metagenomic evidence indicates that a sulfur cycle exists in the nitrate-rich offshore waters of the ETSP region detached from benthic processes (Canfield et al. 2010). With increasing distance from the eutrophic upper shelf, the OMZ becomes further disconnected from the vertical benthic fluxes of sulfide, ammonium, and iron; with fluxes being largely negligible at stations over 200 m water depth (Bohlen et al. 2011; Sommer et al. 2016; Schlosser et al. 2018). Even though dissolved sulfide does not accumulate in these waters, sulfide amendment experiments with waters collected from the offshore OMZ find high, but, variable rates of sulfide oxidation ranging from 2.4 to 22 nmol S L⁻¹ d⁻¹, suggesting that sulfide-oxidizing bacteria, such as SUP05 bacteria, are present and possibly active in these offshore OMZ waters (Canfield et al. 2010). Congruently, sequences affiliated to the SUP05 cluster is one of the most consistently identified taxon, with a sulfur-based metabolism, in the offshore ETSP region and in other OMZs void of sulfide (Fuchs et al. 2005; Stevens and Ulloa 2008; Canfield et al. 2010; Stewart et al. 2012; Wright et al. 2012; Carolan and Beman 2015; Bristow et al. 2017; Callbeck et al. 2018). However, unlike in sulfidic shelf waters where SUP05 bacteria can make up 50% of the microbial community, SUP05-affiliated genes persist outside of sulfidic waters at low to moderate abundances (Fuchs et al. 2005; Stevens and Ulloa 2008; Canfield et al. 2010; Carolan and Beman 2015; Bristow et al. 2017) with SUP05 cell densities comprising between 0% and 17% of the microbial community (Callbeck et al. 2018). In addition, active expression of *rdsr* genes, putatively involved in the oxidation of sulfide, has been reported in the core of the ETSP and ETNP, with most genes being affiliated to SUP05 bacteria (Stewart et al. 2012; Carolan and Beman 2015).

Other clades with a putative role in offshore sulfur and nitrogen transformation include Marinimicrobia (Marine Group A/ Sar406), which is also abundant in sulfidic shelf waters (Wright et al. 2012; Hawley et al. 2017). The persistent and widespread distribution of Marinimicrobia and SUP05 contrasts with other sulfide-oxidizing bacteria. For instance, ETSP *Arcobacter* and *Sulfurovum* are more restricted to the upper shelf, and thereby more dependent on the benthic fluxes of sulfide and sulfur (Callbeck et al. 2018, 2019). Whereas the widespread distribution of SUP05 implies that it has a more versatile ecophysiology, which is less reliant on the benthic sulfide flux (Walsh et al. 2009; Shah et al. 2019).

Sulfate-reducing bacteria have been identified from functional and phylogenetic gene marker surveys in ETSP offshore waters including *Desulfobacca*, *Desulfatibacillum*, *Desulfobacterium*, *Desulfococcus*, and *Syntrophobacter* species (Canfield et al. 2010; Stewart et al. 2012). Moreover, two novel sulfate-reducing bacteria strains within *Desulfovibrio oceani* have been isolated from

offshore OMZ waters off the Peruvian coast (Finster and Kjeldsen 2010). Rates of sulfate reduction have been measured in offshore OMZ waters ranging from 1.3 to 12.0 nmol L⁻¹ d⁻¹ at two stations off the coast of Chile (Canfield et al. 2010). Time-integrated indicators of sulfate reduction have been studied in an attempt to quantify rates of sulfate reduction in the offshore OMZ. Sulfate reduction imparts natural abundance isotope signatures of sulfur (³³S/³²S, ³⁴S/³²S) and oxygen (¹⁸O/¹⁶O), and the isotope composition of sulfate was analyzed to constrain dissimilatory sulfate reduction processes in anoxic waters collected in the ETSP region (Johnston et al. 2014). However, no clear signature of water-column sulfur cycling was observed, in that, the ETSP collected samples were isotopically comparable to the global mean. The lack of a signature in ETSP waters does not necessarily contradict a sulfur cycle operating in offshore waters, as observed experimentally, because the time-integrated maximum rates of sulfate reduction as constrained by the ¹⁸O sulfate data (6.4–64 nmol L⁻¹ d⁻¹ depending on the assumed water residence time) were at or above the mean rate directly measured by Canfield et al. (2010). This demonstrates that the ¹⁸O sulfate method is not yet sensitive enough to capture the ETSP sulfur cycle.

An ETSP model with an implemented nitrogen–sulfur cycling component predicts that organic matter export rates are sufficient to sustain sulfate reduction activity throughout the OMZ (Azhar et al. 2014). Azhar et al. (2014) estimated that depth-integrated sulfate reduction could amount to 0.36 mmol m⁻² d⁻¹ based on the given chemistry and organic matter input, which was in good agreement with measured rates of 0.28–1.00 mmol m⁻² d⁻¹ (Canfield et al. 2010).

Role of microniches and lateral transport processes

How a sulfur cycle occurs in the open ocean ETSP region under nitrate-rich conditions is ambiguous, as sulfate reduction should be outcompeted by nitrate reduction based on energetic considerations. One hypothesis is that the microbes that carry out sulfate reduction and sulfide oxidation are housed within marine snow aggregates (Fig. 5) (Wright et al. 2012). Such aggregates would theoretically act as both a source of organic matter and a substrate for attachment (Karl et al. 1984; Alldredge and Cohen 1987; Woeckel et al. 2007), and nitrate could potentially be depleted internally due to a diffusional limitation (Stief et al. 2016). A model simulation of particle sinking in the ETSP predicts that sulfate reduction could develop in the particle core of both small (< 100 μm) and large (> 0.5 mm) diameter aggregates (Bianchi et al. 2018). Furthermore, larger sinking particles (> 0.5 mm) may even develop anoxic microenvironments in oxic waters above and below the OMZ (Bianchi et al. 2018).

Size fractionation studies have demonstrated that SUP05 has an affinity for growth in association with aggregates (Fuchsman et al. 2011; Ganesh et al. 2014). Microscopy analysis has found both SUP05 bacteria and sulfate-reducing bacteria in close spatial association inside aggregates at both an

offshore and upper shelf ETSP station (Callbeck et al. 2018). Albeit, the offshore station located 70 km from the coast was influenced by cross-shelf transport as discussed below. These in situ observations, in combination with a particle model (Bianchi et al. 2018), suggest that sulfur cycling could be feasibly housed in aggregate microniches. Inside the sinking particle the diffusion of ambient nitrate into the aggregate is likely consumed by sulfide-oxidizing nitrate-reducing bacteria. Subsequently, the nitrate void particle core, in combination with organic matter promotes sulfate reduction, generating a sulfide gradient that drives sulfide-oxidizing bacteria. This microstructuring of the sulfur cycling community does, however, require further validation by state-of-the-art particle embedding techniques combined with confocal laser scanning microscopy (Lukumbuza et al. 2019).

The offshore OMZ sulfur cycle can also be sustained by lateral transport processes from the coast. Previous studies have shown that cross-shelf transport induced by mesoscale eddies is a prevalent phenomenon in OMZs that contributes to the long-range transport of chlorophyll, nutrients, and trace metals, such as iron, from the coast into the open ocean (Gruber et al. 2011; Kondo and Moffett 2015; Nagai et al. 2015; Thomsen et al. 2016b). Mesoscale eddies are known to propagate in shelf waters adjacent to areas of active benthic-pelagic sulfur cycling (Chaigneau et al. 2008, 2009). Despite the absence of dissolved sulfide, recent evidence indicates that the offshore OMZ receives a large inflow of cross-shelf transported elemental sulfur, which forms at the chemocline in a sulfidic event (Callbeck et al. 2018). Cross-shelf transported elemental sulfur can also be observed in remote sensing images in both the ETSP and ETSA regions (Weeks et al. 2002, 2004; Ohde et al. 2007; Ohde 2018; Ohde and Dadou 2018) (e.g., Fig. 2A,B).

An analysis of an offshore advected sulfur-rich water mass demonstrated abundant and active SUP05 bacteria that were enriched in intracellular sulfur and fixed CO₂ into biomass. While outside of the advected plume, SUP05 abundances were markedly lower, and cells contained less sulfur with lower rates of CO₂ assimilation (Callbeck et al. 2018). This contrast at two offshore stations suggested that SUP05 remain active in waters transported offshore from coastal sulfidic events, and are able to sustain their activity by utilizing intracellular and/or co-transported elemental sulfur (Callbeck et al. 2018). Thus, the ETSP-SUP05 bacteria appear to be well adapted to thrive at low-sulfide/sulfur concentrations (Callbeck et al. 2018), which is consistent with the high-affinity sulfide oxidation rates reported in the ETSP region (Crowe et al. 2018), and in line with the eco-physiology of the cultivated SUP05 isolate (Shah et al. 2019).

Cross-shelf transport may additionally contribute the redistribution of coastal particles into the open ocean (Thomsen et al. 2016a). Given the potential for particles to host anoxic microniches (Bianchi et al. 2018), sulfate reduction might be active in advected particles, which could partly account for active sulfate reduction in offshore OMZ waters, but this requires further examination.

The biogeochemical implications of the sulfur cycle on other linked cycles

The transformation of inorganic sulfur, via the reductive and oxidative branches of the sulfur cycle, exerts an important influence over other element cycles including nitrogen, carbon, and phosphorus. We explore the effects of sulfur cycling on these various linked cycles both when sulfide accumulates in upper shelf bottom waters (Fig. 4B), and when water-column sulfide is absent following a sulfidic event (Fig. 4A). In addition, we highlight key sulfur-based microbes that mediate the turnover of nitrogen, carbon and phosphorus. In the last section, we examine the biogeochemical implications of the offshore sulfur cycle and its heterogenous distribution in the OMZ.

N₂, NO₂⁻, and N₂O production

In the OMZ, nitrate is the primary oxidant for reduced sulfur species, and thereby sulfide-/sulfur-oxidizing bacteria contribute directly to the removal of fixed nitrogen via sulfide-/sulfur-dependent denitrification (Figs. 4A,B, 5). Like heterotrophic denitrification, sulfide-dependent denitrification is the stepwise reduction of nitrate to N₂ via intermediates NO₂⁻, NO, and N₂O.

During a sulfidic event (Fig. 4B), the nitrate-sulfide interface in upper shelf OMZ waters supports some of the highest rates of denitrification in marine environments, with maximum rates ranging between 500 and 2500 nmol N L⁻¹ d⁻¹ for moderately sized sulfidic events (~ 10 μM H₂S), with exceptionally high rates of 6500 nmol N L⁻¹ d⁻¹ when sulfide exceeds 20 μM (Kalvelage et al. 2013; Schunck et al. 2013; Galán et al. 2014; Callbeck et al. 2018, 2019). The measured rates of sulfide-driven denitrification in the ETSP region are markedly higher than the maximum rates of anammox reported in the same waters of 8–250 nmol N L⁻¹ d⁻¹ (Kalvelage et al. 2013; Schunck et al. 2013; Galán et al. 2014; Callbeck et al. 2018). In the sulfide-rich bottom waters of the Saanich Inlet, rates of denitrification up to 3360 nmol N L⁻¹ d⁻¹ were observed, which also surpassed rates of anammox (Michiels et al. 2019). In the ETSP region, sulfide-driven denitrification over the shelf off central Chile (~ 4500 km², sulfidic for 200 d) contributes to as much as 0.5 Tg N yr⁻¹ (Galán et al. 2014). Likewise, sulfide-driven denitrification off the coast of Callao-Pisco is estimated to contribute to 0.3 Tg N yr⁻¹ (~ 5500 km², sulfidic for 180 d; Callbeck et al. 2018, 2019). Together, these ETSP-denitrification hotspots total a production of 0.8 Tg N yr⁻¹, which is substantial considering that nitrogen loss by anammox—a key pathway contributing to fixed nitrogen removal in OMZs—is estimated at 3.1 Tg N yr⁻¹ in ETSP shelf waters (Kalvelage et al. 2013). Given the numerous other sulfur plumes identified in ETSP waters (Fig. 2A), it is probable that sulfide-/sulfur-driven denitrification contributes to even greater nitrogen loss.

Nitrite, a substrate required by anammox bacteria, can also be supplied by sulfide-dependent nitrate reduction to nitrite.

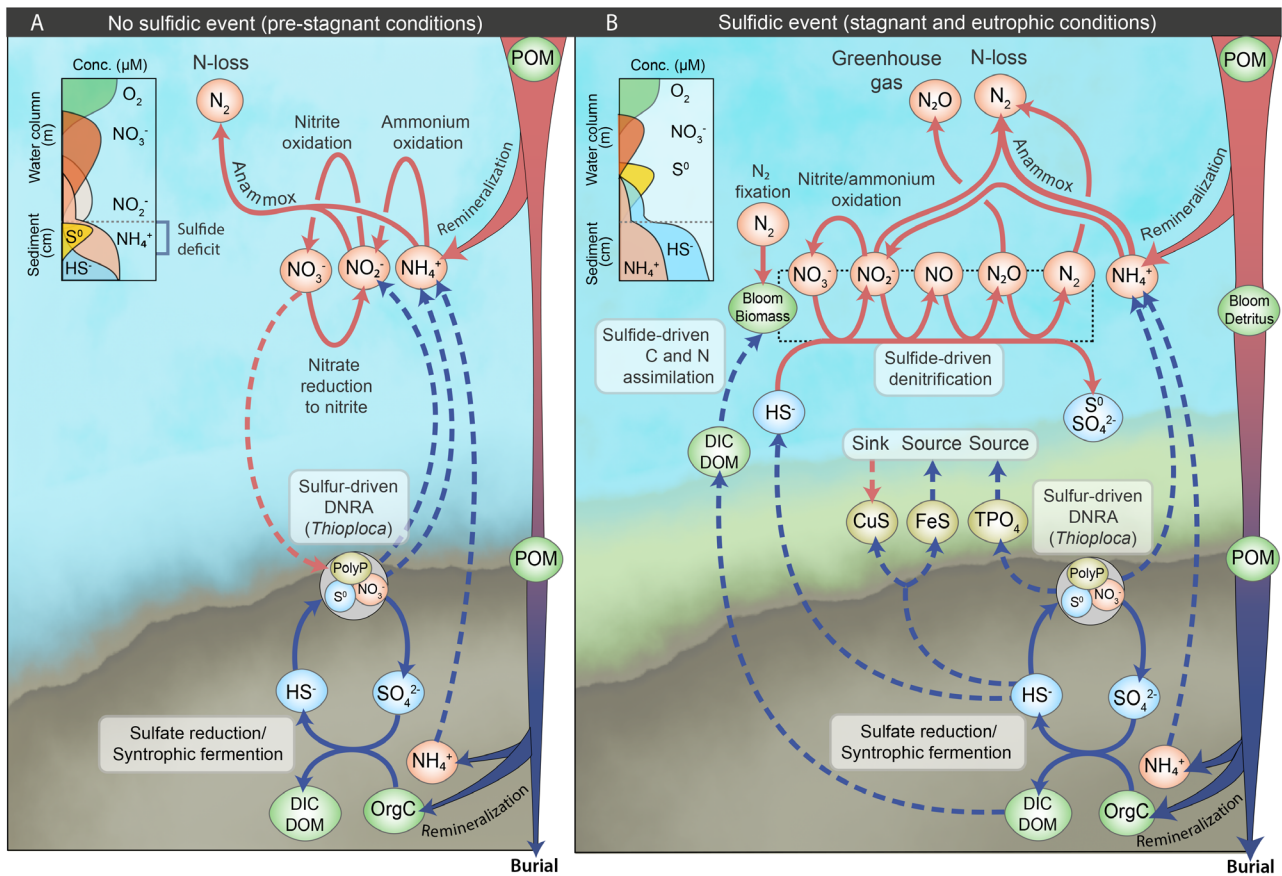


Fig. 4. The upper shelf OMZ sulfur cycle (< 200 m water depth) and its tight coupling with nitrogen, carbon and phosphorous cycling, including its influence on trace metal mineralogy. The schematic model is based on findings reported in previous studies, the values and data pertaining to the schematics and major themes are discussed in-text. Two contrasting upper shelf OMZ scenarios are shown: **(A)** no H_2S bottom waters where nitrate is replenished to the upper shelf (Kuypers et al. 2005; Lam et al. 2009; Bohlen et al. 2011; Noffke et al. 2012; Kalvelage et al. 2013; Dale et al. 2015, 2016, 2017; Füssel et al. 2017); and scenario **(B)** which is characterized by the accumulation of H_2S in bottom waters (Lavik et al. 2009; Schunck et al. 2013; Galán et al. 2014; Dale et al. 2015, 2016; Lomnitz et al. 2016; Sommer et al. 2016; Callbeck et al. 2018, 2019; Schlosser et al. 2018). The yellow-green color in panel **B** represents the accumulation of elemental sulfur, which is generated from the oxidation of sulfide. At the nitrate-sulfide chemocline, benthic released sulfide is oxidized by sulfide-oxidizing nitrate-reducing bacteria (dotted rectangular box), which use dissolved inorganic and organic carbon for growth, otherwise known as chemolithoautotrophy and chemolithoheterotrophy, respectively. If green sulfur bacteria, such as *Chlorobium*, are present at the nitrate-sulfide chemocline, they may contribute to nitrogen fixation, via anoxygenic photosynthesis (Christiansen and Löscher 2019). Solid arrows colored in red and blue indicate processes occurring in the bottom waters and in the sediments, respectively. Dotted colored lines represent water-sediment fluxes. The color of the circles corresponds to different nutrient and chemical compounds involving sulfur (blue), nitrogen (orange), carbon (green), phosphorous and metal-sulfides (yellow). Abbreviations stand for: POM, particulate organic matter; DIC, dissolved inorganic carbon; DOM, dissolved organic matter; TPO₄, total dissolved phosphate; PolyP, polyphosphate; DNRA, dissimilatory nitrate reduction to ammonium.

In sulfide containing co-culture experiments, with anammox and a autotrophic denitrifier (*Sulfurimonas denitrificans*), the sulfide-oxidizing bacteria generated up to 65–75% of the nitrite requirements of anammox (Russ et al. 2014). Furthermore, microbial community models of OMZs have predicted that sulfide-driven nitrate reduction to nitrite is tightly coupled with anammox to produce N_2 gas (Louca et al. 2016; Hawley et al. 2017; Michiels et al. 2019). In the ETSP region, rates of sulfide-driven nitrate reduction to nitrite have been measured from 100 to 2500 $nmol\ N\ L^{-1}\ d^{-1}$. These rates greatly exceed the rates of nitrate reduction to nitrite of 80–250 $nmol\ N\ L^{-1}\ d^{-1}$ at stations outside of the sulfide plume (Kalvelage et al. 2013). If the full size and frequency of the ETSP sulfur plumes

are considered (Fig. 2), sulfide-driven nitrate reduction to nitrite in the ETSP upper shelf could offer a substantial supply of nitrite for anammox.

Sulfide-driven denitrification might also be responsible for the accumulation of N_2O in OMZ shelf regions (Naqvi et al. 2000, 2006; Arevalo-Martinez et al. 2015; Kock et al. 2016; Bourbonnais et al. 2017; Arévalo-Martínez et al. 2019). Interestingly, N_2O production was shown to increase with increasing organic matter input (Frey et al. 2020), which is a key prerequisite to the formation of a sulfidic event. Moreover, in the AS upper shelf, N_2O production was shown to be linked to a transition to water-column anoxia, and eventually the accumulation of bottom water sulfide (Naqvi et al. 2000, 2006). In

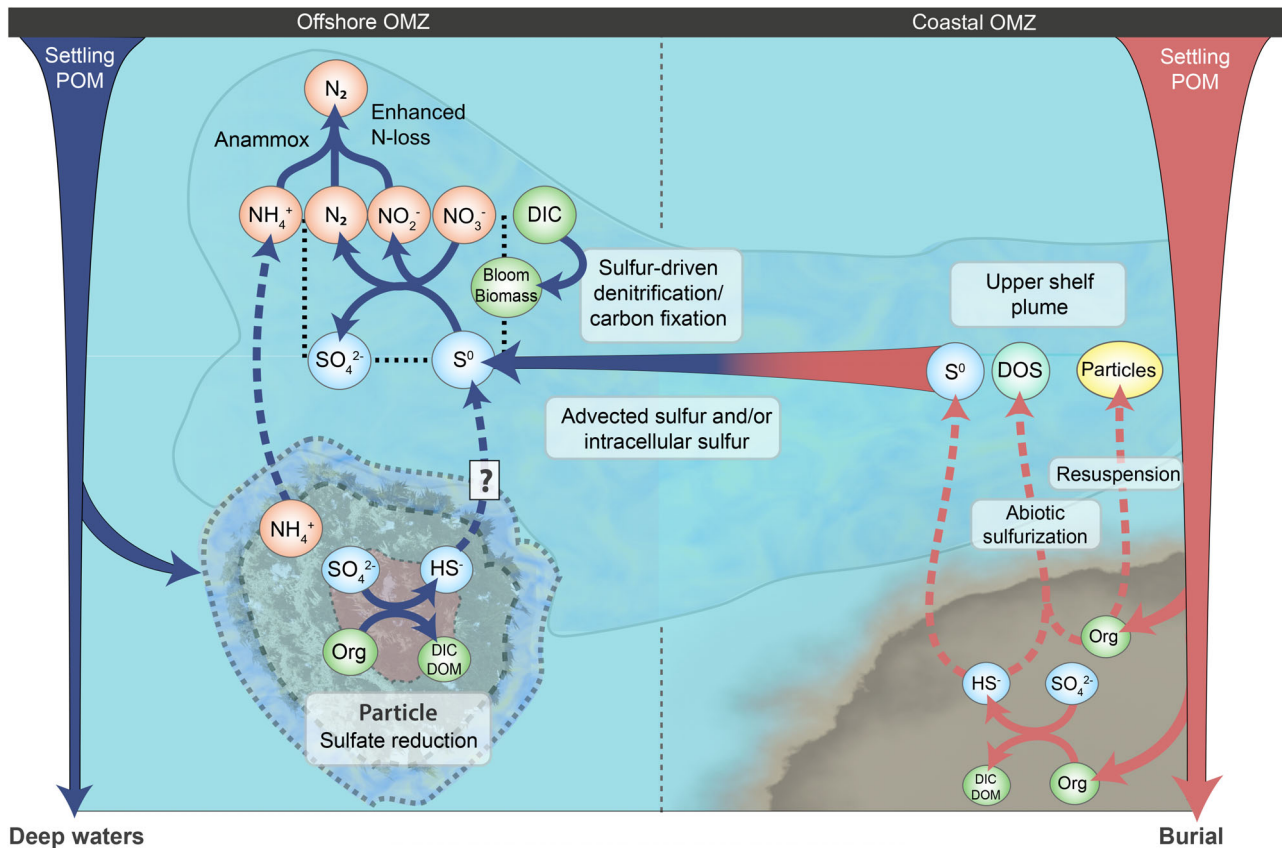


Fig. 5. Lateral transport of elemental sulfur and particle microniches sustain the offshore OMZ sulfur cycle (> 200 m water depth). The schematic represents a synthesis of work discussed in text (Canfield et al. 2010; Bianchi et al. 2018; Callbeck et al. 2018). The sulfide-oxidizing nitrate-reducing SUP05 bacteria are a key catalyst in the offshore sulfur cycle. In the ETSP region, SUP05 cells can be transported from the upper shelf into the offshore OMZ, where they may metabolize advected or intracellular sulfur, driving nitrogen loss, nitrate reduction to nitrite and carbon fixation (dotted rectangular box). SUP05 may also be attached to particles along with other sulfate-reducing bacteria (Callbeck et al. 2018). Note that the sinking particle is not to scale and is exaggerated for illustration purposes. In the environment, particles can range in size from 10 μm to 5 mm in diameter; models predict that both small (< 100 μm) and large (> 0.5 mm) particles sinking in the OMZ can form zones of sulfate reduction in the aggregate core (Bianchi et al. 2018). Solid arrows colored in red and blue indicate processes occurring in the coastal and offshore OMZ, respectively. Dotted colored lines represent water-sediment or water-particle fluxes. The color of the circles corresponds to different nutrient and chemical compounds involving sulfur (blue), nitrogen (orange), carbon and dissolved organic sulfur (green-blue). DIC, dissolved inorganic carbon; DOM, dissolved organic matter; DOS, dissolved organic sulfur; POM, particulate organic matter.

these waters, N_2O accumulated up to 90 nM just above the sulfide plume, near the nitrate-sulfide chemocline (Naqvi et al. 2000). In the ETSP upper shelf, N_2O concentrations were reported to increase, reaching a maxima of 35 nM in the sulfide-rich bottom waters (Schunck et al. 2013). A number of in situ incubation experiments suggest that ETSP sulfide-oxidizing bacteria may contribute to this N_2O production (Canfield et al. 2010; Dalsgaard et al. 2014; Galán et al. 2014). For example, Dalsgaard et al. 2014 showed that the addition of sulfide (1 μM) to incubation experiments with ETSP waters caused an increase in net N_2O production by more than 4.5-fold (up to $\sim 120 \text{ nmol L}^{-1} \text{ d}^{-1}$) relative to nonsulfide amended experiments. Galán et al. 2014 performed similar experiments, except with 5 μM sulfide, and observed a net N_2O production of 12–29 $\text{nmol L}^{-1} \text{ d}^{-1}$, with no N_2O production observed in sulfide-free controls. In other stratified basins,

studies have reported intensive N_2O production at the nitrate-sulfide interface, where rates of N_2O production were similar to rates of nitrate reduction to N_2 (Bonaglia et al. 2016).

Key microbial denitrifiers

Pelagic denitrifying blooms of epsilonproteobacteria and gammaproteobacteria, which comprise of SUP05, *Arcobacter* and *Sulfurovum/Sulfurimonas* are likely candidates that mediate sulfide-driven nitrate reduction to NO_2^- , N_2O , and N_2 . *A. peruensis*, isolated from the ETSP region, contains not only a complete set of denitrification genes, but was further shown to produce N_2 in physiology experiments amended with sulfide, nitrate and organic matter (Callbeck et al. 2019). In addition, *A. peruensis*, was shown to produce nitrite either transiently or as an end-product of nitrate reduction. For instance, when organic matter was limiting, incomplete

nitrate reduction producing nitrite was observed, suggesting that the fate of nitrate reduction was moderated by the availability of organic matter.

The ETSP sulfide-nitrate chemocline exhibits active expression of the nitrate reductase gene, most of which are affiliated to the SUP05 bacteria, suggesting that this group also plays a considerable role in regulating the fate of nitrate (Schunck et al. 2013; Léniz et al. 2017). Whether nitrate is reduced to N_2 , or produces nitrite or N_2O as an end-product, depends on the SUP05 member. For instance, the recovered metagenome of SUP05 bacteria in ETSP waters contains a capacity for sulfide oxidation coupled to complete nitrate reduction to N_2 (Callbeck et al. 2018). While a Saanich Inlet recovered SUP05 metagenome was shown to lack the gene (*nosZ*) necessary for N_2O reduction to N_2 (Walsh et al. 2009), and was also missing the gene involved in nitrite reduction to NO, generating nitrite in laboratory culture experiments (Shah et al. 2016). Alternatively, the Saanich Inlet SUP05 works in consortium with Marinimicrobia to catalyze the last step of N_2O reduction to N_2 (Hawley et al. 2017), possibly contributing to the elevated rates of N_2 production in these sulfide-rich waters (Michiels et al. 2019). Whether the same SUP05-Marinimicrobia interaction is active in ETSP waters, given that ETSP-SUP05 has a capacity for complete denitrification, is unclear.

What ultimately controls the fate of nitrate, and its channeling to end products NO_2^- , N_2O , and N_2 by pelagic SUP05 and *Arcobacter*, thus, appears to be dictated by a few factors: (1) species heterogeneity (e.g., ETSP-SUP05 vs Saanich Inlet SUP05), (2) the coupling of sulfide-oxidizing bacteria with other microbial groups (SUP05-Marinimicrobia), and (3) the availability of certain requisite substrates, such as sulfide and organic matter. These three factors, in addition to the abiotic interaction of sulfide with trace metals that influence the metalloenzymes of denitrification (discussed below), are all possible controls of sulfide-driven denitrification.

NH_4^+ production

Ammonium, another important substrate required by anammox bacteria, can be jointly supplied by benthic sulfate-reducing and sulfide-oxidizing bacteria. The high surface organic matter export rates that promote a sulfidic event (Fig. 2C,D), also enhance benthic sulfate reduction that in consortium with fermenting bacteria, drives organic matter remineralization and the release of benthic ammonium to the water column. Moreover, the enhanced sulfide production in sediments promotes the activity of giant sulfur bacteria *Thioploca* and *Thiomargarita*, which reduce the nitrate stored in their vacuoles to ammonium via DNRA (Fossing et al. 1995; Otte et al. 1999; Schulz et al. 1999). By utilizing the nitrate stored in their vacuoles, DNRA activity by *Thioploca* can be sustained for weeks during prolonged periods of bottom-water anoxia when water-column nitrate is absent during a sulfidic event (Dale et al. 2016). Estimates indicate that sulfide-driven DNRA activity by giant sulfur bacteria can

contribute up to 63% of the benthic ammonium flux. The remainder of the flux is generally ascribed to ammonification by the activities of sulfate-reducing bacteria, acting in consortium with fermenting bacteria (Sommer et al. 2016).

The combined activities of sulfate reduction and sulfide-driven DNRA during a sulfidic event result in high benthic fluxes of ammonium. Measured fluxes can range from 1.5 to 21.2 $mmol NH_4^+ m^{-2} d^{-1}$ with the higher values occurring at shallow stations less than 100 m water depth (Sommer et al. 2016). By comparison, fluxes reported across a similar transect with no apparent sulfide accumulation were between 3.5 and 4.0 $mmol m^{-2} d^{-1}$, suggesting that sulfidic events can enhance the benthic ammonium flux (Bohlen et al. 2011; Sommer et al. 2016). Congruently, elevated ammonium concentrations of 5–10 μM have been reported in sulfide-rich bottom waters (Naqvi et al. 2000; Lavik et al. 2009; Schunck et al. 2013; Callbeck et al. 2018). Some evidence also indicates that water-column rates of DNRA at the nitrate-sulfide chemocline (40 $nmol L^{-1} d^{-1}$, estimated at $\sim 0.1 mmol NH_4^+ m^{-2} d^{-1}$) may supply some additional ammonium (Schunck et al. 2013).

In the ETSP region, the benthic ammonium flux combined with the enhanced rates of nitrite production at the pelagic nitrate-sulfide chemocline, promote twofold higher anammox activity at stations containing bottom water sulfide compared to nonsulfidic stations (Kalvelage et al. 2013; Schunck et al. 2013; Callbeck 2017). While it was previously suggested that anammox is inhibited by sulfide, in situ amendment experiments affirm that anammox activity tolerated sulfide concentrations up to 1–2.5 μM (Dalsgaard et al. 2014; Michiels et al. 2019). Furthermore, anammox genes were found to be actively expressed during a sulfidic event (Schunck et al. 2013). Thus, even in the presence of sulfide, anammox appears to still compete for available nitrite and ammonium generated by the sulfur cycle.

Abiotic interaction of sulfide with trace metals and its feedback on the nitrogen cycle

The production of nitrite and N_2O are tightly regulated by the metalloenzymes of denitrification that produce and consume these intermediates, and these enzymes are influenced by the availability of trace metals such as iron and copper. In sulfidic waters, sulfide may sequester trace metals such as copper in the form of copper-sulfide precipitates. The metalloenzymes of NirK involved in nitrite reduction to nitric oxide, and NosZ involved in the last step of denitrification, N_2O reduction to N_2 , contain copper-rich active sites (Godden et al. 1991; Brown et al. 2000; Nojiri et al. 2007; Glass and Orphan 2012). Laboratory experiments using denitrifying bacteria have shown that inducing Cu-limitation by the addition of chelating agents increases the production of nitrite and N_2O (Granger and Ward 2003; Manconi et al. 2006; Felgate et al. 2012; Moffett et al. 2012). Similar observations are reported with increasing sulfide concentrations, whereby increasing sulfide induces lower nitrite and N_2O reduction

activity, while nitrate reduction to nitrite remains unchanged at all sulfide concentrations (Pan et al. 2013; Pratihary et al. 2014).

In OMZs, the sulfide-rich sediments and bottom waters are likely sinks of copper, analogous to the sulfide-rich Cariaco Basin (Tankéré et al. 2001). Although sulfide sequesters copper (and many other transition metals), sulfide-rich sediments are often a source of dissolved iron, as iron forms a relatively soluble metal sulfide complex with sulfide (Saito et al. 2003; Noffke et al. 2012; Scholz et al. 2014; Schlosser et al. 2018; Plass et al. 2019). During a sulfidic event, the benthic iron flux to overlying waters is substantial (Schlosser et al. 2018), and may alleviate iron constraints for the Fe-rich denitrification enzymes including nitrate reductase (NarGHI: $\text{NO}_3^- \rightarrow \text{NO}_2^-$), the Fe-nitrite reductase (NirS: $\text{NO}_2^- \rightarrow \text{NO}$) and nitric oxide reductase (cNOR: $\text{NO} \rightarrow \text{N}_2\text{O}$) (Glass and Orphan 2012).

In the sulfide-rich bottom waters of the ETSP region, the Cu-nitrite reductase (*nirK*) and nitrous oxide reductase (*nosZ*) exhibited lower levels of expression relative to the Fe-nitrate reductase (Schunck et al. 2013; Léniz et al. 2017). Moreover, in the presence of sulfide, rates of nitrate reduction to nitrite well surpassed potential rates of N_2O reduction to N_2 (Schunck et al. 2013). Copper limitations induced by the addition of sulfide in ETSP amendment experiments might also explain the net increase in N_2O production relative to non-sulfide amended experiments (Dalsgaard et al. 2014; Galán et al. 2014), in line with other studies (Pan et al. 2013; Pratihary et al. 2014). It is therefore tempting to speculate that sulfide–metal interactions might disproportionately affect the various steps of denitrification differently during a sulfidic event controlling the fate of nitrate, and its channeling to end products NO_2^- , N_2O , and N_2 .

Local production of fixed-N and fixed-C in the anoxic zone

Nitrogen and carbon fixation are most active in the oxygenated surface waters, which sustain elevated primary productivity as a result of nutrient upwelling. The sinking of surface generated organic matter, in turn, provides fixed carbon and nitrogen to the OMZ driving an active nitrogen and sulfur cycle. While part of this sinking material is remineralized in the water column by heterotrophs, mounting evidence indicates that sulfidic events could additionally support the local generation of fixed nitrogen and carbon in the anoxic zone.

In the ETSP region, elevated rates of nitrogen fixation were detected in sulfide-rich bottom waters during a sulfidic event, reaching up to $10 \text{ nmol N L}^{-1} \text{ d}^{-1}$, or $0.5 \text{ mmol N m}^{-2} \text{ d}^{-1}$ (Löscher et al. 2014; Sommer et al. 2016). Even though these rates are 2–3-fold lower compared to rates of nitrogen fixation in surface waters (Löscher et al. 2014), newly fixed nitrogen in the anoxic zone could partly offset local nitrogen loss (Halm et al. 2009). A metatranscriptomic survey of these ETSP waters finds active expression of the *NifH* gene—the key enzyme involved in nitrogen fixation—associated to green sulfur bacteria *Chlorobium*, as well as to Desulfovibionales and

Desulfobacterales (orders of sulfate-reducing bacteria) (Christiansen and Löscher 2019, preprint).

Elevated rates of dark carbon fixation are also associated with the sulfide-rich waters, driven by chemolithoautotrophic blooms of sulfide-oxidizing bacteria. Off the coast of Peru and Chile, carbon fixation rates during sulfidic events can reach from 900 to $2800 \text{ nmol C L}^{-1} \text{ d}^{-1}$ (Schunck et al. 2013; Galán et al. 2014; Callbeck et al. 2018, 2019); with the highest rates of carbon fixation occurring when stations contain $> 20 \mu\text{M}$ sulfide (Callbeck et al. 2019). Similarly high rates of carbon fixation have also been reported in the chemoclines of stratified basins up to $\sim 2500 \text{ nmol C L}^{-1} \text{ d}^{-1}$ (Taylor et al. 2001; Glaubitz et al. 2010; Michiels et al. 2019). In the ETSP region, assuming that the total amount of sulfide contained in these waters was oxidized for growth by chemolithoautotrophic bacteria, then a singular sulfidic event can represent up to $\sim 30\%$ of the photoautotrophic carbon fixation (Schunck et al. 2013). This episodic increase in the fraction of dark carbon fixation is similar in magnitude to the amount of photosynthetic surface production exported below the photic zone.

Single-cell CO_2 assimilation measurements indicate that SUP05, and epsilonproteobacteria (most likely *Sulfurovum/Sulfurimonas*), account for a large fraction of the carbon fixation rate in the nitrate-sulfide chemocline (Callbeck et al. 2018, 2019). Namely, the epsilonproteobacteria *Sulfurovum/Sulfurimonas* had a nearly fourfold higher CO_2 fixation rate than compared to SUP05 of 0.72 and $0.19 \text{ fmol cell}^{-1} \text{ d}^{-1}$, respectively (Callbeck et al. 2019). Given the abundance of *Sulfurovum/Sulfurimonas* during a sulfidic event, they are expected to play an important role in generating organic matter in the anoxic zone. Other autotrophic bacteria, such as Marinimicrobia, might further contribute to carbon fixation (Hawley et al. 2017), although in situ rates of CO_2 fixation remain unquantified for this clade.

Apart from lithoautotrophy, emerging evidence indicates that chemolithoheterotrophic bacteria may additionally thrive in these organic- and sulfide-rich bottom waters (Callbeck et al. 2019). *A. peruensis*, isolated from a sulfidic event, is capable of assimilating acetate for growth, while oxidizing sulfide and reducing nitrate. Indeed, previous chemocline studies have observed elevated rates of acetate assimilation in the sulfide-rich Cariaco Basin (Ho et al. 2002). In OMZs, we posit that the anoxic blooms of chemolithoheterotrophic and chemolithoautotrophic bacteria are sustained, in part, by the release of dissolved organic and inorganic carbon from sediments (Dale et al. 2015; Loginova et al. 2016).

The presence of deep anoxic blooms have therefore potential to represent major sinks of dissolved inorganic and organic carbon, providing an input of fixed-C, and fixed-N, below the photic zone. This local input is expected to enforce sulfate reduction and sulfide accumulation in upper shelf sediments (Schunck et al. 2013), and possibly enhance nitrogen loss (e.g., Callbeck et al. 2021).

The release of dissolved phosphate

In OMZs, intensive sulfur cycling at the water–sediment interface plays an important role in moderating the release of dissolved phosphate to the water column. Since phosphate is a key nutrient limiting primary productivity, its release to the water column is predicted to cause greater eutrophication with positive feedback effects on nitrogen and sulfur cycling. While anoxic sediments generally contribute to the benthic release of phosphate, field observations suggest that the benthic phosphate flux to the water column is enhanced during a sulfidic event. For instance, a sulfidic event off the coast of Peru (with up to $33 \mu\text{M HS}^-$ in bottom waters) observed a total benthic dissolved phosphate flux of $1 \text{ mmol m}^{-2} \text{ d}^{-1}$ (Lomnitz et al. 2016), which was twofold higher than the flux measured in the absence of a sulfidic event (Bohlen et al. 2011; Noffke et al. 2012).

The increase in the benthic phosphate flux during a sulfidic event can be partly ascribed to the activities of sulfate-reducing and sulfide-oxidizing bacteria. The high rates of surface exported organic matter that induce a sulfidic event (Fig. 2C,D), also fuel greater sulfate reduction that increases organic matter remineralization producing phosphate in shelf sediments (Lomnitz et al. 2016).

The release of phosphate is further compounded by the activities of giant sulfur bacteria, such as *Thioploca* and *Thiomargarita*. *Thioploca/Thiomargarita* has a capacity to store phosphate inside intracellular vacuoles in the form of polyphosphate. Evidence indicates that these bacteria uptake large amounts of phosphate when sulfide concentrations are low (Schulz and Schulz 2005; Goldhammer et al. 2010), but oxidize stored polyphosphate reserves when sulfide concentrations increase, resulting in an efflux of dissolved phosphate (Brock and Schulz-Vogt 2011). In OMZ sediments, *Thioploca/Thiomargarita* exhibit a spatial correlation with the accumulation of pore-water phosphate and apatite formation (Schulz and Schulz 2005; Goldhammer et al. 2010; Bailey et al. 2013). Furthermore, functional gene surveys affirm that genes related to polyphosphate degradation are upregulated in the presence of sulfide (Jones et al. 2016). Together, the intensive sulfur-based activity at the water–sediment interface not only influences the carbon and nitrogen cycles, but also has consequences for phosphorous cycling in OMZs.

The benthic-pelagic sulfur cycle in the absence of bottom water sulfide

Once the release of benthic sulfide declines (Fig. 4A), the sulfur cycle at the water–sediment interface continues to play a major role in upper shelf biogeochemistry (Dale et al. 2017). Following a sulfidic event, nitrate is replenished to upper shelf bottom waters, while organic matter rain rates are typically reduced compared to an active sulfidic event (Dale et al. 2016, 2017).

Under nitrate-rich conditions, in the absence of sulfide, pelagic rates of sulfide-driven denitrification decrease dramatically,

leaving anammox as the dominate nitrogen removal pathway in the water column. While pelagic denitrification subsides benthic sulfide-driven DNRA continues, which marks a large shift from nitrogen removal to mainly nitrogen recycling by DNRA (Bohlen et al. 2011; Pratihary et al. 2014; Dale et al. 2016; Neumann et al. 2016; Sommer et al. 2016). Some sulfide-driven denitrification remains in sediments, but, giant sulfur bacteria appear to out-compete denitrifying bacteria for available nitrate (Dale et al. 2017), where they draw a downward flux of pelagic nitrate to the sediment to replenish vacuole nitrate stores. Field observations in the ETSP region indicate that benthic fluxes of ammonium are as much as five times lower in the absence of a sulfidic event (Bohlen et al. 2011; Sommer et al. 2016). Nevertheless, benthic sulfide-driven DNRA and ammonification (by sulfate reducing bacteria) continue to release ammonium to the water column at up to $3.7 \text{ mmol m}^{-2} \text{ d}^{-1}$. Estimates suggest that the benthic ammonium flux could account for 50% of the ammonium requirements of anammox activity in OMZ shelf waters (Kavelage et al. 2013; Dale et al. 2016).

In addition, the sulfide-rich shelf sediments can sometimes be a small but significant flux of nitrite to the overlying water column. For instance, nitrite concentrations often increase moving toward the bottom waters of the upper shelf OMZ (Fariás et al. 2009; Füssel et al. 2012, 2017; Galán et al. 2014; Léniz et al. 2017). While a substantial fraction of nitrite production involves pelagic heterotrophic nitrate reduction to nitrite (Lam et al. 2009), another possible source may arise from the activities of giant sulfur bacteria *Thioploca/Thiomargarita* in sediments. In addition to producing ammonium as a result of DNRA, *Thioploca* can also generate nitrite under nitrate limiting conditions, which can leak from the cell and accumulate in subsurface pore waters (Otte et al. 1999; Prokopenko et al. 2006, 2013). A small fraction of this pore-water nitrite accumulation may subsequently diffuse into the water column. For instance, in the ETSP and ETSA upper shelf the maxima benthic nitrite flux was from 5 to $150 \mu\text{mol m}^{-2} \text{ d}^{-1}$, albeit, the nitrite flux is sometimes directed into the sediments depending on the location (Bohlen et al. 2011; Neumann et al. 2016; Sommer et al. 2016).

Benthic-generated nitrite and ammonium likely contribute to the active rates of anammox and nitrification, which are reported in upper shelf bottom waters (Kuyppers et al. 2005; Lam et al. 2009; Lavik et al. 2009; Füssel et al. 2012, 2017; Kavelage et al. 2013; Galán et al. 2014). Thus, despite the absence of sulfide, the highly active sulfur cycle in the water–sediment interface plays an integral role in moderating the pelagic inventories of nitrite and ammonium with important implications for anammox and nitrification year-round (Dale et al. 2017). When conditions promote the benthic release of sulfide, the nitrate-sulfide chemocline exhibits a shift back to nitrogen removal by denitrification, along with accelerated rates of anammox and N_2O production (Fig. 4B).

Moving offshore

In the offshore OMZ, the sulfur cycle is expected to have similar biogeochemical implications for the carbon and nitrogen cycle as to the upper shelf sulfur cycle. Sulfur cycling activity and the other linked processes also appear to be heterogeneously distributed in the offshore OMZ, as a consequence of lateral transport processes. As described earlier, ETSP cross-shelf transport, can contribute to the redistribution of large inventories of elemental sulfur, produced during a sulfidic event into the open ocean OMZ. In addition, the offshore advected plume is associated with active chemolithoautotrophic SUP05 bacteria (Callbeck et al. 2018).

In the ETSP sulfur plume, single-cell measurements indicate that SUP05 bacteria contributed to substantial carbon fixation with rates reaching $8.4 \text{ mmol C m}^{-2} \text{ d}^{-1}$, comparable to the sulfidic upper shelf of $13.4 \text{ mmol C m}^{-2} \text{ d}^{-1}$ (Callbeck et al. 2018). Moreover, the offshore sulfur plume exhibited elevated nitrate reduction to N_2 and nitrate reduction to nitrite with rates averaging 7.9 and $17.8 \text{ nmol N L}^{-1} \text{ d}^{-1}$, respectively (Fig. 5). The ability of SUP05 to store intracellular sulfur, or metabolize advected sulfur, combined with its genomic capacity for denitrification, suggested that it may be responsible for measured rates of nitrate reduction in the offshore advected plume. Overall, denitrification in plume waters accounted for nearly one-fifth of total nitrogen loss, with the remainder attributable to anammox (Callbeck 2017; Callbeck et al. 2018). In addition, the enhanced rates of nitrate reduction to nitrite in the sulfur plume contributed to nearly one-half of the required nitrite for anammox (Callbeck 2017; Callbeck et al. 2018). ETSP rate measurements are also comparable with an ETSP model that estimated that sulfide-driven denitrification could account for nearly one-fourth of total nitrogen loss; while sulfide-driven nitrate reduction to nitrite supports one-fourth of the nitrite supply for anammox (Azhar et al. 2014).

In contrast, in offshore ETSP waters outside of the sulfur plume, SUP05 CO_2 fixation rates were negligible and mean rates of nitrate reduction to N_2 ($0.7 \text{ nmol N L}^{-1} \text{ d}^{-1}$) and nitrate reduction to nitrite ($7.7 \text{ nmol N L}^{-1} \text{ d}^{-1}$) were lower compared to waters sampled inside the sulfur plume. The difference in activity between the two offshore stations sampled in and outside of the sulfur plume, suggests that a large degree of variability is inherent to the offshore ETSP region. Congruently, in past offshore ETSP surveys a similar degree of variability is observed in denitrification rates, with maximum rates ranging from 0 to $19 \text{ nmol N L}^{-1} \text{ d}^{-1}$ (Thamdrup et al. 2006; Hamersley et al. 2007; Lam et al. 2009; Canfield et al. 2010; Dalsgaard et al. 2012; Kalvelage et al. 2013). Unfortunately, ^{15}N -labeled stable isotope experiments as used to quantify nitrogen transformations, are unable to distinguish between heterotrophic or sulfur-driven denitrification. However, the evidence for cross-shelf advected elemental sulfur, and sulfur-accumulating SUP05 bacteria described above, raises the possibility that sulfur-driven denitrification could be another pathway contributing to offshore ETSP nitrogen loss.

Furthermore, the frequent transport of coastal sulfur plumes into the open ocean (Weeks et al. 2002, 2004; Ohde et al. 2007; Ohde 2018; Ohde and Dadou 2018) (e.g., Fig. 2A), implies that sulfur-driven chemolithoautotrophy might have a larger impact on offshore ETSP nitrogen loss and carbon fixation than previously believed.

Apart from the activities of sulfur-driven denitrification, the offshore rates of OMZ sulfate reduction indicate that organic matter remineralization producing ammonium could support nitrogen loss by anammox. Measured rates of sulfate reduction of $12 \pm 5 \text{ nmol L}^{-1} \text{ d}^{-1}$, amounted to 33% of offshore organic carbon remineralization (Canfield et al. 2010). Using Redfieldian C : N ratios, the measured sulfate reduction rate could yield up to $0.30 \text{ mmol NH}_4^+ \text{ m}^{-2} \text{ d}^{-1}$, roughly 22% of the ammonium needed to sustain offshore anammox activity (Canfield et al. 2010). At a station located 44 km from the coast, which had lower average sulfate reduction rates ($1.3 \pm 0.6 \text{ nmol L}^{-1} \text{ d}^{-1}$), sulfate reduction accounted for 8% of anammox ammonium requirements (Canfield et al. 2010). Estimates from an offshore ETSP model suggest that organic matter remineralization by sulfate reduction could account for 36% of offshore remineralization (Azhar et al. 2014). This modeled rate is in close agreement with the measured rates of sulfate reduction (Canfield et al. 2010). A more recent ETSP-OMZ estimate, using a size-resolved particle simulation model, predicts that sulfate reduction could contribute up to 5% of particulate organic matter remineralization (Bianchi et al. 2018). Despite the variability, modeling and rate process measurements suggest that sulfate reduction could be a significant supply of ammonium for anammox bacteria in the ETSP region. Although more direct measurements of sulfate reduction are needed to better understand the full extent and variability of this process in the offshore OMZ.

Potential for DOS degradation in OMZs

The ocean contains nearly 7 Pg (10^{15} g) of DOS (Ksionzek et al. 2016), with marine upwelling regions representing major hotspots of DOS production (Kloster et al. 2006; Lana et al. 2011; Ksionzek et al. 2016; McParland and Levine 2019). Work in the Canary and Benguela upwelling systems indicates that these eutrophic waters are active areas of remineralization of DOS-containing compounds, with indications of preferential DOS removal relative to dissolved organic carbon (DOC) (Ksionzek et al. 2016).

In marine upwelling regions, phytoplankton DOS synthesis and the sinking of their biomass offer an important source of DOS to OMZ waters (Landa et al. 2019). Further contributions occur as a result of local secretions of DOS by diel vertical migrating zooplankton (Clifford et al. 2017; Tutasi and Escribano 2020). Moreover, abiotic sulfurization of organic matter in sulfide-rich sediments is posited to also contribute to the large DOS inventory in OMZs (Pohlabeln et al. 2017). Abiotic sulfur incorporation into DOM has been observed in

sediment cores collected from the Peru margin, with organosulfonates comprising 20–40% of the sulfur species (Eglinton et al. 1994; Vairavamurthy et al. 1994), and extremely high concentrations of DOS (up to 442 nM) have been reported in association with OMZ shelf waters (Andreae 1985; Shenoy et al. 2012).

The large DOS inventory supports organosulfur-based heterotrophy by marine microorganisms (Moran and Durham 2019; Tang 2020). These microbes employ a number of organic matter transport systems and degradation pathways to gain energy from the vast array of DOS compounds available in the marine environment. While a great number of DOS compounds exist as reviewed elsewhere (Moran and Durham 2019; Tang 2020), the chemical composition of DOS is roughly defined according to the chemical oxidation state of the organic sulfur containing moiety. More oxidized sulfur metabolites include taurine, and its derivatives, hypotaurine, methyltaurine, isethionate, and N-acetyltaurine contain a sulfonate moiety (R-SO_3^-); while more reduced forms of DOS, such as dimethylsulfide, contain a methyl-sulfur (S-R_2^+). Subsequently, when DOS is metabolized by heterotrophic microbes it generates reduced and oxidized forms of inorganic sulfur species (e.g., sulfide, thiosulfate and sulfite).

Although our understanding of DOS degradation in OMZs is rudimentary; we briefly explore some key organisms that could ostensibly contribute to DOS recycling in the OMZ and oxycline. We specifically focus on the fate of the organic sulfur metabolite, taurine (Table 1). Taurine is an important labile amino-acid like compound produced from algae and zooplankton, where it can reach concentrations of up to 200 mM inside some cells (Clifford et al. 2017). Once released into the environment, taurine utilization can generate a wide range of energy yields for heterotrophic bacteria ($\Delta G' = -12$ to -1365 kJ mol $^{-1}$; Table 1). In addition, some heterotrophs also use taurine as the sole source of assimilable carbon, nitrogen, and sulfur (Durham et al. 2019). This dual role as an energy source and as a source of assimilable carbon, nitrogen and sulfur may explain why free dissolved taurine concentrations are maintained at low nanomolar levels due to its rapid uptake by marine heterotrophs (Clifford et al. 2019). Indeed, a diverse assemblage of heterotrophs carry a capacity for taurine uptake and remineralization, suggesting that taurine is important to many microbes in the marine realm (Clifford et al. 2019), and the same likely holds true for organic-rich OMZs.

Taurine degradation coupled to S-species oxidation

Due to the oxidized nature of the sulfonate moiety, the desulfonation of taurine leads to sulfoacetaldehyde and eventually to sulfite and acetate generation ($\Delta G' = -302$ kJ mol $^{-1}$; Table 1). The produced sulfite from taurine desulfonation can be further oxidized for energy gain by the rDsr pathway, or by the family of molybdenum-containing sulfite-oxidizing enzymes YedYZ and SorAB (Kappler 2008), producing sulfate (also see

Fig. 1). The initial desulfonation of taurine is catalyzed by the enzyme TauD, which is an oxygenolytic dioxygenase that requires molecular oxygen (Kertesz 2000; Tang 2020). Overall, the complete oxidation of taurine to sulfate, ammonium, and bicarbonate generates significant energy yields when using either nitrate or oxygen as the electron acceptor ($\Delta G' = -1239$ and -1365 kJ mol $^{-1}$; Table 1). In the oxygenated ETSP surface waters, the most prevalent microbes involved in taurine uptake and recycling is mediated by the cosmopolitan members SAR11 and *Roseobacter* (Bergauer et al. 2018; Clifford et al. 2019; Tang 2020).

In deeper ETSP waters, taurine uptake genes are dominated by SAR324 and Arctic96BD-19 (Landa et al. 2019). Arctic96BD-19 within the Gammaproteobacteria is a heterotrophic sister lineage of the SUP05 clade. While SUP05 is widely distributed in OMZs (Fig. 6A), Arctic96BD-19 exhibits an even broader distribution in the ocean than compared to SUP05 (Fig. 6B). SAR324 is found within the Deltaproteobacteria (Yilmaz et al. 2016), and like Arctic96BD-19, it is also omnipresent in the ocean, including all major marine upwelling regions (Stevens and Ulloa 2008; Fuchsman et al. 2011; Wright et al. 2012; Allers et al. 2013; Beman and Carolan 2013; Hawley et al. 2014; Forth et al. 2015; Thrash et al. 2017). Specifically, Sar324 and Arctic96BD-19 distributions tend to correlate with low-oxygen concentrations (< 70 μM) (Aldunate et al. 2018), indicating that these members possibly thrive in the OMZ oxycline. Here, Arctic96BD-19 bacteria putatively grow via a mixotrophic metabolism, with a capacity for autotrophy as well as a reliance on organic matter for growth (Swan et al. 2011; Marshall and Morris 2013; Spietz et al. 2019).

Among the array of organic matter degradation pathways, Arctic96BD-19 encodes for the *tauD*, as well as taurine uptake genes *tauABC* (Marshall and Morris 2015; Landa et al. 2019). Moreover, a Saanich Inlet OMZ Arctic96BD-19 isolate showed some growth on taurine and thiotaurine (Spietz et al. 2019). Other water-column studies of phytoplankton blooms, observed an upregulation of taurine genes associated to Arctic96BD-19 (Georges et al. 2014). Similarly, the mixotrophic SAR324 clade, although poorly characterized, encodes for carbon fixation, including various pathways involved in organic matter degradation and taurine desulfonation by TauD (Swan et al. 2011; Sheik et al. 2014; Landa et al. 2019; Tang 2020). Complementing their heterotrophic capacity, both Sar324 and Arctic96BD-19 carry genes for reduced sulfur degradation via *rdsr* pathways, including genes for sulfite oxidation (Swan et al. 2011; Sheik et al. 2014; Spietz et al. 2019), suggesting that sulfite generation from taurine could be further oxidized to sulfate.

Given that Sar324 and Arctic96BD-19 favor low-oxygen concentrations (< 70 μM) (Aldunate et al. 2018), these mixotrophs are posited to play a role in taurine/DOS degradation coupled to oxygen respiration in the OMZ oxycline. Future work might also consider whether organosulfur-based heterotrophs, such as Sar324 and Arctic96BD-19, are partly

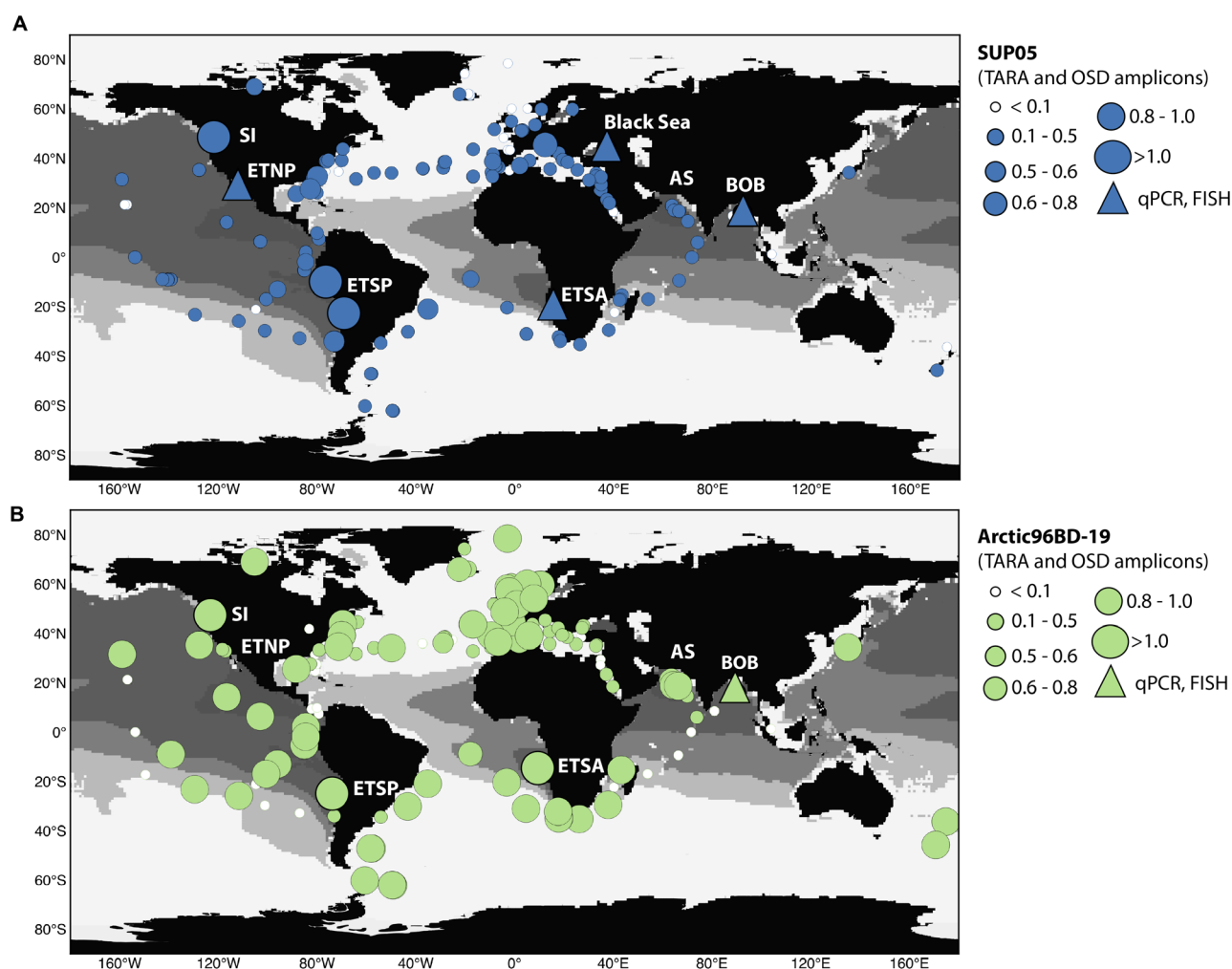


Fig. 6. Distribution of SUP05 and Arctic96BD-19 clades. SUP05 (A) and Arctic96BD-19 (B) abundances are represented as the percentage of associated 16S rRNA sequences in metagenomic and amplicon sequencing datasets from TARA Ocean and OSD, Ocean Sampling Day 2014 (OSD2014) as well as from other OMZ metagenomic data sets (Walsh et al. 2009; Canfield et al. 2010; Wright et al. 2012; Schunck et al. 2013). The highest reported SUP05 and Arctic96BD-19 abundances at each station are indicated. Note that studies using quantitative polymerase chain reaction (qPCR) (Carolan and Beman 2015; Bristow et al. 2017) and fluorescence in situ hybridization (FISH) (Lavik et al. 2009; Glaubitz et al. 2013; Callbeck et al. 2018) based approaches to quantify SUP05 and Arctic96BD-19 bacteria are highlighted with triangles. Map abbreviations indicated stand for: eastern tropical South Pacific (ETSP), eastern tropical North Pacific (ETNP), eastern tropical South Atlantic (ETSA), Arabian Sea (AS), Saanich Inlet (SI), and the Bay of Bengal (BOB). Mapping of 16S rRNA gene sequence reads from the TARA Ocean and OSD data sets was performed according to (Martínez-Pérez et al. 2016). Near full-length published and unpublished 16S rRNA gene sequences from previously identified SUP05 and Arctic96BD-19 species were used as a BLASTn classification reference database. A cutoff of $(\text{percent query coverage} + \text{percent alignment identity})/2 > 98\%$ was used to assign either SUP05 or Arctic96BD-19 identity to a read.

fueled by cross-shelf transported elemental sulfur (Callbeck et al. 2018).

Other members that carry a genetic capacity for DOS degradation include the recently characterized ETSP *Sagittula castanea* within the *Roseobacter* clade, which was isolated from sulfide-rich upper shelf waters (Martínez-Pérez et al. 2018). Previous studies have found *Roseobacter* members in close association with sulfide-rich marine sediments and in the oxic-anoxic redoxcline, suggesting that some members of this diverse phylum can thrive under sulfidic conditions (Sorokin 1995; Lenk et al. 2012). Interestingly, the ETSP *S. castanea*, was capable of both aerobic and anaerobic growth, and its genome encoded

for genes involved in dimethylsulfide utilization as well as a complete Sox pathway akin to other *Roseobacter* members (Martínez-Pérez et al. 2018). Dimethylsulfide degradation is common to *Sagittula stellata* E-37 (the next closest type strain to ETSP *S. castanea*), and also has been shown to oxidize sulfite and thiosulfate, although it is unclear if this is directly connected with organic sulfur degradation (González et al. 1999; Boden et al. 2011). Organic sulfur utilization might also extend to chemolithoautotrophic SUP05 bacteria, which were shown under laboratory conditions to grow using thiotaurine, but not taurine or dimethylsulfoniopropionate (Shah et al. 2019). Whether a similar capacity for organic

sulfur utilization exists in other OMZ-SUP05 bacteria is currently unknown.

Anaerobic taurine degradation coupled to sulfite reduction to sulfide

The presence of oxygen is critical to the function of many desulfonation enzymes (mono-/di-oxygenases), such as TauD, because it enables the C–S bond cleavage in DOS via the generation of oxygen radicals. However, recent emerging evidence has characterized a novel C–S bond cleaving enzyme, within the family of glyceryl radical enzymes called IsIA that does not require oxygen for its catalysis of DOS. The complete anaerobic taurine desulfonation pathway was characterized in the strict anaerobe *Bilophila wadsworthia* (Peck et al. 2019), which proceeds first by deamination of taurine to sulfoacetaldehyde. Sulfoacetaldehyde is then reduced to isethionate by a NADH-dependent reductase (e.g., *Halodesulfobivrio oceani*; Fig. 3H). In the critical C–S bond cleavage step, sulfite is liberated from isethionate catalyzed by the isethionate sulfite-lyase (IsIA). Acetaldehyde is oxidized to acetyl-CoA and eventually incorporated into biomass via gluconeogenesis; while the liberated sulfite is reduced to sulfide by Dsr. Thus, the sulfonate moiety ultimately serves as the source of sulfur (also see Fig. 1). Apart from *B. wadsworthia*, the desulfonation enzyme IsIA, has also been identified in *Desulfobivrio* spp. (62% amino acid identity) as well as a number of other genera associated to the deltaproteobacteria (Peck et al. 2019), more commonly identified in OMZs (Canfield et al. 2010; Finster and Kjeldsen 2010; Schunck et al. 2013).

In the ETSP region, two strains of *D. oceani* were isolated from offshore waters off the coast of Peru (reclassified as *Halodesulfobivrio oceani*; Finster and Kjeldsen 2010; Shivani et al. 2017). Both strains demonstrated a capacity for taurine reduction producing sulfide and ammonium as end products (Finster and Kjeldsen 2010). *Halodesulfobivrio oceani* also demonstrated a capacity to reduce sulfate to sulfide, likely via canonical sulfate reduction. Interestingly, a draft genome of *Halodesulfobivrio spirochaetisodalis* JC271, the next closest type culture (Shivani et al. 2017) has a complete taurine metabolism pathway including taurine outer membrane permeases and the desulfonation gene cluster *isIA* with 72% gene identity to *B. wadsworthia*. The ability for ETSP *H. oceani* to use taurine to generate sulfide (Finster and Kjeldsen 2010), indicates that taurine could function as an alternative electron acceptor to sulfate.

The ability to use taurine as an electron acceptor offers some key advantages. In contrast with sulfate reduction, which requires one ATP to reduce sulfate to sulfite, the use of taurine does not require ATP to generate sulfite as the electron acceptor (Peck et al. 2019). The fermentation of taurine to ammonium, acetate, bicarbonate, and sulfite followed by the reduction of sulfite to sulfide results in a Gibbs free energy yield of -225 kJ mol^{-1} (Table 1), making this reaction favorable under OMZ conditions especially in contrast to canonical sulfate

reduction ($\Delta G' = -88 \text{ kJ mol}^{-1}$). Furthermore, microbes capable of utilizing taurine as the electron acceptor, via IsIA, are not exclusive to sulfate-reducing bacteria (Deltaproteobacteria), but also include microorganisms in the phylum Firmicutes (Peck et al. 2019). Moreover, DOS compounds other than taurine could serve as organic-sulfite donors for anaerobic respiration, including 2,3-dihydroxypropane-1-sulfonate, isethionate and cyseate (Lie et al. 1996; Denger et al. 1997; Burcher et al. 2018).

The capacity of ETSP *H. oceani* to use taurine as an electron acceptor importantly highlights that sulfide generation could extend beyond canonical sulfate reduction in OMZs. Examining this, in combination with the rates of taurine turnover to sulfite and sulfide on a larger scale, presents an exciting avenue for future OMZ research.

Summary

Primary production and the export of organic matter is one of the principal drivers of the OMZ sulfur cycle. Organic matter oxidation coupled to sulfate reduction and organosulfur sulfidogenesis generate sulfide, as well as the various other reduced sulfur intermediates, sulfur, thiosulfate and sulfite (Fig. 1). Collectively, a diverse assemblage of microbes gain energy from the turnover of organic and/or inorganic sulfur species, and these microbes exhibit clear niche partitioning in the OMZ (Fig. 3). In the offshore waters, a number of microbes thrive as mixotrophs with a capacity for both organic and inorganic sulfur transformation, with most exhibiting a stronger reliance on organic matter for growth, including *Roseobacter*, Arctic96BD-19 and Sar324. In coastal waters, the benthic fluxes of sulfide and elemental sulfur support more lithotrophic metabolisms, including *Arcobacter*, *Sulfurovum*, *Thioploca*, and SUP05 (*A. peruensis* is a partial exception since it can grow as a chemolithoheterotroph). These microbes have additionally evolved strategies (e.g., intracellular sulfur storage) to cope with changing reduced sulfur fluxes caused by fluctuating hydrodynamics.

The microbial sulfur cycle, in turn, exerts significant control over other linked biogeochemical cycles involved in carbon, nitrogen and phosphorous (Figs. 4). The influence of the sulfur cycle is most evident in shelf waters with direct contact to the benthos. Here, the water-sediment sulfur cycle controls not only the pools of dissolved inorganic and organic carbon, but contributes to carbon and nitrogen fixation that drives local organic matter generation in the anoxic zone. The local input of organic matter is expected to reinforce a sulfidic event, which is possibly compounded by the release of benthic phosphate at the water-sediment interface stimulating primary productivity in surface waters. Sulfur cycling also contributes to the generation of both nitrite and ammonium—key substrates for anammox and nitrification. In the upper shelf OMZ, the enhanced activities of anammox in the presence of sulfide, in combination, with sulfide-driven

denitrification at the chemocline promote substantial nitrogen loss. Moreover, the abiotic interaction of sulfide with trace metals may further regulate the emission of the climate-active trace gas N_2O . While sulfide/sulfur accumulations were previously considered to be rare (e.g., Fig. 4B), evidence now indicates that these events occur frequently in the ETSP and ETSA shelf waters over prolonged periods of anoxia 180–200 d of the year (Fig. 2C,D).

Similar biogeochemistry to the upper shelf is reported in the offshore OMZ. In these waters detached from benthic processes, sulfur cycling is believed to be sustained by lateral transport processes and particle microniches (Fig. 5). Lateral transport processes drive the redistribution of coastal sulfur plumes into the open ocean along with active sulfide-oxidizing bacteria, such as SUP05. Offshore advected SUP05 bacteria contribute to rates of sulfur-driven denitrification and carbon fixation. Moreover, sinking particles (or particles advected from the coast) are predicted to house microniches that contain an active sulfur cycle that could explain the presence of measured rates of sulfate reduction in the offshore OMZ. These measured rates of sulfate reduction potentially support an important fraction of ammonium driving anammox. Given the intensity of sulfur cycling activity (Figs. 2, 4, 5), we hypothesize that the sulfur cycle plays a quantitatively significant role in biogeochemistry from the upper shelf to the open ocean OMZ.

The potential for large scale sulfur cycling in OMZs is perhaps even greater if DOS turnover is also considered. Microbes with a capacity for organic sulfur degradation (e.g., Arctic96BD-19) are a persistent and widespread feature of organic matter rich OMZs (Fig. 6B). Moreover, DOS compounds, such as taurine, may provide a novel pathway of sulfide generation by sulfate-reducing bacteria in OMZs (e.g., *H. oceani*). The significance of organosulfonate degradation as a source of reducing equivalents for sulfide-oxidizing and sulfate-reducing bacteria in the offshore OMZ remains unquantified, as does its potential linkage to the nitrogen cycle or other elemental cycles.

A century and a half ago, Dr. Burrill observed the presence of a highly active sulfur cycle operating off the coast of Peru. What seemed like a mystery is today understood as a complex benthic–pelagic interaction involving regional oceanography, chemistry, and microbiology. Our still modest understanding of the modern OMZ sulfur cycle continues to evolve at a great pace. We praise the long-term monitoring efforts, which have been instrumental in providing integrated water-column fluxes, process rate measurements, and molecular data; and when supplemented with remote sensing, have provided great insight into the spatial–temporal dynamics of OMZ sulfur cycling. Moreover, we encourage cultivation-dependent techniques, as they continue to help disentangle the multifunctionality of microbes and further serve to verify omic-based metabolic models. Finally, modeling work, with integrated regional hydrodynamics, will be critical to assessing the

ramifications of the OMZ sulfur cycle on the tightly coupled carbon and nitrogen cycles. We hope that work presented in this synthesis will help guide the design of future research in OMZs, and in similar anoxic environments.

References

- Aldunate, M., R. De la Iglesia, A. D. Bertagnolli, and O. Ulloa. 2018. Oxygen modulates bacterial community composition in the coastal upwelling waters off Central Chile. *Deep Sea Res. Part II Top. Stud. Oceanogr.* **156**: 68–79. doi:10.1016/j.DSR2.2018.02.001
- Allredge, A. L., and Y. Cohen. 1987. Can microscale chemical patches persist in the sea? Microelectrode study of marine snow, fecal pellet. *Science* **235**: 689–691. doi:10.1126/science.235.4789.689
- Allers, E., J. J. Wright, K. M. Konwar, C. G. Howes, E. Beneze, S. J. Hallam, and M. B. Sullivan. 2013. Diversity and population structure of Marine Group A bacteria in the north-east subarctic Pacific Ocean. *ISME J.* **7**: 256–268. doi:10.1038/ismej.2012.108
- Andreae, M. O. 1985. Dimethylsulfide in the water column and the sediment porewaters of the Peru upwelling area. *Limnol. Oceanogr.* **30**: 1208–1218. doi:10.4319/lo.1985.30.6.1208
- Arevalo-Martinez, D. L., A. Kock, C. R. Loscher, R. A. Schmitz, and H. W. Bange. 2015. Massive nitrous oxide emissions from the tropical South Pacific Ocean. *Nat. Geosci.* **8**: 530–533. doi:10.1038/ngeo2469
- Arévalo-Martínez, D. L., T. Steinhoff, P. Brandt, A. Körtzinger, T. Lamont, G. Rehder, and H. W. Bange. 2019. N_2O emissions from the Northern Benguela upwelling system. *Geophys. Res. Lett.* **46**: 3317–3326. doi:10.1029/2018GL081648
- Azhar, M., D. Al, E. Canfield, K. Fennel, B. Thamdrup, and C. J. Bjerrum. 2014. A model-based insight into the coupling of nitrogen and sulfur cycles in a coastal upwelling system. *J. Geophys. Res. Biogeosci.* **119**: 264–285. doi:10.1002/2012JG002271
- Bailey, J. V., F. A. Corsetti, S. E. Greene, C. H. Crosby, P. Liu, and V. J. Orphan. 2013. Filamentous sulfur bacteria preserved in modern and ancient phosphatic sediments: Implications for the role of oxygen and bacteria in phosphogenesis. *Geobiology* **11**: 397–405. doi:10.1111/gbi.12046
- Belmadani, A., V. Echevin, B. Dewitte, and F. Colas. 2012. Equatorially forced intraseasonal propagations along the Peru-Chile coast and their relation with the nearshore eddy activity in 1992–2000: A modeling study. *J. Geophys. Res. Ocean.* **117**: 1–20. doi:10.1029/2011JC007848
- Beman, J. M., and M. T. Carolan. 2013. Deoxygenation alters bacterial diversity and community composition in the ocean's largest oxygen minimum zone. *Nat. Commun.* **4**: 2705. doi:10.1038/ncomms3705

- Bergauer, K., A. Fernandez-Guerra, J. A. L. Garcia, R. R. Sprenger, R. Stepanauskas, M. G. Pachiadaki, O. N. Jensen, and G. J. Herndl. 2018. Organic matter processing by microbial communities throughout the Atlantic water column as revealed by metaproteomics. *Proc. Natl. Acad. Sci. USA*. **115**: E400–E408. doi:[10.1073/pnas.1708779115](https://doi.org/10.1073/pnas.1708779115)
- Bertagnolli, A. D., C. C. Padilla, J. B. Glass, B. Thamdrup, and F. J. Stewart. 2017. Metabolic potential and in situ activity of marine Marinimicrobia bacteria in an anoxic water column. *Environ. Microbiol.* **19**: 4392–4416. doi:[10.1111/1462-2920.13879](https://doi.org/10.1111/1462-2920.13879)
- Beulig, F., H. Røy, C. Glombitza, and B. B. Jørgensen. 2018. Control on rate and pathway of anaerobic organic carbon degradation in the seabed. *Proc. Natl. Acad. Sci. USA*. **115**: 367–372. doi:[10.1073/pnas.1715789115](https://doi.org/10.1073/pnas.1715789115)
- Bianchi, D., T. S. Weber, R. Kiko, and C. Deutsch. 2018. Global niche of marine anaerobic metabolisms expanded by particle microenvironments. *Nat. Geosci.* **2018**: 263–268. doi:[10.1038/s41561-018-0081-0](https://doi.org/10.1038/s41561-018-0081-0)
- Boden, R., J. C. Murrell, and H. Schäfer. 2011. Dimethylsulfide is an energy source for the heterotrophic marine bacterium *Sagittula stellata*. *FEMS Microbiol. Lett.* **322**: 188–193. doi:[10.1111/j.1574-6968.2011.02349.x](https://doi.org/10.1111/j.1574-6968.2011.02349.x)
- Bohlen, L., A. W. Dale, S. Sommer, T. Mosch, C. Hensen, A. Noffke, F. Scholz, and K. Wallmann. 2011. Benthic nitrogen cycling traversing the Peruvian oxygen minimum zone. *Geochim. Cosmochim. Acta* **75**: 6094–6111. doi:[10.1016/j.gca.2011.08.010](https://doi.org/10.1016/j.gca.2011.08.010)
- Bonaglia, S., I. Klawonn, L. De Brabandere, B. Deutsch, B. Thamdrup, and V. Brüchert. 2016. Denitrification and DNRA at the Baltic Sea oxic-anoxic interface: Substrate spectrum and kinetics. *Limnol. Oceanogr.* **61**: 1900–1915. doi:[10.1002/lno.10343](https://doi.org/10.1002/lno.10343)
- Böning, P., H.-J. Brumsack, M. E. Böttcher, B. Schmetzger, C. Kriete, J. Kallmeyer, and S. L. Borchers. 2004. Geochemistry of Peruvian near-surface sediments. *Geochim. Cosmochim. Acta* **68**: 4429–4451. doi:<https://doi.org/10.1016/j.gca.2004.04.027>
- Bourbonnais, A., R. T. Letscher, H. W. Bange, V. Échevin, J. Larkum, J. Mohn, N. Yoshida, and M. A. Altabet. 2017. N₂O production and consumption from stable isotopic and concentration data in the Peruvian coastal upwelling system. *Global Biogeochem. Cycles* **31**: 678–698. doi:[10.1002/2016GB005567](https://doi.org/10.1002/2016GB005567)
- Bristow, L. A., and others. 2017. N₂ production rates limited by nitrite availability in the Bay of Bengal oxygen minimum zone. *Nat. Geosci.* **10**: 24–29. doi:[10.1038/ngeo2847](https://doi.org/10.1038/ngeo2847)
- Brock, J., and H. N. Schulz-Vogt. 2011. Sulfide induces phosphate release from polyphosphate in cultures of a marine Beggiatoa strain. *ISME J.* **5**: 497–506. doi:[10.1038/ismej.2010.135](https://doi.org/10.1038/ismej.2010.135)
- Brown, K., M. Tegoni, M. Prudêncio, A. S. Pereira, S. Besson, J. J. Moura, I. Moura, and C. Cambillau. 2000. A novel type of catalytic copper cluster in nitrous oxide reductase. *Nat. Struct. Biol.* **7**: 191–195. doi:[10.1038/73288](https://doi.org/10.1038/73288)
- Brüchert, V., and others. 2006. Biogeochemical and physical control on shelf anoxia and water column hydrogen sulphide in the Benguela upwelling system of Namibia, p. 161–193. *In* N. L. Neretin [ed.], Past and present water column anoxia. Springer.
- Brüchert, V., B. B. Jørgensen, K. Neumann, D. Riechmann, M. Schlösser, and H. Schulz. 2003. Regulation of bacterial sulfate reduction and hydrogen sulfide fluxes in the central Namibian coastal upwelling zone. *Geochim. Cosmochim. Acta* **67**: 4505–4518. doi:[10.1016/S0016-7037\(03\)00275-8](https://doi.org/10.1016/S0016-7037(03)00275-8)
- Burrichter, A., K. Denger, P. Franchini, T. Huhn, N. Müller, D. Spiteller, and D. Schleheck. 2018. Anaerobic degradation of the plant sugar sulfoquinovose concomitant with H₂S production: *Escherichia coli* K-12 and *Desulfovibrio* sp. strain DF1 as co-culture model. *Front. Microbiol.* **9**: 2792. doi:[10.3389/fmicb.2018.02792](https://doi.org/10.3389/fmicb.2018.02792)
- Burt, J. 1852. On fish destroyed by sulphuretted hydrogen in the Bay of Callao. *American J. Sci.* **2**: 433–434.
- Callbeck, C. M. 2017. Distribution and activity of anammox and sulfide-oxidizing nitrate-reducing bacteria in oxygen minimum zones. Ph.D. Diss. Max Planck Institute for Marine Microbiology.
- Callbeck, C. M., and others. 2018. Oxygen minimum zone cryptic sulfur cycling sustained by offshore transport of key sulfur oxidizing bacteria. *Nat. Commun.* **9**: 1729. doi:[10.1038/s41467-018-04041-x](https://doi.org/10.1038/s41467-018-04041-x)
- Callbeck, C. M., and others. 2019. *Arcobacter peruensis* sp. nov., a chemolithoheterotroph isolated from sulfide and organic rich coastal waters off Peru. *Appl. Environ. Microbiol.* **85**: e01344–e01319. doi:[10.1128/AEM.01344-19](https://doi.org/10.1128/AEM.01344-19)
- Callbeck, C. M., B. Ehrenfels, K. B. L. Baumann, B. Wehrli, and C. J. Schubert. 2021. Anoxic chlorophyll maximum enhances local organic matter remineralization and nitrogen loss in Lake Tanganyika. *Nat. Commun.* **12**: 830. doi:[10.1038/s41467-021-21115-5](https://doi.org/10.1038/s41467-021-21115-5)
- Canfield, D. E., K. Erik, and T. Bo. 2005. The sulfur cycle, p. 313–381. *In* E.K. Donald E. Canfield and T. Bo [eds.], Advances in marine biology. Academic Press.
- Canfield, D. E., F. J. Stewart, B. Thamdrup, L. De Brabandere, T. Dalsgaard, E. F. Delong, N. P. Revsbech, and O. Ulloa. 2010. A cryptic sulfur cycle in oxygen-minimum-zone waters off the Chilean coast. *Science* **330**: 1375–1378. doi:[10.1126/science.1196889](https://doi.org/10.1126/science.1196889)
- Carolan, M., and J. M. Beman. 2015. Transcriptomic evidence for microbial sulfur cycling in the eastern tropical North Pacific oxygen minimum zone. *Front. Microbiol.* **6**: 334. doi:[10.3389/fmicb.2015.00334](https://doi.org/10.3389/fmicb.2015.00334)
- Carr, M.-E. 2001. Estimation of potential productivity in Eastern Boundary Currents using remote sensing. *Deep Sea Res. Part II Top. Stud. Oceanogr.* **49**: 59–80. doi:[10.1016/S0967-0645\(01\)00094-7](https://doi.org/10.1016/S0967-0645(01)00094-7)

- Cassman, N., and others. 2012. Oxygen minimum zones harbour novel viral communities with low diversity. *Environ. Microbiol.* **14**: 3043–3065. doi:[10.1111/j.1462-2920.2012.02891.x](https://doi.org/10.1111/j.1462-2920.2012.02891.x)
- Cervantes, F. J., E. R. Meza-Escalante, A.-C. Texier, and J. Gómez. 2009. Kinetic limitations during the simultaneous removal of p-cresol and sulfide in a denitrifying process. *J. Ind. Microbiol. Biotechnol.* **36**: 1417–1424. doi:[10.1007/s10295-009-0628-6](https://doi.org/10.1007/s10295-009-0628-6)
- Chaigneau, A., A. Gizolme, and C. Grados. 2008. Mesoscale eddies off Peru in altimeter records: Identification algorithms and eddy spatio-temporal patterns. *Prog. Oceanogr.* **79**: 106–119. doi:[10.1016/j.pocean.2008.10.013](https://doi.org/10.1016/j.pocean.2008.10.013)
- Chaigneau, A., G. Eldin, and B. Dewitte. 2009. Eddy activity in the four major upwelling systems from satellite altimetry (1992–2007). *Prog. Oceanogr.* **83**: 117–123. doi:[10.1016/j.pocean.2009.07.012](https://doi.org/10.1016/j.pocean.2009.07.012)
- Chaigneau, A., N. Dominguez, G. Eldin, L. Vasquez, R. Flores, C. Grados, and V. Echevin. 2013. Near-coastal circulation in the Northern Humboldt Current System from shipboard ADCP data. *J. Geophys. Res. Ocean.* **118**: 5251–5266. doi:[10.1002/jgrc.20328](https://doi.org/10.1002/jgrc.20328)
- Christiansen, C. F., and C. R. Löscher. 2019. Facets of diazotrophy in the OMZ off Peru revisited- what we couldn't see from a single marker gene approach. *bioRxiv* 558072. doi:[10.1101/558072](https://doi.org/10.1101/558072)
- Clifford, E. L., D. A. Hansell, M. M. Varela, M. Nieto-Cid, G. J. Herndl, and E. Sintés. 2017. Crustacean zooplankton release copious amounts of dissolved organic matter as taurine in the ocean. *Limnol. Oceanogr.* **62**: 2745–2758. doi:[10.1002/lno.10603](https://doi.org/10.1002/lno.10603)
- Clifford, E. L., M. M. Varela, D. De Corte, A. Bode, V. Ortiz, G. J. Herndl, and E. Sintés. 2019. Taurine is a major carbon and energy source for marine prokaryotes in the North Atlantic Ocean off the Iberian Peninsula. *Microb. Ecol.* **78**: 299–312. doi:[10.1007/s00248-019-01320-y](https://doi.org/10.1007/s00248-019-01320-y)
- Cockcroft, A. C. 2002. *Jasus lalandii* “walkouts” or mass strandings in South Africa during the 1990s: An overview. *Mar. Freshw. Res.* **52**: 1085–1093. doi:[10.1071/MF01100](https://doi.org/10.1071/MF01100)
- Codispoti, L. A., J. A. Brandes, J. P. Christensen, A. H. Devol, S. A. W. Naqvi, H. W. Paerl, and T. Yoshinari. 2001. The oceanic fixed nitrogen and nitrous oxide budgets: Moving targets as we enter the anthropocene? *Sci. Mar.* **65**: 85–105.
- Copenhagen, W. J. 1954. The periodic mortality of fish in the Walvis region. *S. Afr. Med. J.* **28**: 381.
- Crowe, S. A., R. P. Cox, C. Jones, D. A. Fowle, J. F. Santibañez-Bustos, O. Ulloa, and D. E. Canfield. 2018. Decrypting the sulfur cycle in oceanic oxygen minimum zones. *ISME J.* **12**: 2322–2329. doi:[10.1038/s41396-018-0149-2](https://doi.org/10.1038/s41396-018-0149-2)
- Dahl, C., S. Engels, A. S. Pott-Sperling, A. Schulte, J. Sander, Y. Lübke, O. Deuster, and D. C. Brune. 2005. Novel genes of the dsr gene cluster and evidence for close interaction of Dsr proteins during sulfur oxidation in the phototrophic sulfur bacterium *Allochromatium vinosum*. *J. Bacteriol.* **187**: 1392–1404. doi:[10.1128/jb.187.4.1392-1404.2005](https://doi.org/10.1128/jb.187.4.1392-1404.2005)
- Dale, A. W., V. Brüchert, M. Alperin, and P. Regnier. 2009. An integrated sulfur isotope model for Namibian shelf sediments. *Geochim. Cosmochim. Acta* **73**: 1924–1944. doi:[10.1016/J.GCA.2008.12.015](https://doi.org/10.1016/J.GCA.2008.12.015)
- Dale, A. W., and others. 2015. Organic carbon production, mineralisation and preservation on the Peruvian margin. *Biogeosciences* **12**: 1537–1559. doi:[10.5194/bg-12-1537-2015](https://doi.org/10.5194/bg-12-1537-2015)
- Dale, A. W., M. Graco, and K. Wallmann. 2017. Strong and dynamic benthic-pelagic coupling and feedbacks in a coastal upwelling system (Peruvian shelf). *Front. Mar. Sci.* **4**: 29. doi:[10.3389/fmars.2017.00029](https://doi.org/10.3389/fmars.2017.00029)
- Dale, A. W. W., S. Sommer, U. Lomnitz, A. Bourbonnais, and K. Wallmann. 2016. Biological nitrate transport in sediments on the Peruvian margin mitigates benthic sulfide emissions and drives pelagic N loss during stagnation events. *Deep Sea Res. Part I Oceanogr. Res. Pap.* **112**: 123–136. <https://doi.org/10.1016/j.dsr.2016.02.013>
- Dalsgaard, T., D. E. Canfield, J. Petersen, B. Thamdrup, and J. Acuna-Gonzalez. 2003. N₂ production by the anammox reaction in the anoxic water column of Golfo Dulce, Costa Rica. *Nature* **422**: 606–608.
- Dalsgaard, T., F. J. Stewart, B. Thamdrup, L. De Brabandere, N. P. Revsbech, O. Ulloa, D. E. Canfield, and E. F. DeLong. 2014. Oxygen at nanomolar levels reversibly suppresses process rates and gene expression in anammox and denitrification in the oxygen minimum zone off Northern Chile. *MBio* **5**: e01966. doi:[10.1128/mBio.01966-14](https://doi.org/10.1128/mBio.01966-14)
- Dalsgaard, T., B. Thamdrup, L. Farías, and N. P. Revsbech. 2012. Anammox and denitrification in the oxygen minimum zone of the eastern South Pacific. *Limnol. Oceanogr.* **57**: 1331–1346. doi:[10.4319/lo.2012.57.5.1331](https://doi.org/10.4319/lo.2012.57.5.1331)
- Denger, K., H. Laue, and M. A. Cook. 1997. Thiosulfate as a metabolic product: The bacterial fermentation of taurine. *Arch. Microbiol.* **168**: 297–301. doi:[10.1007/s002030050502](https://doi.org/10.1007/s002030050502)
- DeVries, T., C. Deutsch, F. Primeau, B. Chang, and A. Devol. 2012. Global rates of water-column denitrification derived from nitrogen gas measurements. *Nat. Geosci.* **5**: 547–550. doi:[10.1038/NNGEO1515](https://doi.org/10.1038/NNGEO1515)
- Diaz, R. J., and R. Rosenberg. 2008. Spreading dead zones and consequences for marine ecosystems. *Science* **321**: 926–929. doi:[10.1126/science.1156401](https://doi.org/10.1126/science.1156401)
- Durham, B. P., and others. 2019. Sulfonate-based networks between eukaryotic phytoplankton and heterotrophic bacteria in the surface ocean. *Nat. Microbiol.* **4**: 1706–1715. doi:[10.1038/s41564-019-0507-5](https://doi.org/10.1038/s41564-019-0507-5)
- Echevin, V., O. Aumont, J. Ledesma, and G. Flores. 2008. The seasonal cycle of surface chlorophyll in the Peruvian upwelling system: A modelling study. *Prog. Oceanogr.* **79**: 167–176. doi:[10.1016/J.POCEAN.2008.10.026](https://doi.org/10.1016/J.POCEAN.2008.10.026)

- Eglinton, T. I., J. E. Irvine, A. Vairavamurthy, W. Zhou, and B. Manowitz. 1994. Formation and diagenesis of macromolecular organic sulfur in Peru margin sediments. *Org. Geochem.* **22**: 781–799. doi:10.1016/0146-6380(94)90139-2
- Espinoza-Morriberón, D., V. Echevin, F. Colas, J. Tam, D. Gutierrez, M. Graco, J. Ledesma, and C. Quispe-Ccalluari. 2019. Oxygen variability during ENSO in the tropical South Eastern Pacific. *Front. Mar. Sci.* **5**: 526. doi:10.3389/fmars.2018.00526
- Fariás, L., C. Fernández, J. Faúndez, M. Cornejo, and M. E. Alcaman. 2009. Chemolithoautotrophic production mediating the cycling of the greenhouse gases N₂O and CH₄ in an upwelling ecosystem. *Biogeosciences* **6**: 3053–3069. doi:10.5194/bg-6-3053-2009
- Felgate, H., G. Giannopoulos, M. J. Sullivan, A. J. Gates, T. A. Clarke, E. Baggs, G. Rowley, and D. J. Richardson. 2012. The impact of copper, nitrate and carbon status on the emission of nitrous oxide by two species of bacteria with biochemically distinct denitrification pathways. *Environ. Microbiol.* **14**: 1788–1800. doi:10.1111/j.1462-2920.2012.02789.x
- Ferdelman, T. G., C. Lee, S. Pantoja, J. Harder, B. M. Bebout, and H. Fossing. 1997. Sulfate reduction and methanogenesis in a *Thioploca*-dominated sediment off the coast of Chile. *Geochim. Cosmochim. Acta* **61**: 3065–3079. doi:10.1016/S0016-7037(97)00158-0
- Ferdelman, T. G., H. Fossing, K. Neumann, and H. D. Schulz. 1999. Sulfate reduction in surface sediments of the Southeast Atlantic continental margin between 15°38'S and 27°57'S (Angola and Namibia). *Limnol. Oceanogr.* **44**: 650–661. doi:10.4319/lo.1999.44.3.0650
- Finster, K. 2011. Microbiological disproportionation of inorganic sulfur compounds. *J. Sulfur Chem.* **29**: 281–292. doi:10.1080/17415990802105770
- Finster, K. W., and K. U. Kjeldsen. 2010. *Desulfovibrio oceani* subsp. *oceani* sp. nov., subsp. nov. and *Desulfovibrio oceani* subsp. *galataeae* subsp. nov., novel sulfate-reducing bacteria isolated from the oxygen minimum zone off the coast of Peru. *Antonie Van Leeuwenhoek* **97**: 221–229. doi:10.1007/s10482-009-9403-y
- Fonseca, A., T. Isohoy, C. Espinoza, D. Pérez-Pantoja, A. Manghisi, M. Morabito, A. Salas-Burgos, and V. A. Gallardo. 2017. Genomic features of “*Candidatus Venteria ishoeyi*,” a new sulfur-oxidizing macrobacterium from the Humboldt Sulfuretum off Chile. *PLoS One* **12**: e0188371. doi:10.1371/journal.pone.0188371
- Forth, M., B. Liljebladh, A. Stigebrandt, P. O. J. Hall, and A. H. Treusch. 2015. Effects of ecological engineered oxygenation on the bacterial community structure in an anoxic fjord in western Sweden. *ISME J.* **9**: 656–669. doi:10.1038/ismej.2014.172
- Fossing, H. 1990. Sulfate reduction in shelf sediments in the upwelling region off Central Peru. *Cont. Shelf Res.* **10**: 355–367. doi:10.1016/0278-4343(90)90056-R
- Fossing, H., and others. 1995. Concentration and transport of nitrate by the mat-forming sulphur bacterium *Thioploca*. *Nature* **374**: 713–715.
- Frey, C., and others. 2020. Regulation of nitrous oxide production in low-oxygen waters off the coast of Peru. *Biogeosciences* **17**: 2263–2287. doi:10.5194/bg-17-2263-2020, 8
- Frigaard, N.-U., and C. Dahl. 2008. Sulfur metabolism in phototrophic sulfur bacteria, p. 103–200. *In* K. P. Robert [ed.], *Advances in microbial physiology*. Academic Press.
- Fuchs, B. M., D. Woebken, M. V. Zubkov, P. Burkill, and R. Amann. 2005. Molecular identification of picoplankton populations in contrasting waters of the Arabian Sea. *Aquat. Microb. Ecol.* **39**: 145–157. doi:10.3354/ame039145
- Fuchsman, C. A., J. B. Kirkpatrick, W. J. Brazelton, J. W. Murray, and J. T. Staley. 2011. Metabolic strategies of free-living and aggregate-associated bacterial communities inferred from biologic and chemical profiles in the Black Sea suboxic zone. *FEMS Microbiol. Ecol.* **78**: 586–603. doi:10.1111/j.1574-6941.2011.01189.x
- Fuenzalida, R., W. Schneider, J. Garcés-Vargas, L. Bravo, and C. Lange. 2009. Vertical and horizontal extension of the oxygen minimum zone in the Eastern South Pacific Ocean. *Deep Sea Res. Part II Top. Stud. Oceanogr.* **56**: 992–1003. <https://doi.org/10.1016/j.dsr2.2008.11.001>
- Füssel, J., P. Lam, G. Lavik, M. M. Jensen, M. Holtappels, M. Gunter, and M. M. M. Kuypers. 2012. Nitrite oxidation in the Namibian oxygen minimum zone. *ISME J.* **6**: 1200–1209. doi:10.1038/ismej.2011.178
- Füssel, J., and others. 2017. Adaptability as the key to success for the ubiquitous marine nitrite oxidizer *Nitrococcus*. *Sci. Adv.* **3**: e1700807. doi:10.1126/sciadv.1700807
- Galán, A., J. Faúndez, B. Thamdrup, J. F. Santibáñez, and L. Fariás. 2014. Temporal dynamics of nitrogen loss in the coastal upwelling ecosystem off Central Chile: Evidence of autotrophic denitrification through sulfide oxidation. *Limnol. Oceanogr.* **59**: 1865–1878. doi:10.4319/lo.2014.59.6.1865
- Ganesh, S., D. J. Parris, E. F. DeLong, and F. J. Stewart. 2014. Metagenomic analysis of size-fractionated picoplankton in a marine oxygen minimum zone. *ISME J.* **8**: 187–211. doi:10.1038/ismej.2013.144
- Georges, A. A., H. El-Swais, S. E. Craig, W. K. Li, and D. A. Walsh. 2014. Metaproteomic analysis of a winter to spring succession in coastal Northwest Atlantic Ocean microbial plankton. *ISME J.* **8**: 1301–1313. doi:10.1038/ismej.2013.234
- Ghosh, W., and B. Dam. 2009. Biochemistry and molecular biology of lithotrophic sulfur oxidation by taxonomically and ecologically diverse bacteria and archaea. *FEMS Microbiol. Rev.* **33**: 999–1043. doi:10.1111/j.1574-6976.2009.00187.x
- Glass, J., and V. Orphan. 2012. Trace metal requirements for microbial enzymes involved in the production and

- consumption of methane and nitrous oxide. *Front. Microbiol.* **3**: 61. doi:10.3389/fmicb.2012.00061
- Glaubitx, S., M. Labrenz, G. Jost, and K. Jurgens. 2010. Diversity of active chemolithoautotrophic prokaryotes in the sulfidic zone of a Black Sea pelagic redoxcline as determined by rRNA-based stable isotope probing. *FEMS Microbiol. Ecol.* **74**: 32–41. doi:10.1111/j.1574-6941.2010.00944.x
- Glaubitx, S., K. Kiesslich, C. Meeske, M. Labrenz, and K. Jurgens. 2013. SUP05 dominates the gammaproteobacterial sulfur oxidizer assemblages in pelagic redoxclines of the Central Baltic and black seas. *Appl. Env. Microbiol.* **79**: 2767–2776. doi:10.1128/AEM.03777-12
- Godden, J. W., S. Turley, D. C. Teller, E. T. Adman, M. Y. Liu, W. J. Payne, and J. LeGall. 1991. The 2.3 angstrom X-ray structure of nitrite reductase from *Achromobacter cycloclastes*. *Science* **253**: 438 LP–442. doi:10.1126/science.1862344
- Goldhammer, T., V. Brüchert, T. G. Ferdelman, and M. Zabel. 2010. Microbial sequestration of phosphorus in anoxic upwelling sediments. *Nat. Geosci.* **3**: 557–561. doi:10.1038/ngeo913
- González, J. M., R. P. Kiene, and M. A. Moran. 1999. Transformation of sulfur compounds by an abundant lineage of marine bacteria in the alpha-subclass of the class Proteobacteria. *Appl. Environ. Microbiol.* **65**: 3810–3819.
- Graco, M. I., S. Purca, B. Dewitte, C. G. Castro, O. Morón, J. Ledesma, G. Flores, and D. Gutiérrez. 2017. The OMZ and nutrient features as a signature of interannual and low-frequency variability in the Peruvian upwelling system. *Biogeosciences* **14**: 4601–4617. doi:10.5194/bg-14-4601-2017
- Granger, J., and B. B. Ward. 2003. Accumulation of nitrogen oxides in copper-limited cultures of denitrifying bacteria. *Limnol. Oceanogr.* **48**: 313–318. doi:10.4319/lo.2003.48.1.0313
- Grote, J., G. Jost, M. Labrenz, G. J. Herndl, and K. Jurgens. 2008. Epsilonproteobacteria represent the major portion of chemoautotrophic bacteria in sulfidic waters of pelagic redoxclines of the Baltic and Black Seas. *Appl. Env. Microbiol.* **74**: 7546–7551. doi:10.1128/AEM.01186-08
- Grote, J., T. Schott, C. G. Bruckner, F. O. Glockner, G. Jost, H. Teeling, M. Labrenz, and K. Jurgens. 2012. Genome and physiology of a model epsilonproteobacterium responsible for sulfide detoxification in marine oxygen depletion zones. *Proc. Natl. Acad. Sci.* **109**: 506–510. doi:10.1073/pnas.1111262109
- Gruber, N., Z. Lachkar, H. Frenzel, P. Marchesiello, M. Munnich, J. C. McWilliams, T. Nagai, and G.-K. Plattner. 2011. Eddy-induced reduction of biological production in eastern boundary upwelling systems. *Nat. Geosci.* **4**: 787–792. doi:10.1038/ngeo1273
- Gutiérrez, D., E. Enríquez, S. Purca, L. Quipúzcoa, R. Marquina, G. Flores, and M. Graco. 2008. Oxygenation episodes on the continental shelf of central Peru: Remote forcing and benthic ecosystem response. *Prog. Oceanogr.* **79**: 177–189. doi:10.1016/j.pcean.2008.10.025
- Halm, H., and others. 2009. Co-occurrence of denitrification and nitrogen fixation in a meromictic lake, Lake Cadagno (Switzerland). *Env. Microbiol.* **11**: 1945–1958. doi:10.1111/j.1462-2920.2009.01917.x
- Hammersley, M. R., and others. 2007. Anaerobic ammonium oxidation in the Peruvian oxygen minimum zone. *Limnol. Oceanogr.* **52**: 923–933. doi:10.4319/lo.2007.52.3.0923
- Hamukuaya, H., M. J. O’Toole, and P. M. J. Woodhead. 1998. Observations of severe hypoxia and offshore displacement of Cape hake over the Namibian shelf in 1994. *South African J. Mar. Sci.* **19**: 57–59. doi:10.2989/025776198784126809
- Hawley, A. K., H. M. Brewer, A. D. Norbeck, L. Paša-Tolić, and S. J. Hallam. 2014. Metaproteomics reveals differential modes of metabolic coupling among ubiquitous oxygen minimum zone microbes. *Proc. Natl. Acad. Sci.* **111**: 11395–11400. doi:10.1073/pnas.1322132111
- Hawley, A. K., and others. 2017. Diverse Marinimicrobia bacteria may mediate coupled biogeochemical cycles along ecothermodynamic gradients. *Nat. Commun.* **8**: 1507. doi:10.1038/s41467-017-01376-9
- Hayes, M. K., G. T. Taylor, Y. Astor, and M. I. Scranton. 2006. Vertical distributions of thiosulfate and sulfite in the Cariaco Basin. *Limnol. Oceanogr.* **51**: 280–287. doi:10.4319/lo.2006.51.1.0280
- Ho, T.-Y., M. I. Scranton, G. T. Taylor, R. Varela, R. C. Thunell, and F. Muller-Karger. 2002. Acetate cycling in the water column of the Cariaco Basin: Seasonal and vertical variability and implication for carbon cycling. *Limnol. Oceanogr.* **47**: 1119–1128. doi:10.4319/lo.2002.47.4.1119
- Hogslund, S., and others. 2009. Physiology and behaviour of marine *Thioploca*. *ISME J.* **3**: 647–657.
- Huettel, M., S. Forster, S. Kloser, and H. Fossing. 1996. Vertical migration in the sediment-dwelling sulfur bacteria *Thioploca* spp. in overcoming diffusion limitations. *Appl. Environ. Microbiol.* **62**: 1863–1872.
- Hutchings, L., and others. 2009. The Benguela current: An ecosystem of four components. *Prog. Oceanogr.* **83**: 15–32. doi:10.1016/j.pcean.2009.07.046
- Jensen, M. M., P. Lam, N. P. Revsbech, B. Nagel, B. Gaye, M. S. Jetten, and M. M. Kuypers. 2011. Intensive nitrogen loss over the Omani Shelf due to anammox coupled with dissimilatory nitrite reduction to ammonium. *ISME J.* **5**: 1660–1670. doi:10.1038/ismej.2011.44
- Johnston, D. T., F. Wolfe-Simon, A. Pearson, and A. H. Knoll. 2009. Anoxygenic photosynthesis modulated proterozoic oxygen and sustained earth’s middle age. *Proc. Natl. Acad. Sci.* **106**: 16925–16929. doi:10.1073/pnas.0909248106
- Johnston, D. T., B. C. Gill, A. Masterson, E. Beirne, K. L. Casciotti, A. N. Knapp, and W. Berelson. 2014. Placing an

- upper limit on cryptic marine sulphur cycling. *Nature* **513**: 530–533. doi:[10.1038/nature13698](https://doi.org/10.1038/nature13698)
- Jones, D. S., B. E. Flood, and J. V. Bailey. 2016. Metatranscriptomic insights into polyphosphate metabolism in marine sediments. *ISME J.* **10**: 1015–1019. doi:[10.1038/ismej.2015.169](https://doi.org/10.1038/ismej.2015.169)
- Jørgensen, B. B. 1982. Mineralization of organic matter in the sea bed—The role of sulphate reduction. *Nature* **296**: 643–645. doi:[10.1038/296643a0](https://doi.org/10.1038/296643a0)
- Jørgensen, B. B., A. J. Findlay, and A. Pellerin. 2019. The biogeochemical sulfur cycle of marine sediments. *Front. Microbiol.* **10**: 849. doi:[10.3389/fmicb.2019.00849](https://doi.org/10.3389/fmicb.2019.00849)
- Kalvelage, T., and others. 2013. Nitrogen cycling driven by organic matter export in the South Pacific oxygen minimum zone. *Nat. Geosci.* **6**: 228–234. doi:[10.1038/ngeo1739](https://doi.org/10.1038/ngeo1739)
- Kappler, U. 2008. Bacterial sulfite-oxidizing enzymes – Enzymes for chemolithotrophs only? p. 151–169. *In* C. Dahl and C. G. Friedrich [eds.], *Microbial sulfur metabolism*. Springer.
- Karl, D. M., G. A. Knauer, J. H. Martin, and B. B. Ward. 1984. Bacterial chemolithotrophy in the ocean is associated with sinking particles. *Nature* **309**: 54–56.
- Karstensen, J., L. Stramma, and M. Visbeck. 2008. Oxygen minimum zones in the eastern tropical Atlantic and Pacific oceans. *Prog. Oceanogr.* **77**: 331–350. doi:[10.1016/j.pocan.2007.05.009](https://doi.org/10.1016/j.pocan.2007.05.009)
- Kasten, S., and B. B. Jørgensen. 2000. Sulfate reduction in marine sediments, p. 263–281. *In* H. D. Schulz and M. Zabel [eds.], *Marine geochemistry*. Springer.
- Kertesz, M. A. 2000. Riding the sulfur cycle—Metabolism of sulfonates and sulfate esters in Gram-negative bacteria. *FEMS Microbiol. Rev.* **24**: 135–175. doi:[10.1111/j.1574-6976.2000.tb00537.x](https://doi.org/10.1111/j.1574-6976.2000.tb00537.x)
- Kloster, S., J. Feichter, E. Maier-Reimer, K. D. Six, P. Stier, and P. Wetzell. 2006. DMS cycle in the marine ocean-atmosphere system—A global model study. *Biogeosciences* **3**: 29–51. doi:[10.5194/bg-3-29-2006](https://doi.org/10.5194/bg-3-29-2006)
- Kock, A., D. L. Arévalo-Martínez, C. R. Löscher, and H. W. Bange. 2016. Extreme N₂O accumulation in the coastal oxygen minimum zone off Peru. *Biogeosciences* **13**: 827–840. doi:[10.5194/bg-13-827-2016](https://doi.org/10.5194/bg-13-827-2016)
- Kondo, Y., and J. W. Moffett. 2015. Iron redox cycling and subsurface offshore transport in the eastern tropical South Pacific oxygen minimum zone. *Mar. Chem.* **168**: 95–103. doi:[10.1016/j.marchem.2014.11.007](https://doi.org/10.1016/j.marchem.2014.11.007)
- Ksionzek, K. B., O. J. Lechtenfeld, S. L. McCallister, P. Schmitt-Kopplin, J. K. Geuer, W. Geibert, and B. P. Koch. 2016. Dissolved organic sulfur in the ocean: Biogeochemistry of a petagram inventory. *Science* **354**: 456–459. doi:[10.1126/science.aaf7796](https://doi.org/10.1126/science.aaf7796)
- Kuypers, M. M. M., G. Lavik, D. Woebken, M. Schmid, B. M. Fuchs, R. Amann, B. B. Jørgensen, and M. S. M. Jetten. 2005. Massive nitrogen loss from the Benguela upwelling system through anaerobic ammonium oxidation. *Proc. Natl. Acad. Sci. USA.* **102**: 6478–6483. doi:[10.1073/pnas.0502088102](https://doi.org/10.1073/pnas.0502088102)
- Kuypers, M. M. M., and others. 2003. Anaerobic ammonium oxidation by anammox bacteria in the Black Sea. *Nature* **422**: 608–611.
- Lahme, S., C. M. Callbeck, L. E. Eland, A. Wipat, D. Enning, I. M. Head, and C. R. J. Hubert. 2020. Comparison of sulfide-oxidizing *Sulfurimonas* strains reveals a new mode of thiosulfate formation in subsurface environments. *Environ. Microbiol.* **22**: 1784–1800. doi:[10.1111/1462-2920.14894](https://doi.org/10.1111/1462-2920.14894)
- Lam, P., and others. 2009. Revising the nitrogen cycle in the Peruvian oxygen minimum zone. *Proc. Natl. Acad. Sci. USA.* **106**: 4752–4757. doi:[10.1073/pnas.0812444106](https://doi.org/10.1073/pnas.0812444106)
- Lam, P., and M. M. M. Kuypers. 2011. Microbial nitrogen cycling processes in oxygen minimum zones. *Ann. Rev. Mar. Sci.* **3**: 317–345. doi:[10.1146/annurev-marine-120709-142814](https://doi.org/10.1146/annurev-marine-120709-142814)
- Lamont, T., R. J. W. Brewin, and R. G. Barlow. 2018. Seasonal variation in remotely-sensed phytoplankton size structure around southern Africa. *Remote Sens. Environ.* **204**: 617–631. doi:[10.1016/j.rse.2017.09.038](https://doi.org/10.1016/j.rse.2017.09.038)
- Lamont, T., R. G. Barlow, and R. J. W. Brewin. 2019. Long-term trends in phytoplankton chlorophyll a and size structure in the Benguela upwelling system. *J. Geophys. Res. Ocean.* **124**: 1170–1195. doi:[10.1029/2018JC014334](https://doi.org/10.1029/2018JC014334)
- Lana, A., and others. 2011. An updated climatology of surface dimethylsulfide concentrations and emission fluxes in the global ocean. *Global Biogeochem. Cycles* **25**: 1–17. doi:[10.1029/2010GB003850](https://doi.org/10.1029/2010GB003850)
- Landa, M., and others. 2019. Sulfur metabolites that facilitate oceanic phytoplankton–bacteria carbon flux. *ISME J.* **13**: 2536–2550. doi:[10.1038/s41396-019-0455-3](https://doi.org/10.1038/s41396-019-0455-3)
- Lavik, G., and others. 2009. Detoxification of sulphidic African shelf waters by blooming chemolithotrophs. *Nature* **457**: 581–584. doi:[10.1038/nature07588](https://doi.org/10.1038/nature07588)
- Léniz, B., A. A. Murillo, S. Ramírez-Flandes, and O. Ulloa. 2017. Diversity and transcriptional levels of RuBisCO form II of sulfur-oxidizing γ -proteobacteria in coastal-upwelling waters with seasonal anoxia. *Front. Mar. Sci.* **4**: 213. doi:[10.3389/fmars.2017.00213](https://doi.org/10.3389/fmars.2017.00213)
- Lenk, S., and others. 2012. Roseobacter clade bacteria are abundant in coastal sediments and encode a novel combination of sulfur oxidation genes. *ISME J.* **6**: 2178–2187. doi:[10.1038/ismej.2012.66](https://doi.org/10.1038/ismej.2012.66)
- Levin, L. A., and others. 2009. Effects of natural and human-induced hypoxia on coastal benthos. *Biogeosciences* **6**: 2063–2098. doi:[10.5194/bg-6-2063-2009](https://doi.org/10.5194/bg-6-2063-2009)
- Li, X., G. T. Taylor, Y. Astor, and M. I. Scranton. 2008. Relationship of sulfur speciation to hydrographic conditions and chemoautotrophic production in the Cariaco Basin. *Mar. Chem.* **112**: 53–64. doi:[10.1016/j.marchem.2008.06.002](https://doi.org/10.1016/j.marchem.2008.06.002)
- Lie, T. J., T. Pitta, E. R. Leadbetter, W. Godchaux III, and J. R. Leadbetter. 1996. Sulfonates: Novel electron acceptors in

- anaerobic respiration. *Arch. Microbiol.* **166**: 204–210. doi:[10.1007/s002030050376](https://doi.org/10.1007/s002030050376)
- Loginova, A. N., S. Thomsen, and A. Engel. 2016. Chromophoric and fluorescent dissolved organic matter in and above the oxygen minimum zone off Peru. *J. Geophys. Res. Ocean.* **121**: 7973–7990. doi:[10.1002/2016jc011906](https://doi.org/10.1002/2016jc011906)
- Lomnitz, U., S. Sommer, A. W. Dale, C. R. Löscher, A. Noffke, K. Wallmann, and C. Hensen. 2016. Benthic phosphorus cycling in the Peruvian oxygen minimum zone. *Biogeosciences* **13**: 1367–1386. doi:[10.5194/bg-13-1367-2016](https://doi.org/10.5194/bg-13-1367-2016)
- Löscher, C. R., and others. 2014. Facets of diazotrophy in the oxygen minimum zone waters off Peru. *ISME J.* **8**: 2180–2192. doi:[10.1038/ismej.2014.71](https://doi.org/10.1038/ismej.2014.71)
- Louca, S., and others. 2016. Integrating biogeochemistry with multiomic sequence information in a model oxygen minimum zone. *Proc. Natl. Acad. Sci.* **113**: E5925–E5933. doi:[10.1073/pnas.1602897113](https://doi.org/10.1073/pnas.1602897113)
- Lüdke, J., and others. 2019. Influence of intraseasonal eastern boundary circulation variability on hydrography and biogeochemistry off Peru. *Ocean Sci. Discuss.* **2019**: 1–31. doi:[10.5194/os-2019-93](https://doi.org/10.5194/os-2019-93)
- Lukumbuzya, M., M. Schmid, P. Pjevac, and H. Daims. 2019. A multicolor fluorescence in situ hybridization approach using an extended set of fluorophores to visualize microorganisms. *Front. Microbiol.* **10**: 1383. doi:[10.3389/fmicb.2019.01383](https://doi.org/10.3389/fmicb.2019.01383)
- Maier, S., and V. A. Gallardo. 1984. *Thioploca araucae* sp. nov. and *Thioploca chilae* sp. nov. *Int. J. Syst. Bacteriol.* **34**: 414–418. doi:[10.1099/00207713-34-4-414](https://doi.org/10.1099/00207713-34-4-414)
- Maltby, J., S. Sommer, A. W. Dale, and T. Treude. 2016. Microbial methanogenesis in the sulfate-reducing zone of surface sediments traversing the Peruvian margin. *Biogeosciences* **13**: 283–299. doi:[10.5194/bg-13-283-2016](https://doi.org/10.5194/bg-13-283-2016)
- Manconi, I., P. van der Maas, and P. Lens. 2006. Effect of copper dosing on sulfide inhibited reduction of nitric and nitrous oxide. *Nitric Oxide Biol. Chem.* **15**: 400–407. doi:[10.1016/j.niox.2006.04.262](https://doi.org/10.1016/j.niox.2006.04.262)
- Marschall, E., M. Jogler, U. Henßge, and J. Overmann. 2010. Large-scale distribution and activity patterns of an extremely low-light-adapted population of green sulfur bacteria in the Black Sea. *Environ. Microbiol.* **12**: 1348–1362. doi:[10.1111/j.1462-2920.2010.02178.x](https://doi.org/10.1111/j.1462-2920.2010.02178.x)
- Marshall, K. T., and R. M. Morris. 2013. Isolation of an aerobic sulfur oxidizer from the SUP05/Arctic96BD-19 clade. *ISME J.* **7**: 452–455. doi:[10.1038/ismej.2012.78](https://doi.org/10.1038/ismej.2012.78)
- Marshall, K. T., and R. M. Morris. 2015. Genome sequence of “*Candidatus Thioglobus singularis*” strain PS1, a mixotroph from the SUP05 clade of marine gammaproteobacteria. *Genome Announc.* **3**: e01155–15. doi:[10.1128/genomeA.01155-15](https://doi.org/10.1128/genomeA.01155-15)
- Martens, C. S., and J. Val Klump. 1980. Biogeochemical cycling in an organic-rich coastal marine basin—I. Methane sediment-water exchange processes. *Geochim. Cosmochim. Acta* **44**: 471–490. doi:[10.1016/0016-7037\(80\)90045-9](https://doi.org/10.1016/0016-7037(80)90045-9)
- Martens, C. S., D. B. Albert, and M. J. Alperin. 1998. Biogeochemical processes controlling methane in gassy coastal sediments—Part 1. A model coupling organic matter flux to gas production, oxidation and transport. *Cont. Shelf Res.* **18**: 1741–1770. doi:[10.1016/S0278-4343\(98\)00056-9](https://doi.org/10.1016/S0278-4343(98)00056-9)
- Martínez-Pérez, C., and others. 2016. The small unicellular diazotrophic symbiont, UCYN-A, is a key player in the marine nitrogen cycle. *Nat. Microbiol.* **1**: 16163. doi:[10.1038/nmicrobiol.2016.163](https://doi.org/10.1038/nmicrobiol.2016.163)
- Martínez-Pérez, C., and others. 2018. Metabolic versatility of a novel N₂-fixing Alphaproteobacterium isolated from a marine oxygen minimum zone. *Environ. Microbiol.* **20**: 755–768. doi:[10.1111/1462-2920.14008](https://doi.org/10.1111/1462-2920.14008)
- McParland, E. L., and N. M. Levine. 2019. The role of differential DMSP production and community composition in predicting variability of global surface DMSP concentrations. *Limnol. Oceanogr.* **64**: 757–773. doi:[10.1002/lno.11076](https://doi.org/10.1002/lno.11076)
- Meier, D. V., P. Pjevac, W. Bach, S. Hourdez, P. R. Girguis, C. Vidoudez, R. Amann, and A. Meyerdierks. 2017. Niche partitioning of diverse sulfur-oxidizing bacteria at hydrothermal vents. *ISME J.* **11**: 1545–1558. doi:[10.1038/ismej.2017.37](https://doi.org/10.1038/ismej.2017.37)
- Michiels, C. C., J. A. Huggins, K. E. Giesbrecht, J. S. Spence, R. L. Simister, D. E. Varela, S. J. Hallam, and S. A. Crowe. 2019. Rates and pathways of N₂ production in a persistently Anoxic Fjord: Saanich inlet, British Columbia. *Front. Mar. Sci.* **6**: 1–23. doi:[10.3389/fmars.2019.00027](https://doi.org/10.3389/fmars.2019.00027)
- Moffett, J. W., C. B. Tuit, and B. B. Ward. 2012. Chelator-induced inhibition of copper metalloenzymes in denitrifying bacteria. *Limnol. Oceanogr.* **57**: 272–280. doi:[10.4319/lo.2012.57.1.0272](https://doi.org/10.4319/lo.2012.57.1.0272)
- Monteiro, P. M. S., and A. K. van der Plas. 2006. Low oxygen water (LOW) variability in the Benguela system: Key processes and forcing scales relevant to forecasting, p. 71–90. *In* V. Shannon, G. Hempel, P. Malanotte-Rizzoli, C. Moloney, and J. Woods [eds.], *Large marine ecosystems*. Elsevier.
- Monteiro, P. M. S., A. K. van der Plas, J. L. Mélice, and P. Florenchie. 2008. Interannual hypoxia variability in a coastal upwelling system: Ocean–shelf exchange, climate and ecosystem-state implications. *Deep Sea Res. Part I Oceanogr. Res. Pap.* **55**: 435–450. doi:[10.1016/j.dsr.2007.12.010](https://doi.org/10.1016/j.dsr.2007.12.010)
- Moran, M. A., and B. P. Durham. 2019. Sulfur metabolites in the pelagic ocean. *Nat. Rev. Microbiol.* **17**: 665–678. doi:[10.1038/s41579-019-0250-1](https://doi.org/10.1038/s41579-019-0250-1)
- Muyzer, G., and A. J. M. Stams. 2008. The ecology and biotechnology of sulphate-reducing bacteria. *Nat. Rev. Micro.* **6**: 441–454.
- Nagai, T., N. Gruber, H. Frenzel, Z. Lachkar, J. C. McWilliams, and G.-K. Plattner. 2015. Dominant role of eddies and filaments in the offshore transport of carbon and nutrients in the California current system. *J. Geophys. Res. Ocean.* **120**: 5318–5341. doi:[10.1002/2015jc010889](https://doi.org/10.1002/2015jc010889)

- Naqvi, S. W. A., D. A. Jayakumar, P. V. Narvekar, H. Naik, V. V. S. S. Sarma, W. D'Souza, S. Joseph, and M. D. George. 2000. Increased marine production of N₂O due to intensifying anoxia on the Indian continental shelf. *Nature* **408**: 346–349. doi:[10.1038/35042551](https://doi.org/10.1038/35042551)
- Naqvi, S. A. W., H. Naik, D. A. Jayakumar, M. S. Shailaja, and P. V. Narvekar. 2006. Seasonal oxygen deficiency over the western continental shelf of India, p. 195–224. *In* N. L. Neretin [ed.], *Past and present water column anoxia*. Springer.
- Neretin, L. N., M. E. Böttcher, and V. A. Grinenko. 2003. Sulfur isotope geochemistry of the Black Sea water column. *Chem. Geol.* **200**: 59–69. doi:[10.1016/s0009-2541\(03\)00129-3](https://doi.org/10.1016/s0009-2541(03)00129-3)
- Neumann, A., N. Lahajnar, and K.-C. Emeis. 2016. Benthic remineralisation rates in shelf and slope sediments of the northern Benguela upwelling margin. *Cont. Shelf Res.* **113**: 47–61. doi:[10.1016/j.csr.2015.12.009](https://doi.org/10.1016/j.csr.2015.12.009)
- Noffke, A., C. Hensen, S. Sommer, F. Scholz, L. Bohlen, T. Mosch, M. Graco, and K. Wallmann. 2012. Benthic iron and phosphorus fluxes across the Peruvian oxygen minimum zone. *Limnol. Oceanogr.* **57**: 851–867. doi:[10.4319/lo.2012.57.3.0851](https://doi.org/10.4319/lo.2012.57.3.0851)
- Nojiri, M., and others. 2007. Structure and function of a hexameric copper-containing nitrite reductase. *Proc. Natl. Acad. Sci.* **104**: 4315–4320. doi:[10.1073/pnas.0609195104](https://doi.org/10.1073/pnas.0609195104)
- Ohde, T. 2018. Coastal sulfur plumes off Peru during El Niño, La Niña, and neutral phases. *Geophys. Res. Lett.* **45**: 7075–7083. doi:[10.1029/2018GL077618](https://doi.org/10.1029/2018GL077618)
- Ohde, T., and I. Dadou. 2018. Seasonal and annual variability of coastal sulphur plumes in the northern Benguela upwelling system. *PLoS One* **13**: e0192140.
- Ohde, T., H. Siegel, J. Reißmann, and M. Gerth. 2007. Identification and investigation of sulphur plumes along the Namibian coast using the MERIS sensor. *Cont. Shelf Res.* **27**: 744–756. doi:[10.1016/j.csr.2006.11.016](https://doi.org/10.1016/j.csr.2006.11.016)
- Otte, S., and others. 1999. Nitrogen, carbon, and sulfur metabolism in natural thioploca samples. *Appl. Environ. Microbiol.* **65**: 3148–3157.
- Overmann, J., and A. K. Manske. 2006. Anoxygenic phototrophic bacteria in the Black Sea chemocline, p. 523–541. *In* L. N. Neretin [ed.], *Past and present water column anoxia*. Springer.
- Pan, Y., L. Ye, and Z. Yuan. 2013. Effect of H₂S on N₂O reduction and accumulation during denitrification by methanol utilizing denitrifiers. *Environ. Sci. Technol.* **47**: 8408–8415. doi:[10.1021/es401632r](https://doi.org/10.1021/es401632r)
- Peck, S. C., K. Denger, A. Burrichter, S. M. Irwin, E. P. Balskus, and D. Schleheck. 2019. A glycyl radical enzyme enables hydrogen sulfide production by the human intestinal bacterium *Bilophila wadsworthia*. *Proc. Natl. Acad. Sci.* **116**: 3171–3176. doi:[10.1073/pnas.1815661116](https://doi.org/10.1073/pnas.1815661116)
- Pietri, A., and others. 2013. Finescale vertical structure of the upwelling system off southern Peru as observed from glider data. *J. Phys. Oceanogr.* **43**: 631–646. doi:[10.1175/JPO-D-12-035.1](https://doi.org/10.1175/JPO-D-12-035.1)
- Pjevac, P., A. Kamyshny Jr., S. Dyksma, and M. Mußmann. 2014. Microbial consumption of zero-valence sulfur in marine benthic habitats. *Environ. Microbiol.* **16**: 3416–3430. doi:[10.1111/1462-2920.12410](https://doi.org/10.1111/1462-2920.12410)
- Plass, A., C. Schlosser, S. Sommer, A. W. Dale, E. P. Achterberg, and F. Scholz. 2019. The control of hydrogen sulfide on benthic iron and cadmium fluxes in the oxygen minimum zone off Peru. *Biogeosci. Discuss.* **2019**: 1–52. doi:[10.5194/bg-2019-390](https://doi.org/10.5194/bg-2019-390)
- Plominsky, A. M., N. Trefault, S. Podell, J. M. Blanton, R. De la Iglesia, E. E. Allen, P. von Dassow, and O. Ulloa. 2018. Metabolic potential and in situ transcriptomic profiles of previously uncharacterized key microbial groups involved in coupled carbon, nitrogen and sulfur cycling in anoxic marine zones. *Environ. Microbiol.* **20**: 2727–2742. doi:[10.1111/1462-2920.14109](https://doi.org/10.1111/1462-2920.14109)
- Pohlbeln, A. M., G. V. Gomez-Saez, B. E. Noriega-Ortega, and T. Dittmar. 2017. Experimental evidence for abiotic sulfurization of marine dissolved organic matter. *Front. Mar. Sci.* **4**: 364.
- Pratihary, A. K., S. W. A. Naqvi, G. Narvenkar, S. Kurian, H. Naik, R. Naik, and B. R. Manjunatha. 2014. Benthic mineralization and nutrient exchange over the inner continental shelf of Western India. *Biogeosciences* **11**: 2771–2791. doi:[10.5194/bg-11-2771-2014](https://doi.org/10.5194/bg-11-2771-2014)
- Prokopenko, M. G., D. E. Hammond, W. M. Berelson, J. M. Bernhard, L. Stott, and R. Douglas. 2006. Nitrogen cycling in the sediments of Santa Barbara basin and eastern subtropical North Pacific: Nitrogen isotopes, diagenesis and possible chemosymbiosis between two lithotrophs (*Thioploca* and *Anammox*)—"riding on a glider". *Earth Planet. Sci. Lett.* **242**: 186–204. doi:<https://doi.org/10.1016/j.epsl.2005.11.044>
- Prokopenko, M. G., and others. 2013. Nitrogen losses in anoxic marine sediments driven by *Thioploca*-*anammox* bacterial consortia. *Nature* **500**: 194–198. doi:[10.1038/nature12365](https://doi.org/10.1038/nature12365)
- Ramos, A., K. Keller, J. Wall, and I. A. Pereira. 2012. The membrane QmoABC complex interacts directly with the dissimilatory adenosine 5'-phosphosulfate reductase in sulfate reducing bacteria. *Front. Microbiol.* **3**: 1–10. doi:[10.3389/fmicb.2012.00137](https://doi.org/10.3389/fmicb.2012.00137)
- Revsbech, N. P., L. H. Larsen, J. Gundersen, T. Dalsgaard, O. Ulloa, and B. Thamdrup. 2009. Determination of ultra-low oxygen concentrations in oxygen minimum zones by the STOX sensor. *Limnol. Oceanogr. Methods* **7**: 371–381. doi:[10.4319/lom.2009.7.371](https://doi.org/10.4319/lom.2009.7.371)
- Rodriguez-Mora, M. J., M. I. Scranton, G. T. Taylor, and A. Y. Chistoserdov. 2013. Bacterial community composition in a large marine anoxic basin: A Cariaco Basin time-series survey. *FEMS Microbiol. Ecol.* **84**: 625–639. doi:[10.1111/1574-6941.12094](https://doi.org/10.1111/1574-6941.12094)

- Roux, S., and others. 2014. Ecology and evolution of viruses infecting uncultivated SUP05 bacteria as revealed by single-cell- and meta-genomics. *Elife* **3**: e03125. doi:10.7554/eLife.03125
- Roux, S., and others. 2016. Ecogenomics and potential biogeochemical impacts of globally abundant ocean viruses. *Nature* **537**: 689–693. doi:10.1038/nature19366
- Russ, L., D. R. Speth, M. S. M. Jetten, H. J. M. Op den Camp, and B. Kartal. 2014. Interactions between anaerobic ammonium and sulfur-oxidizing bacteria in a laboratory scale model system. *Env. Microbiol.* **16**: 3487–3498. doi:10.1111/1462-2920.12487
- Saito, M. A., D. M. Sigman, and F. M. Morel. 2003. The bioinorganic chemistry of the ancient ocean: The co-evolution of cyanobacterial metal requirements and biogeochemical cycles at the Archean–Proterozoic boundary? *Inorganica Chim. Acta* **356**: 308–318. doi:10.1016/S0020-1693(03)00442-0
- Santos, A. A., S. S. Venceslau, F. Grein, W. D. Leavitt, C. Dahl, D. T. Johnston, and I. A. C. Pereira. 2015. A protein trisulfide couples dissimilatory sulfate reduction to energy conservation. *Science* **350**: 1541–1545. doi:10.1126/science.aad3558
- Schlosser, C., P. Streu, M. Frank, G. Lavik, P. L. Croot, M. Dengler, and E. P. Achterberg. 2018. H₂S events in the Peruvian oxygen minimum zone facilitate enhanced dissolved Fe concentrations. *Sci. Rep.* **8**: 12642. doi:10.1038/s41598-018-30580-w
- Schmaljohann, R., M. Drews, S. Walter, P. Linke, U. Von Rad, and J. F. Imhoff. 2001. Oxygen-minimum zone sediments in the northeastern Arabian Sea off Pakistan: A habitat for the bacterium *Thioploca*. *Mar. Ecol. Prog. Ser.* **211**: 27–42. doi:10.3354/meps211027
- Scholz, F., J. McManus, A. C. Mix, C. Hensen, and R. R. Schneider. 2014. The impact of ocean deoxygenation on iron release from continental margin sediments. *Nat. Geosci.* **7**: 433–437. doi:10.1038/ngeo2162
- Schubert, C. J., T. G. Ferdelman, and B. Strotmann. 2000. Organic matter composition and sulfate reduction rates in sediments off Chile. *Org. Geochem.* **31**: 351–361. doi:10.1016/S0146-6380(00)00005-X
- Schubert, C. J., J. Niggemann, G. Klockgether, and T. G. Ferdelman. 2005. Chlorin index: A new parameter for organic matter freshness in sediments. *Geochem. Geophys. Geosyst.* **6**: 1–12. doi:10.1029/2004GC000837
- Schulz, H. N., T. Brinkhoff, T. G. Ferdelman, M. H. Mariné, A. Teske, and B. B. Jørgensen. 1999. Dense populations of a giant sulfur bacterium in Namibian shelf sediments. *Science* **284**: 493–495. doi:10.1126/science.284.5413.493
- Schulz, H. N., and H. D. Schulz. 2005. Large sulfur Bacteria and the formation of phosphorite. *Science* **307**: 416–418. doi:10.1126/science.1103096
- Schunck, H., and others. 2013. Giant hydrogen sulfide plume in the oxygen minimum zone off Peru supports chemolithoautotrophy. *PLoS One* **8**: e68661. doi:10.1371/journal.pone.0068661
- Shah, V., and R. M. Morris. 2015. Genome sequence of “*Candidatus Thioglobus autotrophica*” strain EF1, a chemoautotroph from the SUP05 clade of marine gammaproteobacteria. *Genome Announc.* **3**: e01156–e01115. doi:10.1128/genomeA.01156-15
- Shah, V., B. X. Chang, and R. M. Morris. 2016. Cultivation of a chemoautotroph from the SUP05 clade of marine bacteria that produces nitrite and consumes ammonium. *ISME J.* **11**: 263–272. doi:10.1038/ismej.2016.87
- Shah, V., X. Zhao, R. A. Lundeen, A. E. Ingalls, D. Nicastro, and R. M. Morris. 2019. Morphological plasticity in a sulfur-oxidizing marine bacterium from the SUP05 clade enhances dark carbon fixation. *MBio* **10**: e00216–e00219. doi:10.1128/mBio.00216-19
- Sheik, C. S., S. Jain, and G. J. Dick. 2014. Metabolic flexibility of enigmatic SAR324 revealed through metagenomics and metatranscriptomics. *Env. Microbiol.* **16**: 304–317. doi:10.1111/1462-2920.12165
- Shenoy, D. M., K. B. Sujith, M. U. Gauns, S. Patil, A. Sarkar, H. Naik, P. V. Narvekar, and S. W. A. Naqvi. 2012. Production of dimethylsulphide during the seasonal anoxia off Goa. *Biogeochemistry* **110**: 47–55. doi:10.1007/s10533-012-9720-5
- Shirodkar, G., S. W. A. Naqvi, H. Naik, A. K. Pratihary, S. Kurian, and D. M. Shenoy. 2018. Methane dynamics in the shelf waters of the West coast of India during seasonal anoxia. *Mar. Chem.* **203**: 55–63. doi:10.1016/J.MARCHEM.2018.05.001
- Shivani, Y., Y. Subhash, C. Sasikala, and C. V. Ramana. 2017. *Halodesulfobvibrio spirochaetisodalis* gen. nov. sp. nov. and reclassification of four *Desulfobvibrio* spp. *Int. J. Syst. Evol. Microbiol.* **67**: 87–93. doi:10.1099/ijsem.0.001574
- Sievert, S. M., E. B. A. Wieringa, C. O. Wirsen, and C. D. Taylor. 2007. Growth and mechanism of filamentous-sulfur formation by *Candidatus Arcobacter sulfidicus* in opposing oxygen-sulfide gradients. *Env. Microbiol.* **9**: 271–276. doi:10.1111/j.1462-2920.2006.01156.x
- Smith, D. A., A. L. Sessions, K. S. Dawson, N. Dalleska, and V. J. Orphan. 2017. Rapid quantification and isotopic analysis of dissolved sulfur species. *Rapid Commun. Mass Spect.* **31**: 791–803. doi:10.1002/rcm.7846
- Sommer, S., J. Gier, T. Treude, U. Lomnitz, M. Dengler, J. Cardich, and A. W. Dale. 2016. Depletion of oxygen, nitrate and nitrite in the Peruvian oxygen minimum zone cause an imbalance of benthic nitrogen fluxes. *Deep Sea Res. Part I Oceanogr. Res. Pap.* **112**: 113–122. doi:10.1016/j.dsr.2016.03.001
- Sørensen, K. B., and D. E. Canfield. 2004. Annual fluctuations in sulfur isotope fractionation in the water column of a euxinic marine basin. *Geochim. Cosmochim. Acta* **68**: 503–515. doi:10.1016/s0016-7037(03)00387-9
- Sorokin, D. Y. 1995. *Sulfitobacter pontiacus* gen. nov., sp. nov. A new heterotrophic bacterium from the black sea, specialized on sulfite oxidation. *Mikrobiologiya* **64**: 354–365.

- Spietz, R. L., R. A. Lundeen, X. Zhao, D. Nicastro, A. E. Ingalls, and R. M. Morris. 2019. Heterotrophic carbon metabolism and energy acquisition in *Candidatus Thioglobus singularis* strain PS1, a member of the SUP05 clade of marine *Gammaproteobacteria*. *Environ. Microbiol.* **21**: 2391–2401. doi:10.1111/1462-2920.14623
- Stevens, H., and O. Ulloa. 2008. Bacterial diversity in the oxygen minimum zone of the eastern tropical South Pacific. *Env. Microbiol* **10**: 1244–1259. doi:10.1111/j.1462-2920.2007.01539.x
- Stewart, F. J. 2011. Dissimilatory sulfur cycling in oxygen minimum zones: An emerging metagenomics perspective. *Biochem. Soc. Trans.* **39**: 1859–1863. doi:10.1042/BST20110708
- Stewart, F. J., O. Ulloa, and E. F. DeLong. 2012. Microbial metatranscriptomics in a permanent marine oxygen minimum zone. *Env. Microbiol* **14**: 23–40. doi:10.1111/j.1462-2920.2010.02400.x
- Stief, P., A. Kamp, B. Thamdrup, and R. N. Glud. 2016. Anaerobic nitrogen turnover by sinking diatom aggregates at varying ambient oxygen levels. *Front. Microbiol.* **7**: 98. doi:10.3389/fmicb.2016.00098
- Stramma, L., T. Fischer, D. S. Grundle, G. Krahlmann, H. W. Bange, and C. A. Marandino. 2016. Observed El Niño conditions in the eastern tropical Pacific in October 2015. *Ocean Sci.* **12**: 861–873. doi:10.5194/os-12-861-2016
- Suess, E., L. Kulm, and J. Killingly. 1987. Coastal upwelling and a history of organic-rich mudstone deposition off Peru, p. 181–197. *In* J. Brooks and A. J. Fleet [eds.], *Marine Petroleum Source Rocks*. Geological Society, London.
- Swan, B. K., and others. 2011. Potential for chemolithoautotrophy among ubiquitous bacteria lineages in the dark ocean. *Science* **333**: 1296–1300. doi:10.1126/science.1203690
- Tang, K. 2020. Chemical diversity and biochemical transformation of biogenic organic sulfur in the ocean. *Front. Mar. Sci.* **7**: 1–15. doi:10.3389/fmars.2020.00068
- Tankéré, S. P., F. L. Muller, J. Burton, P. Statham, C. Guieu, and J.-M. Martin. 2001. Trace metal distributions in shelf waters of the Northwestern Black Sea. *Cont. Shelf Res.* **21**: 1501–1532. doi:10.1016/S0278-4343(01)00013-9
- Taylor, G. T., and others. 2001. Chemoautotrophy in the redox transition zone of the Cariaco Basin: A significant midwater source of organic carbon production. *Limnol. Oceanogr.* **46**: 148–163. doi:10.4319/lo.2001.46.1.0148
- Thamdrup, B., and D. E. Canfield. 1996. Pathways of carbon oxidation in continental margin sediments off Central Chile. *Limnol. Oceanogr.* **41**: 1629–1650. doi:10.4319/lo.1996.41.8.1629
- Thamdrup, B., T. Dalsgaard, M. M. Jensen, O. Ulloa, L. Farías, and R. Escobedo. 2006. Anaerobic ammonium oxidation in the oxygen-deficient waters off northern Chile. *Limnol. Oceanogr.* **51**: 2145–2156. doi:10.4319/lo.2006.51.5.2145
- Thomsen, S., T. Kanzow, F. Colas, V. Echevin, G. Krahlmann, and A. Engel. 2016a. Do submesoscale frontal processes ventilate the oxygen minimum zone off Peru? *Geophys. Res. Lett.* **43**: 8133–8142. doi:10.1002/2016gl070548
- Thomsen, S., T. Kanzow, G. Krahlmann, R. J. Greatbatch, M. Dengler, and G. Lavik. 2016b. The formation of a subsurface anticyclonic eddy in the Peru-Chile undercurrent and its impact on the near-coastal salinity, oxygen, and nutrient distributions. *J. Geophys. Res. Ocean.* **121**: 476–501. doi:10.1002/2015jc010878
- Thrash, J. C., K. W. Seitz, B. J. Baker, B. Temperton, L. E. Gillies, N. N. Rabalais, B. Henrissat, and O. U. Mason. 2017. Metabolic roles of uncultivated bacterioplankton lineages in the Northern Gulf of Mexico “Dead Zone”. *MBio* **8**: e01017–e01017. doi:10.1128/mBio.01017-17
- Tiano, L., E. Garcia-Robledo, T. Dalsgaard, A. H. Devol, B. B. Ward, O. Ulloa, D. E. Canfield, and N. Peter Revsbech. 2014. Oxygen distribution and aerobic respiration in the north and south eastern tropical Pacific oxygen minimum zones. *Deep Sea Res. Part I Oceanogr. Res. Pap.* **94**: 173–183. doi:10.1016/j.dsr.2014.10.001
- Tutasi, P., and R. Escobedo. 2020. Zooplankton diel vertical migration and downward C flux into the oxygen minimum zone in the highly productive upwelling region off northern Chile. *Biogeosciences* **17**: 455–473. doi:10.5194/bg-17-455-2020
- Vairavamurthy, A., W. Zhou, T. Eglinton, and B. Manowitz. 1994. Sulfonates: A novel class of organic sulfur compounds in marine sediments. *Geochim. Cosmochim. Acta* **58**: 4681–4687. doi:10.1016/0016-7037(94)90200-3
- van Vliet, D. M., F. A. B. von Meijenfildt, B. E. Dutilh, L. Villanueva, J. S. Sinninghe Damsté, A. J. M. Stams, and I. Sánchez-Andrea. 2020. The bacterial sulfur cycle in expanding dysoxic and euxinic marine waters. *Environ. Microbiol.* 1–24. doi:10.1111/1462-2920.15265
- Walsh, D. A., E. Zaikova, C. G. Howes, Y. C. Song, J. J. Wright, S. G. Tringe, P. D. Tortell, and S. J. Hallam. 2009. Metagenome of a versatile chemolithoautotroph from expanding oceanic dead zones. *Science* **326**: 578–582. doi:10.1126/science.1175309
- Ward, B. B., A. H. Devol, J. J. Rich, B. X. Chang, S. E. Bulow, H. Naik, A. Pratihary, and A. Jayakumar. 2009. Denitrification as the dominant nitrogen loss process in the Arabian Sea. *Nature* **461**: 78–81. doi:10.1038/nature08276
- Wasmund, K., M. Mußmann, and A. Loy. 2017. The life sulfuric: Microbial ecology of sulfur cycling in marine sediments. *Environ. Microbiol. Rep.* **9**: 323–344. doi:10.1111/1758-2229.12538
- Weeks, S. J., B. Currie, and A. Bakun. 2002. Satellite imaging: Massive emissions of toxic gas in the Atlantic. *Nature* **415**: 493–494. doi:10.1038/415493b
- Weeks, S. J., B. Currie, A. Bakun, and K. R. Peard. 2004. Hydrogen sulphide eruptions in the Atlantic Ocean off southern Africa: Implications of a new view based on SeaWiFS

- satellite imagery. *Deep Sea Res. Part I Oceanogr. Res. Pap.* **51**: 153–172. doi:[10.1016/j.dsr.2003.10.004](https://doi.org/10.1016/j.dsr.2003.10.004)
- Widdel, F. 1988. Microbiology and ecology of sulfate- and sulfur-reducing bacteria, p. 469–585. In A. J. B. Zehnder [ed.], *Biology of anaerobic organisms*. John Wiley.
- Winkel, M., V. Salman-Carvalho, T. Woyke, M. Richter, H. N. Schulz-Vogt, B. E. Flood, J. V. Bailey, and M. Mußmann. 2016. Single-cell sequencing of thiomargarita reveals genomic flexibility for adaptation to dynamic redox conditions. *Front. Microbiol.* **7**: 964. doi:[10.3389/fmicb.2016.00964](https://doi.org/10.3389/fmicb.2016.00964)
- Woebken, D., B. M. Fuchs, M. M. M. Kuypers, and R. Amann. 2007. Potential interactions of particle-associated anammox bacteria with bacterial and archaeal partners in the Namibian upwelling system. *Appl. Environ. Microbiol.* **73**: 4648–4657. doi:[10.1128/aem.02774-06](https://doi.org/10.1128/aem.02774-06)
- Wright, J. J., K. M. Konwar, and S. J. Hallam. 2012. Microbial ecology of expanding oxygen minimum zones. *Nat. Rev. Microbiol.* **10**: 381–394. doi:[10.1038/nrmicro2778](https://doi.org/10.1038/nrmicro2778)
- Wright, J. J., K. Mewis, N. W. Hanson, K. M. Konwar, K. R. Maas, and S. J. Hallam. 2014. Genomic properties of Marine Group A bacteria indicate a role in the marine sulfur cycle. *ISME J.* **8**: 455–468. doi:[10.1038/ismej.2013.152](https://doi.org/10.1038/ismej.2013.152)
- Yilmaz, P., P. Yarza, J. Z. Rapp, and F. O. Glöckner. 2016. Expanding the world of marine bacterial and archaeal clades. *Front. Microbiol.* **6**: 1–29. doi:[10.3389/fmicb.2015.01524](https://doi.org/10.3389/fmicb.2015.01524)
- Zopfi, J., T. G. Ferdelman, B. B. Jørgensen, A. Teske, and B. Thamdrup. 2001a. Influence of water column dynamics on sulfide oxidation and other major biogeochemical processes in the chemocline of (Mariager Fjord Denmark). *Mar. Chem.* **74**: 29–51.
- Zopfi, J., T. Kjær, L. P. Nielsen, and B. B. Jørgensen. 2001b. Ecology of *Thioploca* spp.: Nitrate and sulfur storage in relation to chemical microgradients and influence of *Thioploca* spp. on the sedimentary nitrogen cycle. *Appl. Environ. Microbiol.* **67**: 5530–5537. doi:[10.1128/AEM.67.12.5530-5537.2001](https://doi.org/10.1128/AEM.67.12.5530-5537.2001)

Acknowledgments

The authors would like to thank Gesa Eirund for plotting of the World Ocean Atlas data 2013. The authors are thankful to Frank Stewart and three anonymous reviewers for their insightful comments and discussion. This work was supported by the MPG and the Sonderforschungsbereich (SFB754) GEOMAR, Kiel as well as the Villum Foundation (DEC) and the European Research Council (NOVAMOX to B.T., Grant no. 695599). The stipend of C.M.C was also supported by a Natural Sciences and Engineering Research Council of Canada (NSERC) scholarship.

Conflict of Interest

None declared.

Submitted 18 November 2020

Revised 05 February 2021

Accepted 02 March 2021

Associate editor: Florence Schubotz